Machinability of Aluminum 7075 Alloys

by

Seyed Mohammad Ali TAHMASEBI KANJOUR

THESIS PRESENTED TO ÉCOLE DE TECHNOLOGIE SUPÉRIEURE
IN PARTIAL FULFILLMENT FOR A MASTER'S DEGREE WITH THESIS
IN MECHANICAL ENGINEERING
M. A. SC.

MONTREAL, MARCH 5, 2024

ÉCOLE DE TECHNOLOGIE SUPÉRIEURE
UNIVERSITÉ DU QUÉBEC

BOARD OF EXAMINERS

THIS THESIS HAS BEEN EVALUATED

BY THE FOLLOWING BOARD OF EXAMINERS

Mr. Victor Songmene, Thesis Supervisor
Department of mechanical Engineering, École de technologie supérieure

Mr. Fawzy-Hosny Samuel, co-director
Department of mechanical Engineering, École de technologie supérieure

Mr. Jean-Pierre Kenne, chair (président of jury)
Department of mechanical Engineering, École de technologie supérieure

Mr. Ehab Elsharkawi, member
Department of Engineering Associate Professor Saint Mary's University

THIS THESIS WAS PRENSENTED AND DEFENDED

IN THE PRESENCE OF A BOARD OF EXAMINERS AND PUBLIC

ON FEBRUARY 23, 2024

AT ÉCOLE DE TECHNOLOGIE SUPÉRIEURE

ACKNOWLEDGMENT

I am deeply grateful to my research advisor, Professor Victor Songmene, for his unwavering guidance, encouragement, patience, and tireless support throughout the development of this thesis.

I would also like to express my gratitude to Prof. Fawzy Hosny Samuel and Dr. Agnes Samuel. Without their continuous support, guidance, and assistance in the revision process, the success of my research would not have been possible. Their valuable input and encouragement played a crucial role in shaping the outcome of this thesis.

My heartfelt thanks also go to Dr. Jules Kouam, Dr. Yasser Zedan, and all the technicians at the machine workshop for their invaluable help and support during the experimental tests.

Finally, I would like to express my profound gratitude to my family for their unlimited support and encouragement. Their unwavering backing played a crucial role in helping me persevere through this challenging period of my life and complete this thesis.

USINABILITÉ DES ALLIAGES D'ALUMINIUM 7075

Seyed Mohammad Ali TAHMASEBI KANJOUR

RESUMÉ

Cette étude porte sur le fraisage (à sec et lubrifié) de trois alliages d'aluminium 7075: Al7075, Al7075 - Sc (avec un ajout de 0,1 % de Sc), et Al7075 - Sc - Li (avec un ajout de 0,1 % de Sc et de 2,2 % de Li). L'objectif principal est d'explorer comment les paramètres de coupe (vitesse de coupe et vitesse d'avance), le traitement thermique, la composition de l'alliage et les méthodes de refroidissement influencent les trois facteurs clés de l'usinabilité : la rugosité de la surface, les forces de coupe et l'émission de particules. L'étude d'usinage était concentrée sur les conditions de traitement thermique qui ont donné les duretés les plus élevées et les plus faibles, afin d'analyser l'impact de la dureté sur l'usinabilité. L'objectif était d'examiner les effets de la vitesse d'avance, de la vitesse de coupe et des méthodes de refroidissement sur les critères d'usinabilité spécifiés. L'étude a utilisé une approche expérimentale à plusieurs niveaux pour générer des résultats d'usinage, qui ont ensuite fait l'objet d'une analyse statistique.

Les résultats du processus de traitement thermique ont montré que de tous les alliages, le traitement thermique de 24 heures à 120°C conduit à la dureté la plus élevée et, en revanche, les valeurs de dureté les plus faibles ont été observées à la fois dans le vieillissement simple (8 heures à 280°C) et le vieillissement double (8 heures à 280°C suivies de 24 heures à 120°C), ce qui souligne le rôle primordial de la température de vieillissement sur la dureté, indépendamment du fait que le processus de vieillissement soit simple ou double.

Les résultats de l'usinage montrent que dans les trois alliages utilisés dans notre étude, la vitesse d'avance a l'effet le plus significatif sur le paramètre Ra de rugosité. La vitesse de coupe et la dureté plus élevée ont eu un effet négatif sur la qualité de la surface. Les résultats ont également révélé que la vitesse d'avance est le paramètre affectant le plus significativement la force de coupe. L'usinage sous arrosage a réduit considérablement la force de coupe, et cette réduction est relativement plus importante lors de l'usinage d'alliages durs. Il a été également observé qu'une dureté plus élevée entraîne une augmentation de la force de coupe pour les trois alliages. Dans cette étude, la vitesse de coupe n'a pas eu d'effet significatif sur la force de coupe. L'émission des particules a été significativement affectée par l'utilisation d'un liquide de coupe. La vitesse de coupe a été le deuxième paramètre significatif sur l'émission de particules.

Mots clés : Usinabilité, Aluminium, Al7075, Traitement thermique, Rugosité de surface, Forces de coupe, Emission de particules

MACHINABILITY OF ALUMINUM 7075 ALLOYS

Seyed Mohammad Ali TAHMASEBI KANJOUR

ABSTRACT

This study delves into the dry and wet end milling of three distinct Aluminum 7075 alloys: AL7075, AL7075 – Sc (with a 0.1% Sc addition), and AL7075 – Sc – Li (featuring a 0.1% Sc and 2.2% Li addition). The primary objective is to explore how cutting parameters (cutting speed and feed rate), heat treatment, alloy composition, and cooling methods influence three key machinability factors: surface roughness, cutting force, and particle emission. In the initial phase of the investigation, all three alloys underwent heat treatment at five different aging times and temperatures. Subsequently, the machining process focused on the alloys' hardest and softest conditions achieved through these heat treatments, aiming to analyze the impact of hardness on machinability. The second phase involved end milling using the same tool and a consistent depth of cut under both dry and wet conditions. This was done to scrutinize the effects of feed rate, cutting speed, and cooling methods on the specified machinability criteria. The study employed a multi-level experimental approach to generate machining results, which would then undergo statistical analysis.

The results in the heat treatment process showed that between all alloys, 24-hour heat treatment at 120°C leads to highest hardness and in contrast the lowest hardness values were observed in both single aging (8 hours at 280°C) and double aging (8 hours at 280°C followed by 24 hours at 120°C) that underscores the primary role of aging temperature in influencing alloy hardness and strength, regardless of whether the aging process is single or double.

The machining results illustrated that in all three alloys used in our study, the feed rate had the most significant effect on surface roughness (Ra). The cutting speed and higher hardness had negative effect on surface quality. The results also revealed that feed rate is the most significant affective parameter on cutting force. Wet machining significantly reduces cutting force, and this reduction is relatively more when machining hard alloys. It was also evident that higher hardness results in increased cutting force in all three alloys. In this study cutting speed did not show significant effect on the cutting force. Particle emission was significantly affected when using cutting fluid. Cutting speed was the second significant effective parameter on particle emission.

Keywords: Machinability, Aluminum, Al7075, Heat treatment, Surface roughness, Cutting forces, Particle emission

TABLE OF CONTENTS

Page

LIST OF TABLES

Page

LIST OF FIGURES

Page

LIST OF ABREVIATIONS

ANOVA	Analysis of variance.
BUE	Built-Up Edge.
ISO	International standard organizations.
SEM	Scanning electron microscopy.
EDS	Energy-dispersive x-ray spectroscopy
CNC	Computer numerical control
MQL	Minimum quantity lubrication
APS	Aerosol Particle Sizer
CPC	Condensation Particle Counter
PFZ	Precipitate free zone

LIST OF SYMBOLS AND UNITS OF MEAUREMENT

f	feed rate (mm/th)
v	Cutting speed (m/min)
ap	Depth of cut (mm)
h	hardness (VHN)
c	cooling mode
Fx, Fy, Fz	Force components in the X, Y and Z directions (N)
Ra	The arithmetic average height (µm)
Rq	Root mean square roughness (µm)
Rt	The maximum height of the profile (µm)
Rz	Ten-point height (µm)
Rp	The maximum height of peaks (µm)

INTRODUCTION

In this study, we empirically examine the impact of cutting parameters, workpiece characteristics, and machining conditions on machinability criteria. The materials studied include three Aluminum 7075 alloys: Al 7075, Al 7075 – Sc (with a 0.1% Sc addition), and Al 7075-Li-Sc (with a 0.1% Sc and 2.2% Li addition). Variations in cutting parameters involve feed rate and cutting speed, with a constant depth of cut set at 2 mm. Machining was performed under both dry and wet conditions using a 10 mm uncoated carbide end mill as the cutting tool. The machinability criteria explored encompass surface roughness (Ra), cutting force, and particle emission. The next paragraphs will enumerate the steps taken during the investigation.

In the initial phase of the study, we carried out five distinct heat treatments for each of the three alloys under investigation. Following these treatments, the microhardness of the alloys was measured as a critical mechanical property criterion. This allowed us to establish a correlation between the achieved microhardness and the specific aging processes applied to each alloy.

To attain a comprehensive understanding of the aging effects on microstructure and the underlying factors contributing to the achieved hardness, this study delved into the examination of SEM (Scanning Electron Microscopy) and EDS (Energy-Dispersive X-ray Spectroscopy) images for selected heat-treated alloys. Going forward, a strategic choice was made to explore the impact of hardness on machinability. We selected the alloys that exhibited the highest and lowest microhardness values as a result of the heat treatment process.

Shaping an aluminum 7075 part through machining is a widespread practice, yet it comes with its set of challenges. The high strength and low thermal conductivity of the material make the machining process intricate, leading to issues such as tool wear, built-up edge formation, and the generation of rough surface finishes. Consequently, a profound comprehension of the machinability of aluminum 7075 becomes imperative. Such understanding not only allows for the optimization of the machining process but also contributes significantly to enhancing the overall quality of the final product.

The machining process was carried out using a 3-axis CNC milling machine under both dry and wet conditions, with variations in cutting parameters such as cutting speed and feed rate.

Throughout the machining process, a three-component dynamometer with a data acquisition system was employed to determine cutting forces in the X, Y, and Z directions.

Additionally, particle emissions, considered another machinability criterion, were measured. Subsequently, a surface roughness tester was utilized to measure the roughness of the machined surfaces.

The purposes and objectives of the study

The purpose of this research is to develop a comprehensive understanding of the fundamental machining of Aluminum 7075 alloys, including Al 7075, Al 7075–Sc (with a 0.1% Sc addition), and Al 7075–Sc–Li (with a 0.1% Sc and 2.2% Li addition).

The specific objectives of the study are:

1) To investigate how precipitation hardening, with variations in aging times and temperatures, and alloying with lithium, affects the mechanical properties of Al 7075 alloys.

2) To measure the roughness of machined surfaces and assess the impact of cutting parameters, workpiece material properties, and machining conditions on surface quality.

3) To investigate cutting forces during the machining of Al 7075 alloys and analyze how the specified inputs influence cutting forces in these specific alloys.

4) To research particle emissions during machining, identifying machining conditions and cutting parameters that result in lower particle generation, considering this a critical criterion for maintaining a safe workshop environment.

Structure of thesis

This thesis is comprised of five main chapters: it commences with an introduction, followed by the first chapter, which is dedicated to a comprehensive literature review. The second chapter provides detailed information on the workpiece material and methodology employed in this study. Moving forward, the third chapter is allocated to presenting and discussing the results of the heat treatment process. In the fourth chapter, the focus shifts to the machining results, where findings are presented and discussed. Finally, the last part encompasses the conclusion, along with recommendations for future work.

At the outset of each chapter, readers will find a presentation of the experimental conditions and parameters used in this research work. This deliberate structure ensures that each chapter is introduced with clarity and relevance. A brief discussion is structured as follows for each chapter.

Chapter 1 presents a comprehensive overview of aluminum characteristics, with a specific emphasis on Al 7075 and its machinability. Initially, the chapter conducts a thorough review of the Aluminum series, alloying, and the hardening process, with a particular focus on precipitation hardening. Subsequently, it delves into the concepts of machining and machinability, covering cutting parameters, machining conditions, and machinability criteria such as roughness, cutting force, and particle emissions. Finally, the chapter narrows its focus to the machining of Aluminum and Al 7075, highlighting relevant research that has been conducted in this field.

Chapter 2 details the experimental work conducted during both workpiece preparation and the machining process. The chemical compositions and heat treatments applied to the studied alloys, namely Al 7075, Al 7075–Sc, and Al 7075–Li –Sc, are presented. To structure the experimental plan, a multi-level factorial design is employed. The chapter introduces all the devices utilized throughout the various stages, including sample preparation, heat treatment, machining processes, and data acquisition. The investigated factors in this study encompass cutting parameters (feed rate, cutting speed), material properties (chemical compositions and hardness), and machining conditions (dry and wet machining).

Chapter 3 is dedicated to the results of the heat treatment processes conducted on the studied alloys. For each alloy, the impact of the adopted heat treatments on micro hardness is thoroughly examined. Furthermore, the chapter delves into an analysis of SEM (Scanning Electron Microscopy) and EDS (Energy-Dispersive X-ray Spectroscopy) images to elucidate the reasons behind the observed behaviors of the heat-treated alloys.

Finally, the concluding section provides a synthesis of the most significant summaries and conclusions derived from the findings presented in Chapters 3 and 4. It encapsulates the key insights gained from the heat treatment processes (Chapter 3) and the machining experiments

(Chapter 4). Furthermore, this section offers practical suggestions aimed at enhancing machinability criteria. Additionally, it addresses pertinent industrial considerations and emphasizes environmental aspects associated with the studied processes. The conclusion serves as a comprehensive wrap-up, tying together the research outcomes and providing actionable recommendations for both industry and environmental stewardship.

CHAPTER 1

LITERATURE REVIEW

1.1 Introduction

Aluminum alloys are widely used in various industries due to their excellent properties such as high strength-to-weight ratio, corrosion resistance, and good thermal and electrical conductivity (Ashkenazi 2019). Machining of aluminum alloys is a crucial process in the manufacturing of various components, including aircraft parts, automotive components, and consumer electronics. The process involves removing material from the workpiece to obtain the desired shape and size using various cutting tools and techniques (Soren, Kumar et al. 2019). Milling is a common machining process used in the manufacturing of aluminum alloy components. Milling of aluminum alloys can be challenging due to the material's low thermal conductivity and the tendency to produce built-up edge and burrs, which can affect the quality of the finished product. Therefore, it is essential to choose appropriate milling techniques and parameters to achieve optimal results (Tsao 2009).

1.2 Aluminum alloys

Significant progress has been made in the technological structures of materials used in modern vehicles over the last decade. A combination of safety, emission control, and comfort are essential for the development and production of next-generation vehicles, while reducing the vehicle's mass is also imperative (Stojanovic and Epler 2018). High strength-to-weight ratio, high fatigue resistance, good formability, excellent thermal conductivity, and good corrosion resistance in various extreme environments, are some of the considerable properties that have made Aluminum an attractive material for a wide range of applications, including automotive components; airplanes, trains, and ships, electrical and packaging industries, architecture, and food industries (Ashkenazi 2019). Figure 1.1 presents global aluminum consumption of primary aluminum between 2010 and 2016:

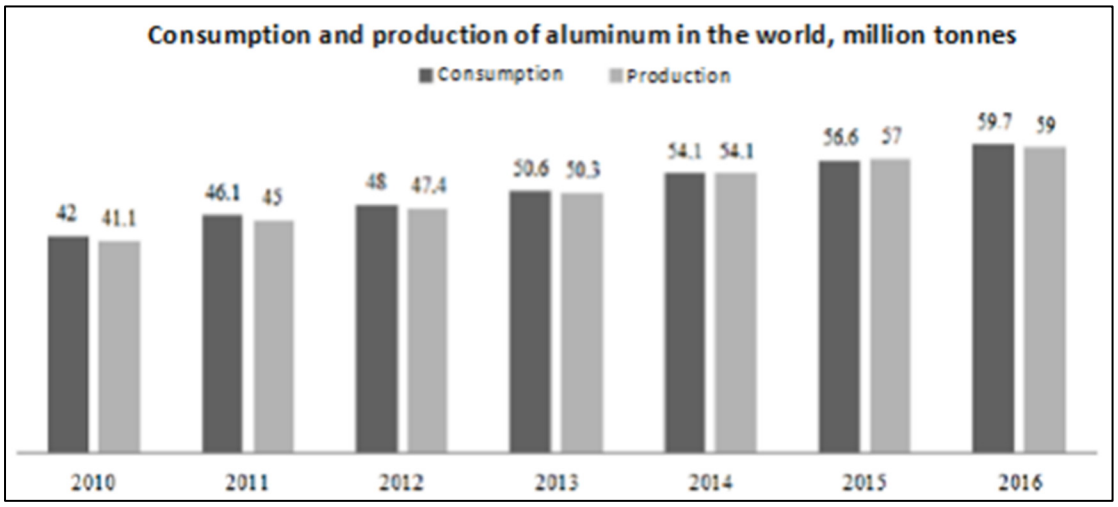

Figure 1.1 World aluminium consumption and production.categories of aluminum alloys Taken from Galevsky, Rudneva and Aleksandrov (2018)

Cast alloys and wrought alloys are the two basic categories of aluminum alloys. According to the strengthening working processes, aluminum wrought alloys are divided into heat-treatable and non-heat-treatable classifications. As a result, aluminum alloy properties can vary widely, providing numerous potential uses (Georgantzia, Gkantou and Kamaris 2021). Cast aluminum alloys are also divided into two subcategories according to whether the alloys can be strengthened by heat treatment or not (Deng, Xia and Wang 2022). Table 1.1 summarizes the classification of aluminum alloys.

1.2.1 Alloying elements used with aluminum alloys

As a strategy for developing alloys, one or two major elements are selected for primary properties, and minor elements are added as alloying additions to modify the microstructure and properties of the alloys (Wang, Wang et al. 2012).

The selection of alloying elements is determined by their effects on the microstructure, and adaptability. These include major and minor alloying elements, microstructure modifiers, and impurities. Alloying elements that are impurities in some alloys can be major elements in others.

Table 1.1 Classification of aluminum alloys

Category	Subcategory	Series
Wrought aluminum alloy	Heat-treated strengthening aluminum alloy	Al-Cu series alloy—2XXX series, such as 2024 alloy Al–Mg–Si series alloy—6XXX series, such as 6063 alloy Al–Zn–Mg–Cu series alloy—7XXX series, such as 7075 alloy Al–Li series alloy—8XXX series, such as 8089 alloy
	Non-heat-treated strengthening aluminum alloy	Pure aluminum—1XXX series, such as 1050 alloy Al–Mn series alloy—3XXX series, such as 3004 alloy Al–Si series alloy—4XXX series, such as 4032 alloy Al–Mg series alloy—5XXX series, such as 5083 alloy
Cast aluminum alloy	Heat-treated strengthening aluminum alloy	Al–Mg–Si series alloy, such as ZL107 alloy Al-Cu–Mg–Si series alloy, such as ZL110 alloy Al–Mg–Si series alloy, such as ZL104 alloy Al–Zn–Mg series alloy, such as ZL402 alloy Al–Zn–Si series alloy, such as ZL401 alloy
	Non-heat-treated strengthening aluminum alloy	Pure aluminum Al–Si series alloy, such as ZL102 alloy Al–Mg series alloy, such as ZL301 alloy

Silicon (Si) lowers the melting point of aluminum and increases its fluidity throughout the casting process. Silicon addition provides a moderate increase in strength. Aluminum strength and hardness are also affected by copper (Cu) addition, due to its ability to increase the alloy matrix hardness. This facilitates the machining process.

Addition of magnesium (Mg) to aluminum alloys significantly strengthens the alloy and improves its work-hardening characteristics. Furthermore, weldability, corrosion resistance, and high strength can all be enhanced by magnesium addition (Rana, Purohit and Das 2012). Increasing the zinc (Zn) content first increases the strength, but then decreases it; also, this increase in Zn content leads to continual reduction of the elongation.

Based on the study of Xu et al.(Xu, Zhang et al. 2021) the addition of 8 percent Zn as the main alloying element in 7xxx alloys provides optimum strength, elongation, and hot-tearing sensitivity to the alloys.

Among major alloying elements, there are only a few elements that have sufficient solid solubility in aluminum. These include Cu, Mg, Si, Zn, and lithium (Li). Aluminum alloys based on their major alloying elements are classified in different series. Table 1.2 lists the wrought aluminum alloys series, their major alloying elements, and their main properties.

1.2.2 Hardening processes

The mechanical, physical, and chemical properties of aluminum alloys depend upon the alloy composition and microstructure. The alloying and hardening processes to which the alloy is subjected control these two factors. Therefore, it can be concluded that the optimal properties of heat-treatable aluminum alloys are achieved by alloying and heat-treating which modify the microstructure. During heat treatment, small hard precipitates form, which obstruct dislocation motion and thus improve mechanical properties. Additionally, strain hardening can be applied to non-heat treatable alloys in order to improve their properties (Isadare, Aremo et al. 2013). Processes of hardening are classified according to whether or not the alloy is heat treatable. Heat-treatable alloys are hardened by precipitation hardening, whereas non-heat treatable alloys are hardened by strain hardening.

Table 1.2 Wrought aluminum alloys series and their main properties

Alloy Series	Major alloying elements	Main properties
1XXX	Pure Al	• Strain hardenable • High formability, corrosion resistance, and electrical conductivity • Typical ultimate tensile strength range: 10 to 27 ksi
2XXX	Copper (Cu)	• Heat treatable • High strength, at room and elevated temperatures • Typical ultimate tensile strength range: 27-62 ksi • Corrosion resistant but not as good as other alloys
3XXX	Manganese (Mn)	• High formability and corrosion resistance with medium strength • Typical ultimate tensile strength range: 16-41 ksi • Hardened by strain hardening
4XXX	Silicon (Si)	• Some heat treatable • Good flow characteristics, medium strength • Typical ultimate tensile strength range: 25-55 ksi
5XXX	Magnesium (Mg)	• Strain hardenable • Excellent corrosion resistance, toughness, weldability, moderate strength • Building and construction, automotive, cryogenic, marine pplications • Typical ultimate tensile strength range: 18-51 ksi
6XXX	Mg-Si	• High corrosion resistance, moderate strength • Typical ultimate tensile strength range: 18-58 ksi • Outstanding extrudability
7XXX	Zinc (Zn)	• Heat treatable • Very high strength, special high toughness versions • Typical ultimate tensile strength range: 32-88 ksi • Mechanically joined

1.2.2.1 Precipitation hardening through heat treatment

Three steps are involved in precipitation hardening: (i) Solution heat treating; (ii) rapidly quenching the solution heat-treated sample to a lower temperature, followed by: (iii) aging (natural aging or artificial aging at a specific temperature and for a specified duration).

During solution heat treatment, the alloy is heated to a temperature at which the alloying elements dissolve in the alloy. To keep the alloying elements trapped in solution, the solution-treated alloy is rapidly quenched to room temperature. Quenching is followed by the aging process in which dissolved alloying elements start to form fine particles, leading to an enhancement of the alloy hardness. The main reason why these fine particles increase the alloy hardness is that they create obstacles preventing dislocation movement. Natural aging and artificial aging are two possible aging processes for aluminum alloys. In the natural aging of Al alloys, precipitation takes place at room temperature, usually after a long period of time, while artificial aging is accomplished through heating to a predetermined temperature for a certain amount of time (Campbell Jr., 2011).

1.2.2.2 Strain hardening

In the plastic forming of metals, while most of the energy during the working process is converted to heat, some of this energy is stored in the form of dislocations produced in the microstructure, which cause the hardening. Therefore, because of most working and forming operations such as extrusion, drawing, and rolling on aluminum and its alloys, work hardening, or strain hardening occurs. In aluminum alloys, the stored energy per unit volume is 0.05, which means that 5% of the work done in deformation is held in the metal and the rest of the energy is released as heat (Dorward 2018).

1.2.3 Aluminum 7000 series alloys

The 7000 series of aluminum alloys are known for their high strength-to-weight ratio, making them popular for use in aerospace and other high-stress applications. They are often used in high performance components and applications such as aircraft, aerospace, and competitive sporting equipment. These alloys utilize Zn as the major alloying element and when combined with a smaller amount of Mg, the result is a heat-treatable alloy which offers very high strength.

Extrusion, casting, rolling, and powder metallurgy are among the different production methods used for the 7000 series of aluminum alloys, depending on the desired form of the component produced and its application (Johnson 1990).

The commercial 7000 series aluminum alloys in the market are listed as below (Miller, Zhuang et al. 2000, Williams and Starke Jr 2003).

1- 7075 Aluminum Alloy: This is the most well-known and widely used alloy in the 7000 series. It has excellent strength-to-weight ratio, good fatigue resistance, and excellent machinability. It is used in the aerospace, automotive, and defense industries.
2- 7050 Aluminum Alloy: This alloy is like 7075 in terms of strength and toughness, but with better corrosion resistance. It is used in aerospace and defense applications.
3- 7175 Aluminum Alloy: This alloy has high strength and toughness and is used in applications such as aircraft and missile components, and other high-stress structural applications.
4- 7475 Aluminum Alloy: This alloy has high strength and toughness and is used in aerospace applications such as wing skin and bulkhead components.

1.2.4 Aluminum 7075 alloys

The aluminum 7075 series is a high-strength aluminum alloy that contains zinc as its major alloying element. It is known for its excellent mechanical properties, particularly its high strength-to-weight ratio. It is worth noting that the specific mechanical properties of aluminum 7075 alloys can vary, depending on the exact composition and processing conditions. Different heat treatments and processing techniques may be used to modify the mechanical properties of the alloy to tailor them to specific applications. The mechanical and physical properties of aluminum 7075 alloys are listed in the Table 1.3 and Table 1.4 (Johnson 1990, Maechler, Uggowitzer et al. 1991).

Table 1.3 Mechanical properties of aluminum 7075 alloys
Taken from Johnson 1990, Maechler, Uggowitzer et al. (1991)

Property	
Tensile Strength	572 MPa (83 ksi)
Yield Strength	503 MPa (73 ksi)
Elongation	11%
Modulus of Elasticity	71.7 GPa (10.4 x 10^6 psi)
Shear Strength	331 MPa (48 ksi)

Table 1.4 Physical properties of aluminum 7075 alloys
Taken from Johnson 1990, Maechler, Uggowitzer et al. (1991)

Property	
Density	2.81 g/cm^3 (0.102 lb/in^3)
Melting Point	477-635°C (890-1175°F)
Thermal Conductivity	130 W/(m*K) at 25°C (77°F)
Electrical Conductivity	34.7 MS/m at 20°C (68°F)
Coefficient of Thermal Expansion	23.6 x 10^{-6}/K at 20°C (68°F)

1.2.4.1 Hardness of aluminum 7075 alloys

The hardness and strength of aluminum 7075 alloys can be attributed to several strengthening mechanisms that occur during the heat treatment process including solid solution strengthening, precipitation hardening, grain refinement, and cold working. A combination of these mechanisms can lead to a significant increase in the hardness and strength of the alloy, making it suitable for high-stress applications in the aerospace, automotive, and defense industries (LI JF 2008, Tajally and Emadoddin 2011).

1.2.5 Aluminum lithium alloys

Aluminum-lithium (Al-Li) alloys are a family of lightweight alloys that have been developed to meet the high-performance requirements of aerospace and defense applications. These alloys typically have a higher strength-to-weight ratio and stiffness compared to conventional aluminum alloys. The mechanical and physical properties of Al-Li alloys are listed in the Table 1.5 and Table 1.6 (Prasad, Gokhale and Wanhill 2013).

Table 1.5 Mechanical properties of Al-Li alloys
Taken from Prasad, Gokhale and Wanhill (2013)

Property	
Tensile Strength	450 MPa to 700 MPa
Yield Strength	300 MPa to 600 MPa
Elongation	1% to 6%
Fatigue strength	110 MPa to 190 MPa

Table 1.6 Physical properties of Al-Li alloys
Taken from Prasad, Gokhale and Wanhill (2013)

Property	
Density	2.4 g/cm^3 to 2.7 g/cm^3
Melting Point	560°C to 650°C
Thermal Conductivity	160 W/mK to 200 W/mK
Electrical Conductivity	30% to 60% IACS

1.2.5.1 Commercial Al-Li alloys

Some common Al-Li alloys and their compositions (Wanhill and Bray 2014) include:

1. AA2091 (composition wt%): Contains 2.8-3.1% Li, 0.5-1.5% Cu, and 0.05-0.15% Zr. This alloy possesses high toughness, ductility, and corrosion resistance.
2. AA2050 (composition wt%): Contains 2.0-2.6% Li, 0.15-0.25% Cu, and 0.05-0.15% Zr. This alloy exhibits high strength, stiffness, and corrosion resistance.
3. AA2195 (composition wt%): Contains 1.9-2.4% Li, 0.15-0.25% Cu, and 0.1-0.2% Zr. This alloy also displays high strength, toughness, and corrosion resistance.
4. AA8090 (composition wt%): Contains 1.5-2.5% Li, 0.8-1.8% Cu, and 0.06-0.15% Zr. Like AA2090 alloy, this alloy also displays high strength, stiffness, and fatigue resistance.

1.2.5.2 Hardness of Al-Li alloys

The hardness of Al-Li alloys varies depending on the specific alloy composition and processing parameters.

However, in general, Al-Li alloys are known to have higher strength and hardness compared to conventional aluminum alloys (Jiang, Xiang and Zheng 2010).

1.3 Material removal and machining

To ensure that the manufactured parts perform as expected throughout their service life, dimensional tolerances and surface finish must be controlled. For the parts formed, cast, or shaped by other processes, additional operations are often required to achieve an accurate and precise final product. These additional processes involve material removal (Kumar, Zindani et al. 2018). A material removal process refers to removing excess materials from a workpiece or part in order to obtain the desired shape.

A significant portion of this process is performed through machining operations such as turning, drilling, milling, etc., as shown in Figure 1.2. These cutting operations are accomplished by using cutting tools that are harder and stronger than the metal being machined (Groover 2020).

From another point of view, machining can be considered as a chip-forming process in which metal is removed in the form of plastically deformed chips (Stephenson and Agapiou 2018).

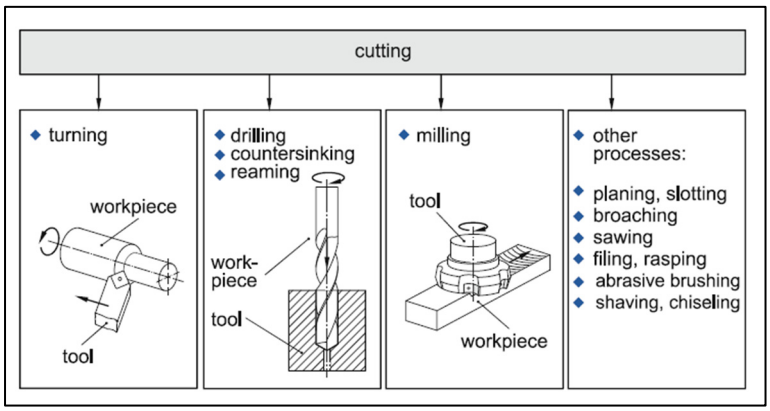

Figure 1.2 Manufacturing processes
Taken from Toenshoff and Denkena (2013)

1.3.1 Milling

Milling is a fundamental machining process used in die, aerospace, automotive, and machinery design, as well as in manufacturing industries to remove metal, and obtain milled surfaces which are widely used to mate with other parts (Zhang, Chen and Kirby 2007).

In the milling operation, a rotating cutting tool provides the cutting action while the movement of the workpiece clamped on a table performs the feed action. The shapes of milling cutters and the number of their cutting edges (teeth) vary, depending on the application. Each tooth cuts away an arc-shaped segment whose thickness is determined by the feed or tooth load.

Although feeds in this operation are typically light, ranging between 0.025 mm and 0.25 mm, the metal removal rate is relatively high due to the high cutting speed and the large number of teeth involved (Trent and Wright 2000). The cutting speed can be calculated using Equation 1.1 where V is the cutting speed, N is the rotational speed of the spindle, and D is the cutting tool diameter (Stephenson and Agapiou 2018).

$$V = \pi ND \tag{1.1}$$

Equation 1.2 describes the relationship between feed rate f_r, feed per revolution f, and feed per tooth f_t, where N is the rotational speed of the spindle and n_t is the number of tool cutting edges (teeth).

$$f_r = Nf = n_t N f_t \tag{1.2}$$

1.3.1.1 Categories of milling operations

Peripheral (or plain) milling, and face milling are the two basic milling operations, as shown in Figure 1.3. The surface generated by peripheral milling is parallel to the axis of rotation, while the surface generated by face milling is normal to the rotation axis. End milling is a peripheral milling operation that is generally used for profiling and slotting, but in pocketing operations, end milling may be used in lieu of face milling.

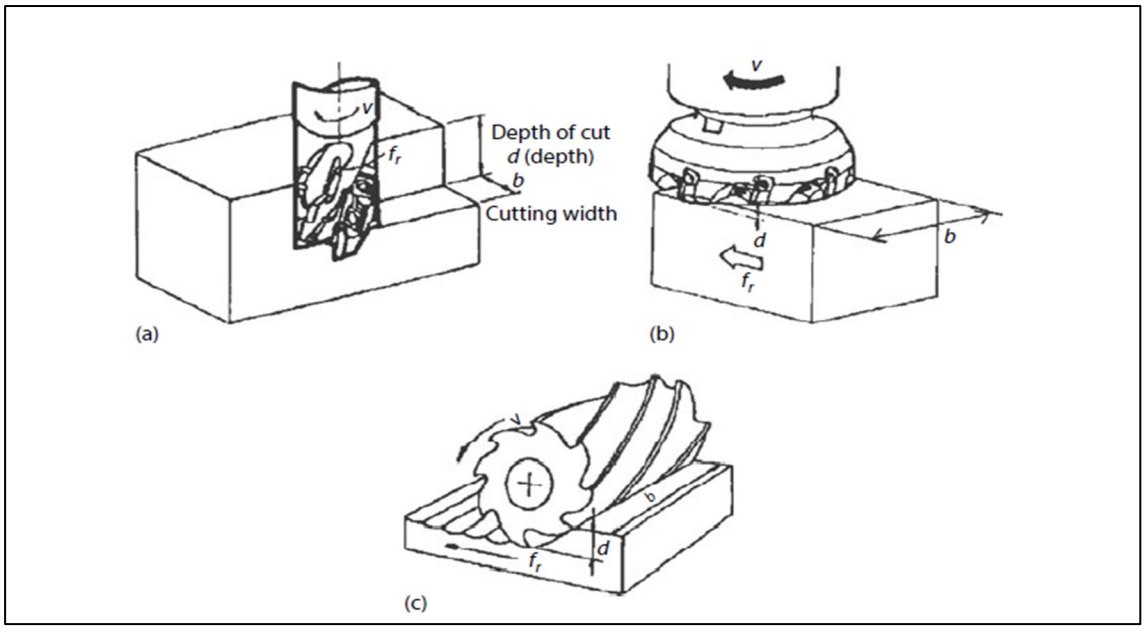

Figure 1.3 Milling operation types: (a) end milling, (b) face milling, and (c) peripheral milling
Taken from Stephenson and Agapiou (2018)

In addition, the milling operations can be divided into *up* (conventional) and *down* (climb) milling as shown in Figure 1.4. During up-milling, the cutter rotates against the feed direction, while in the case of down-milling, the cutter rotates in the same direction as the feed.

Uncut chip thickness increases with cutter rotation in up milling, whereas in down milling, it decreases to zero as the cutter rotates. There are advantages to both up and down-milling depending on the circumstances. Up-milling is generally more appropriate when there is backlash in the spindle and feed drive as well as when there are significant vibrations in the part. During down-milling, chips often become trapped between the insert and cutter, resulting in tool breakage. Also, in down-milling, cutting tool engagement time per volume of removed material is relatively higher compared to up-milling, resulting in a higher tool wear rate (Stephenson and Agapiou 2018).

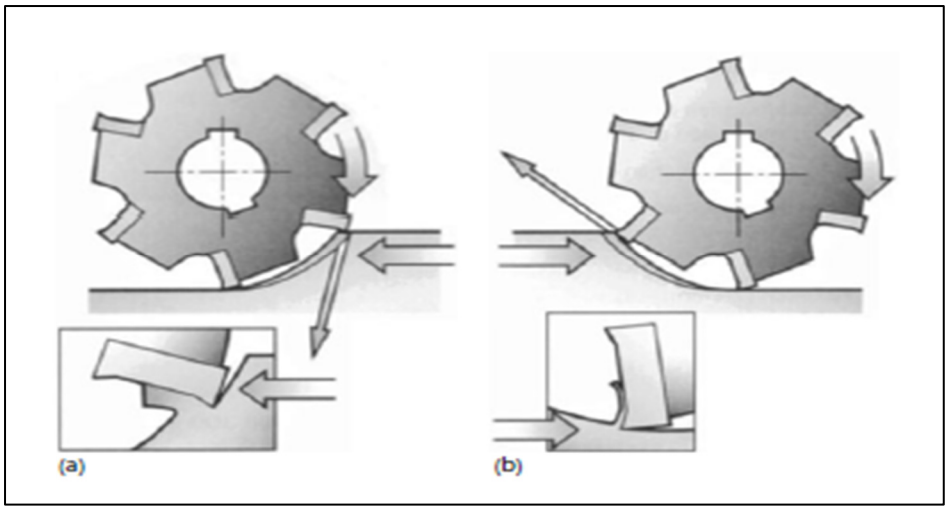

Figure 1.4 Cutting direction: (a) Down-milling (climb), and (b) up-milling (conventional) Taken from Stephenson and Agapiou (2018)

1.3.2 Machining parameters

From a system-oriented perspective, black boxes with input and output variables are a good way to describe cutting processes. As indicated in Figure 1.5, input variables, also known as independent variables, can be categorized into system variables, and manipulated variables. System variables that remain constant over a relatively long period of time, include the machine tool, workpiece properties such as strength, shape, and chemical composition, and tool material and geometry. The manipulated variables, however, are adjusted either manually or by using a computer program for each machining process. These variables include the cutting speed, feed rate, depth of cut, and volume of cutting liquid used.

The output variables that are identified as dependent variables or responses, can be classified as process variables and effect variables. Process variables emerge during the process; therefore, they are detectable and measurable only during the machining process. Cutting force, chip formation zone temperature, and acoustic emissions are some of the well-known outputs of this category. After machining, effect variables can be measured for different elements including the workpiece (dimension accuracy, surface roughness), the tool (wear), the machine tool (increase in temperature, wear), and the cutting fluids (increase in temperature) (Toenshoff and Denkena 2013).

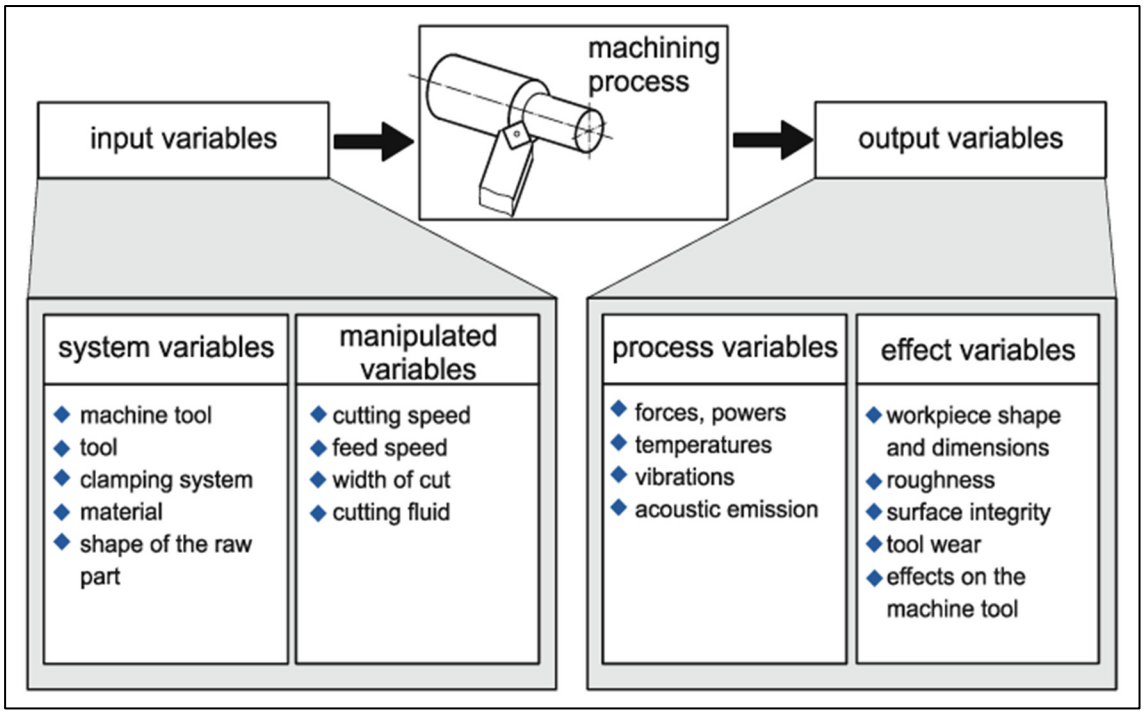

Figure 1.5 Cutting processes as a black box system
Taken from Toenshoff and Denkena (2013)

1.3.3 Machinability

The term “machinability” refers to the property and characteristic of the work material that influences machining success. Therefore, the machinability of a material can be defined as its relative ease of machining. Machinability can be evaluated according to a variety of factors, including tool life, cutting force, power used in the operation, surface finish, cutting temperature, and ease of chip disposal (Groover 2010).

In spite of this simple definition of machinability and repetitive usage of this phrase in numerous books and articles, its concept is relatively difficult and ambiguous. The machinability of a material could be good according to one criterion, but poor according to another. It is also possible for machinability to change if a different operation is carried out or different machining conditions are applied. Consequently, it is not acceptable to claim that a material has good or poor machinability.

A better approach to dealing with this complex situation might be to investigate the machinability criteria behavior of metals under different cutting conditions (Trent and Wright 2000). The machinability of a metal is usually compared to the machinability of a standard metal (usually AISI 1112 steel). The results are expressed as an index number named machinability rate (MR), where the standard material is given a score of 1.0. Higher scores indicate easier machinability, while lower scores indicate more difficult machinability (Boubekri, Rodriguez and Asfour 2003).

1.3.4 Machining outputs or machinability criteria

The machinability section of this thesis explores various criteria that influence the machining process. These criteria include Force, Roughness (Surface Quality), Particle Emissions, Cooling Mode, and Cutting Fluids.

Force is a critical parameter affecting tool wear and material removal, while Roughness directly relates to the quality of the machined surface. Particle Emissions are of environmental concern and can be linked to tool wear.

Cooling mode and the application of cutting fluids play essential roles in temperature control and lubrication during machining, impacting tool life and workpiece integrity.
Understanding and optimizing these criteria is crucial for enhancing the efficiency, quality, and sustainability of machining operations.

1.3.4.1 Cutting force

The cutting forces required for metal cutting operations have been considered in research programs covering many metals and alloys, due to their importance in machinability investigations.

Oftentimes, measured cutting forces are used to compare machinability of materials, especially when tool life tests cannot be conducted due to time constraints or limited material supplies. Furthermore, machine power requirements and bearing loads are influenced by cutting forces. High forces can also result in deflection of the part, tool, or machine structure, as well as high cutting temperatures and excessive vibrations (Stephenson and Agapiou 2018).

For metals of commercial purity like iron, nickel, copper, and aluminum, the forces are high due to the large contact area on the rake face, small shear plane angle, and thick chips that move away at slow speeds.

Alloying pure metals typically increases the yield strength but reduces tool forces during machining due to a shorter contact length on the rake face. Reduction of forces by restricting contact on the rake face is not always practical because it weakens the tool. The rake angle is the most important parameter influencing cutting force. An increase in the rake angle reduces both the cutting and feeding force but weakens the edge of the tool and can cause fractures.

The use of cutting lubricants can significantly affect the contact length and cutting forces. At very low cutting speeds, the lubricant can prevent seizure and greatly reduce the forces. Although at higher speeds, seizure cannot be prevented near the edge, liquid or gaseous lubricants can restrict the area of seizure to a small region by penetrating from the periphery (Trent and Wright 2000).

Several models have been introduced for predicting cutting forces (Han, Jin and Fu 2015). However, due to the vast number of variables involved, such as cutting parameters, tool and machine tool conditions, workpiece properties, and various unpredictable noise factors that affect the cutting force, these models are unable to predict the cutting force with high precision. Consequently, experimental models are considered more reliable, as they take into account the impact of all the mentioned variables and noise factors (Coelho, A et al. 2003).

The cutting force measuring methods are generally divided into direct and indirect categories. In indirect force measurements, some sensors are applied to measure a variety of physical quantities such as displacement. Although these methods are cheaper than the direct methods, they are not accurate enough, being easily affected by environmental factors like temperature and humidity.

The most common direct cutting force measurement is done employing a table dynamometer in which piezoelectric sensors are located between two plates. The piezoelectric sensors generate an electrical charge when they are exposed to mechanical stress (Wan, Yin and Zhang 2016). As the table remains stationary or is moving with constant speed while the workpiece is fixed and machining occurs, the forces applied to the table are in equilibrium. As a result, the cutting forces transform into the pressure change of the piezoelectric sensors.

In the milling process, the cutting forces in the X-Y plane are measured by four sensors, as shown schematically in Figure 1.6. Under these conditions, all applied forces are balanced as shown in Equation 1.3. Therefore the forces in the X and Y directions can be calculated using Equation 1.4 (Luo, Chong and Liu 2018).

$$\begin{cases} \sum_{i=1}^{n} \mathrm{Fx}i = 0 \\ \sum_{i=1}^{n} \mathrm{Fy}i = 0 \end{cases} \quad i = 1, 2, 3, 4 \tag{1.3}$$

$$\begin{cases} F_x = \frac{\sqrt{2}}{2} F_3 - \frac{\sqrt{2}}{2} F_4 \\ F_y = F_1 + F_2 - \frac{\sqrt{2}}{2} F_3 - \frac{\sqrt{2}}{2} F_4 \end{cases} \tag{1.4}$$

For measuring cutting force in the Z direction, three sensors are located at the bottom of the table as shown in Figure 1.7, and the force in this direction is expressed as given in Equation 1.5.

$$F_z = F_{z1} = F_{z2} = F_{z3} \tag{1.5}$$

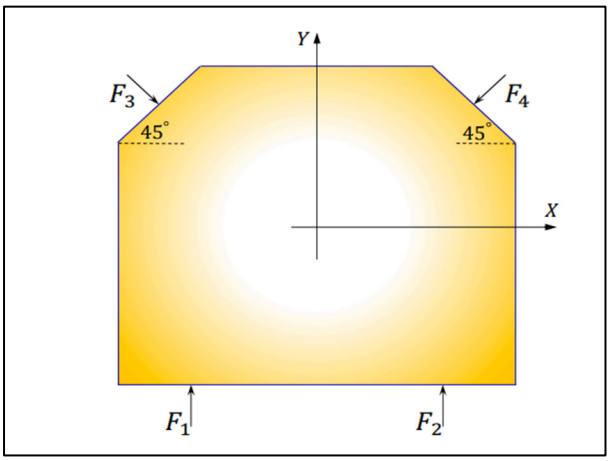

Figure 1.6 Cutting forces in the X-Y plane
Taken from Luo, Chong and Liu (2018)

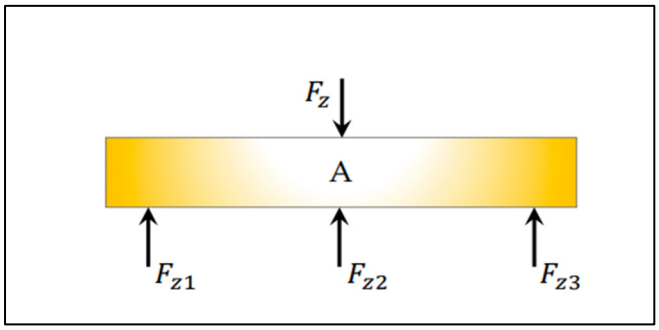

Figure 1.7 Cutting force in the Z direction
Taken from Luo, Chong and Liu (2018)

1.3.4.2 Roughness

The assessment of workpiece surface quality and the level of surface smoothness depends on the surface roughness. Surface roughness refers to the micro-geometry of a processed surface, including the size and interval of small peaks, valleys, and irregularities. Low roughness indicates high surface smoothness. Workpiece fatigue strength, contact stiffness, and corrosion resistance can all be impacted by surface roughness. Additionally, surface roughness affects the durability and reliability of the machined products. If the surface quality is poor, it can lead

to a decline in the workpiece performance, causing it to fail earlier than its expected lifetime (Zhenjing, Changhe et al. 2021).

The evaluation of the machined surface finish is typically conducted using a profilometer, which is a stylus-type profile meter. The profilometer measures the vertical movement of a stylus as it traverses the surface, and then amplifies this motion. The result is a two-dimensional profile of the surface segment that has been traced, which magnifies surface contours and irregularities in both the normal and tangential directions as shown in Figure 1.8.

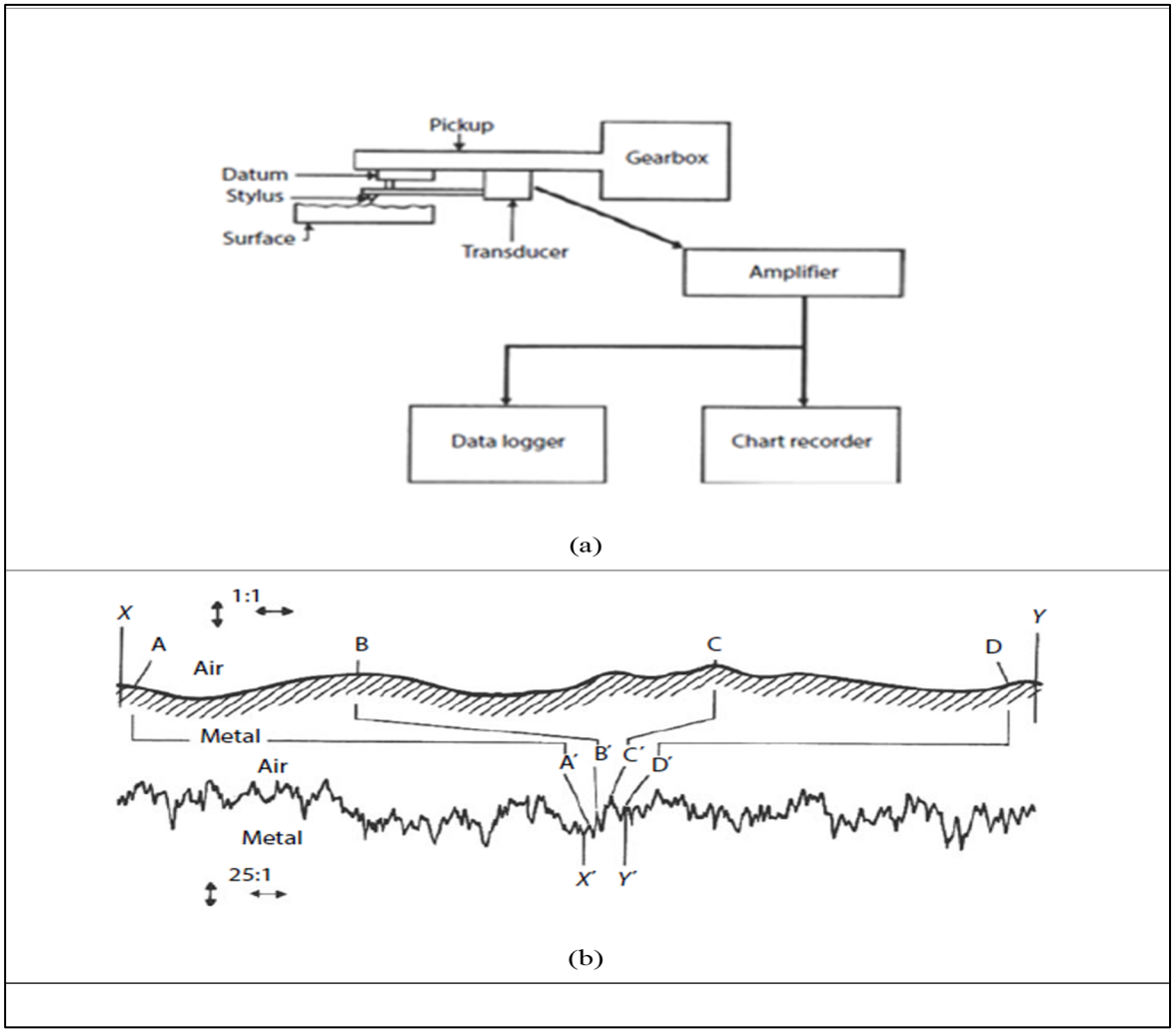

Figure 1.8 Schematic illustration of a profilometer (a), and typical unamplified and amplified surface profile traces (b)

Taken from Stephenson and Agapiou (2018)

Numerous parameters have been suggested to describe surface roughness. However, national, and international standards have established a set of commonly used parameters and standard measurement techniques, which are widely interchangeable. These standard roughness parameters include the average roughness (Ra), maximum peak height (Rp), maximum valley depth (Rv), peak to valley height (Rt), average maximum profile height (Rz), and maximum roughness depth (Rmax).

To define parameters Ra, Rv, Rp, and Rt, the centerline of a filtered stylus trace is used as a reference point, as shown in Figure 1.9. Before determining the centerline, filtering is performed to remove any slope or fluctuations present in the trace. Afterward, the centerline is established as the mean line of the surface profile.

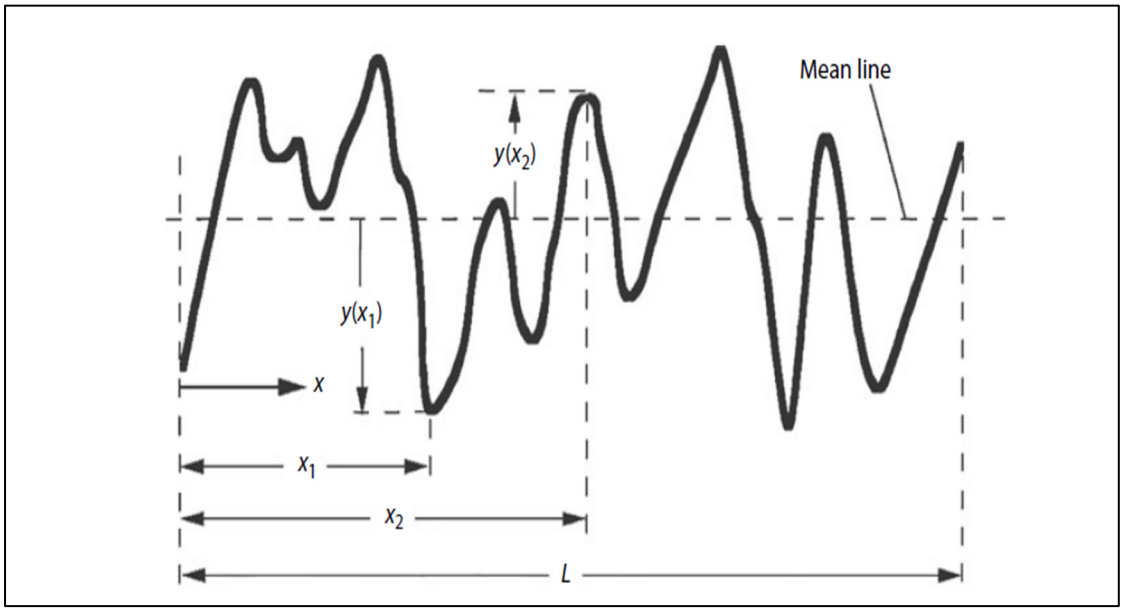

Figure 1.9 Profile parameters used to compute the roughness parameters Ra, Rp, Rv, and Rt
Taken from Stephenson and Agapiou (2018)

The profile parameters are defined and calculated as follows.

Ra is the arithmetic average of the absolute values of the deviations of the stylus trace from the centerline within the evaluation length and is calculated using Equation 1. 6.

$$R_a = \frac{1}{L}\int_0^L |y(x)|\, dx \tag{1.6}$$

Rp is the distance from the highest peak of the surface profile to the centerline within the evaluation length.

$$R_p = \text{Max } y(x),\ 0 < x < L \tag{1.7}$$

Rv, the maximum depth of valley below the centerline, is defined as Equation 1.8.

$$R_v = |Miny(x)|, 0 < x < L \tag{1.8}$$

Rt is the distance between the highest peak and deepest valley within the evaluation length.

$$Rt = Rp + Rv \tag{1.9}$$

Equations 1.10 and 1.11 define the average maximum profile height R_z and maximum roughness depth R_{max} (as shown in Figure 1.10) as the mean and maximum values of the profile heights, respectively, taken over five consecutive sampling intervals.

$$Rz = \frac{1}{5}\sum_{i=1}^{5} R_{zi} \tag{1.10}$$

$$Rmax = max\ (Rzi) \tag{1.11}$$

R_q or RMS (Root Mean Square) indicates the standard deviation of the surface height distribution which is a significant statistical measure for describing surface roughness. Compared to the arithmetic average height (R_a), RMS is more responsive to significant deviations from the mean line. R_q is calculated with the help of Equation 1.12 as shown below:

$$\sqrt{\frac{1}{l}\int_0^l \{y(x)\}^2 dx} \tag{1.12}$$

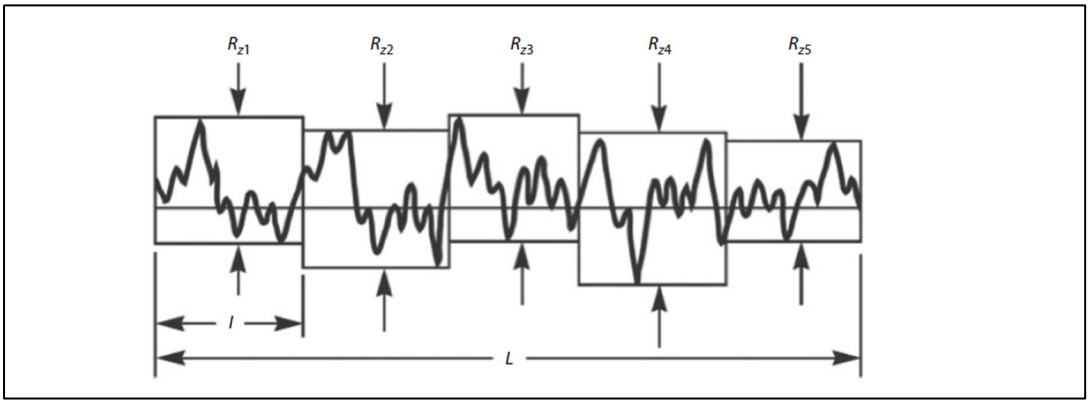

Figure 1.10 The profile heights over five successive sampling intervals
Taken from Stephenson and Agapiou (2018)

Surface roughness is an important quality characteristic in the machining of aluminum alloys. Achieving the desired surface finish is crucial in ensuring the functionality and performance of the machined component. However, the low thermal conductivity and high ductility of aluminum alloys can make achieving a smooth surface finish challenging.

Various machining parameters, such as cutting speed, feed rate, and depth of cut, can affect surface roughness in the machining of aluminum alloys. Therefore, it is essential to carefully select and optimize these parameters to achieve the desired surface finish.

1.3.4.3 Particle emission

Despite providing significant benefits to humans, the modern industry also has negative impacts on natural environments and human health.

Machining of aluminum alloys generates aerosols and metallic particles that are dangerous to the health of operators and the environment. Furthermore, machine-tool parts can be damaged by these particles. Metal particles can lead to severe pulmonary disease, especially when their aerodynamic diameters of these particles are less than 2.5 μm (PM 2.5). Such particles can penetrate into the alveoli and deepest parts of the lungs, leading to various health problems like asthma, respiratory diseases, and different types of cancer (Khettabi, Songmene et al. 2010).

Measurements of air quality are often conducted in a location far from the cutting area. However, this approach is not suitable for determining emissivity because it requires testing large volumes of air, increases testing time, and lowers dust concentration. When examining dust emissions in a laboratory situation, it is essential to consider the following points (Khettabi, Songmene and Masounave 2007):

1. In the environment, separated particles move randomly (Brownian motion, atmospheric composition, turbulence caused by machine-tool motion and ventilation).
2. Due to the chaotic motion of the air, the particles do not easily spread in the air.
3. Different sources of emission are present during machining operations, including multiple zones of emission with varying quantities of particle emission, depending on the process type and stability.

The largest amount of particles is generated in three main zones. As shown in Figure 1.11, the cutting force and heat cause plastic deformation of materials in the first deformation zone labeled I and, as a result, friction occurs between the tool and workpiece materials. Metal dust particles are formed when the energy level reaches the activation energy needed to release metallic micro-particles from the two materials. Thus, in the deformation zone II, in addition to compressive deformation, friction occurs between chips and rake faces, leading to dust generation. Finally, Zone III also generates dust due to the friction between the flank face of the tool and the machined surface of the workpiece (Cheng, Liu et al. 2014).

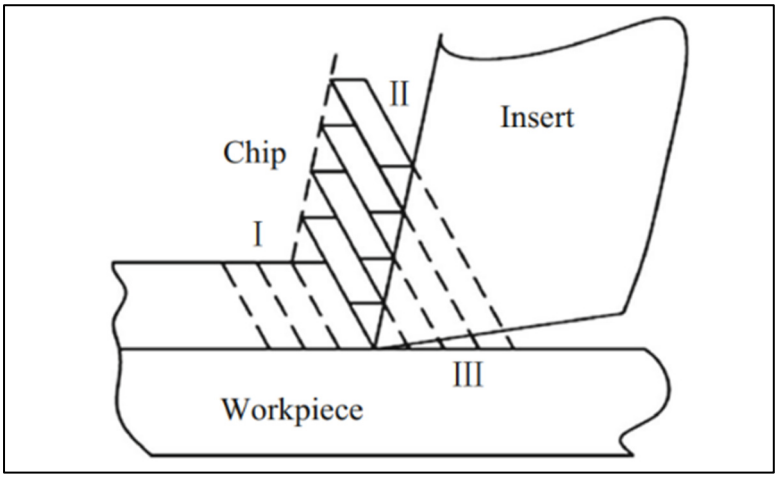

Figure 1.11 Schematic of the chip formation process
Taken from Cheng, Liu et al. (2014)

A variety of phenomena cause the formation of fine particles during the cutting process, among them macroscopic and microscopic friction, plastic deformation, and chip formation. Brittle materials produce chips through brittle fracture, resulting in a minimal contact length between the chip and the tool. In contact with the tool material, the irregular chip surface can release particles from its internal surface. Particle size is affected by several factors, including the tool's rake face, cutting conditions, and workpiece material. Furthermore, during the cutting process, the temperature can influence the mechanical properties of the material, the mode of chip formation, and the emission of particles (Khettabi, Songmene et al. 2010).

1.3.5 Cooling mode in machining

Cooling during the machining process is crucial in maintaining the cutting tool's performance and prolonging its life. The cooling methods used during the machining process can be classified into three main categories: dry machining, flood cooling, and minimum quantity lubrication (MQL).

In dry machining, no cutting fluid is used, and the machining is carried out in a dry environment.

In flood cooling, a large amount of cutting fluid is sprayed onto the cutting zone, whereas in MQL, a small amount of cutting fluid is supplied to the cutting zone in the form of a mist or

spray (Yoshimura, Moriwaki et al. 2006). The cooling mode used during the machining process affects the cutting performance, tool wear, and surface integrity of the machined part.

Dry machining can result in high temperatures at the cutting zone, leading to tool wear and poor surface quality.

Flood cooling can reduce the cutting temperature and improve the surface quality, but it can also lead to poor chip evacuation and reduced tool life.

The MQL method offers a balance between the two, providing adequate cooling while minimizing the amount of cutting fluid used, resulting in better surface quality and longer tool life (Ye, Wang and Yu 2022).

1.3.6 Cutting fluids

The use of cutting fluids is essential to many metal cutting operations. Cutting fluids provide lubrication, cooling, and chip clearing capabilities, allowing for increased cutting speeds and feed rates, and improving chip formation, tool life, surface finish, and dimensional accuracy. Additionally, they prevent built-up edge and part rust in most cases (Stephenson and Agapiou 2018).

1.3.6.1 Classification of cutting fluids

The industry does not have a standard classification system for cutting fluids.

The following categories can be considered as one of the most popular list of classifications (Sales, Diniz and Machado 2001).

I. Air

II. Water based cutting fluids

- water
- emulsions (soluble oil)
- chemical solutions (or synthetic fluids)

III. Neat oils

- mineral oils
- fatty oils
- composed oils
- pressure oils (EP)
- multiple use oils

1.3.7 Machining of aluminum

Machining ductile materials like aluminum, generates large chip-tool contact areas and high chip thickness ratios, leading to higher cutting forces, greater power consumption and heat generation, and producing long chips and poor surface finish of the machined part.

On the other hand, the low shear strength of aluminum makes it relatively easy to machine. While thermal or mechanical treatments and the addition of certain chemical elements can improve the hardness and strength of aluminum alloys, they also increase the force required for machining. However, this increase in force can be compensated by reducing the chip-tool contact area (Santos, Machado et al. 2016, Wieroński, Pezda and Ponikwia 2016).

The input variables include different heat treatments, material composition manipulations, and machining parameters such as cutting speed, feed rate, depth of cut, and cooling mode have effect on the machinability. Hence, it is imperative to investigate the impact of these factors on the machining process. Demir and Gündüz (Demir and Gündüz 2009) have shown in their study that the effect of heat treatment of Al 6061 alloy on cutting force is not prominent at higher cutting speeds; in contrast, at lower cutting speeds, the cutting forces of softer work-pieces during machining are lower compared to other materials.

Regarding the influence of cutting speed on cutting force, it is generally observed that the cutting forces decrease across all workpieces as the cutting speed increases. This decrease in cutting forces can be due to two factors: first, a reduction in the tool-chip contact area, and second, a decrease in the shear strength of the material due to an increase in the temperature of the cutting zone, as displayed in Figures 1.12 and 1.13.

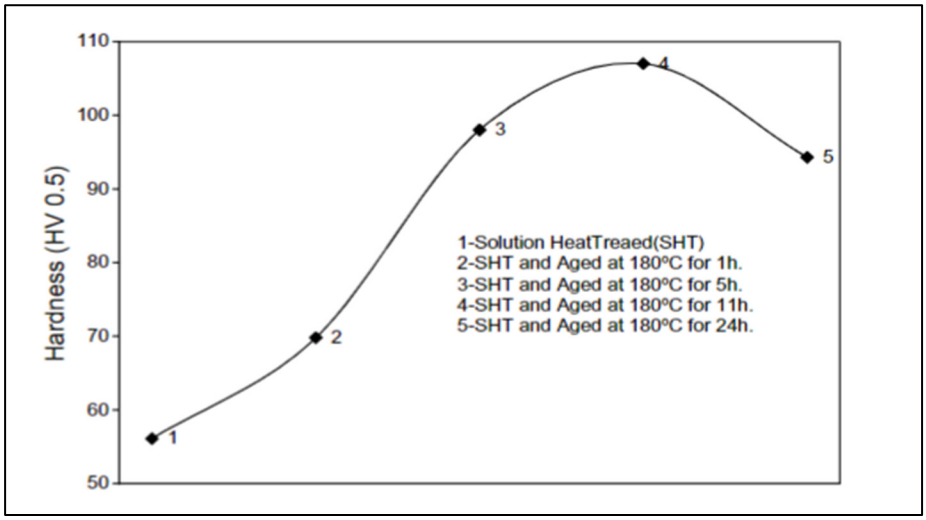

Figure 1.12 Hardness values of Al 6061 alloy following different heat treatments

Taken from Demir and Gündüz (2009)

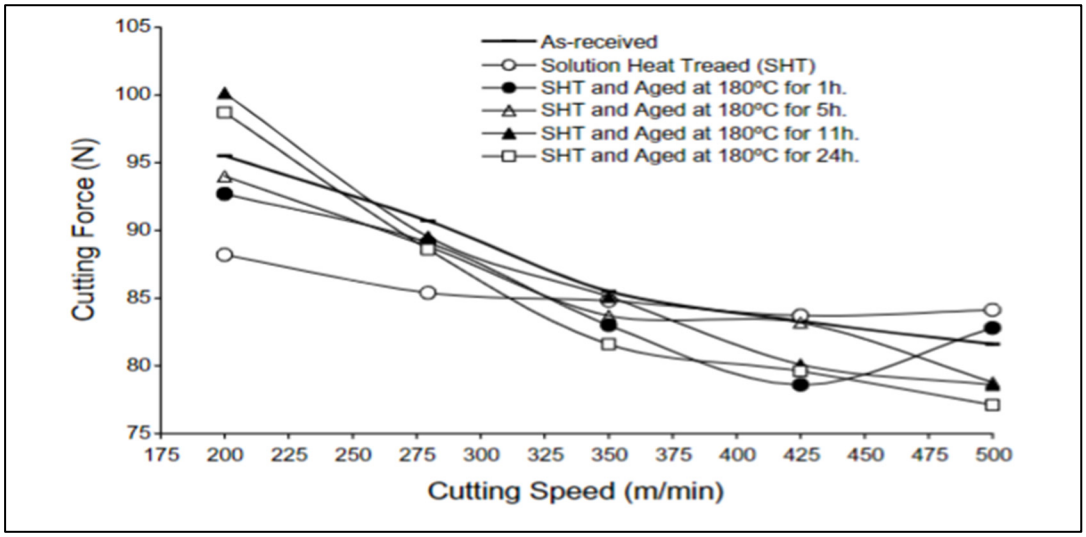

Figure 1.13 The effect of heat treatment conditions and cutting speeds on cutting force

Taken from Demir and Gündüz (2009)

Another investigation was conducted by Zagórski and Warda (Zagórski and Warda 2018) to analyze the impact of cutting speed, feed rate on the surface roughness of heat-treated aluminum alloys Al 2024, Al 7075, and Al 6082. Their findings indicated that the surface roughness exhibited no significant variations among the three alloys. Furthermore, at the same feed rate, the influence of cutting speed was negligible. According to this study, it is evident that the feed

rate has a crucial effect on surface roughness. Figures 11.14 and 11.15 show the reaction of surface roughness to feed rate and cutting speed (Zagórski and Warda 2018)

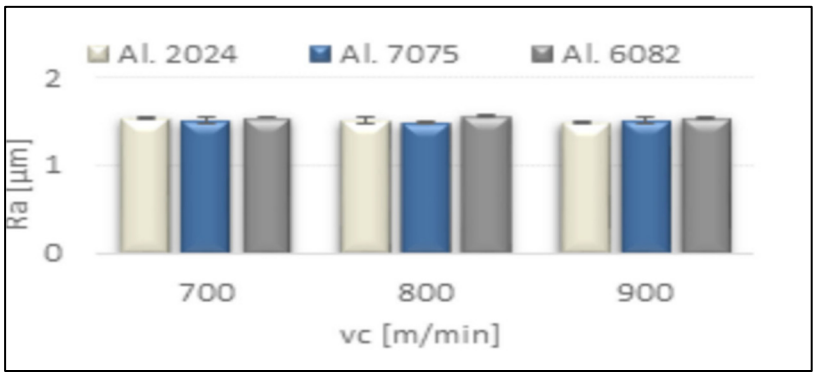

Figure 1.14 The effect of change in cutting speed on surface roughness at constant feed rate Taken from Zagórski and Warda (2018)

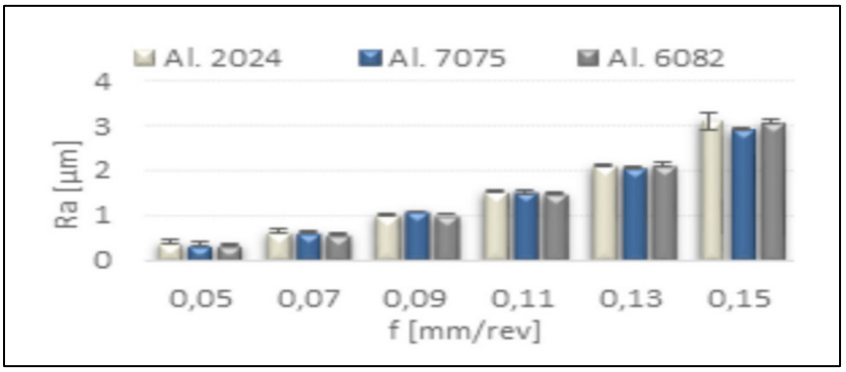

Figure 1.15 The effect of change in feed rate on surface roughness at constant cutting speed Taken from Zagórski and Warda (2018)

1.3.7.1 Machining of aluminum 7000 series alloys

Aluminum 7000 series alloys are widely used in various aerospace and automotive applications due to their high strength-to-weight ratio, excellent fatigue properties, and good corrosion resistance. However, these alloys are known to have poor machinability characteristics, which make the machining process challenging and time-consuming.

In recent years, there has been a growing interest in the development of new machining strategies and cutting tools to improve the machinability of aluminum 7000 series alloys. One of

the key factors that influence the machinability of these alloys is the presence of intermetallic particles, such as Fe-rich particles, which are known to cause tool wear and surface defects during the machining process. (Ping, Xiujie et al. 2021) conducted experiments to evaluate the effects of cutting parameters on tool wear and surface roughness in the milling of Al 7050 alloy. The results showed that higher cutting speeds and lower feed rates led to lower tool wear and a better surface finish.

Another approach to improve the machinability of the 7000 series alloys is to use advanced cutting tools, such as coated carbide, ceramic, and diamond tools, which have better wear resistance and can withstand high temperatures and cutting forces.

The choice of a cutting tool and its influence on the machining process carries substantial significance. (Kumar, Pattnaik et al. 2019) evaluated the performance of diamond-coated and uncoated carbide tools in the milling of Al 7050 alloy. The results showed that the diamond-coated tool had lower tool wear and produced a better surface finish than the uncoated carbide tool.

In addition to conventional machining processes, such as milling and turning, some researchers have investigated the use of advanced machining techniques, such as laser machining and electrochemical machining, for machining of aluminum 7000 series alloys. For example, (Yilbas, Khan et al. 2010) studied the effects of laser power and scanning speed on the surface quality and microstructure of laser-machined aluminum 7050 alloy. The results showed that higher laser power and slower scanning speed led to better surface quality and a finer microstructure.

1.3.7.1.1 Machining of aluminum 7075 alloy

Aluminum 7075 is a popular aluminum alloy that is widely used in the aerospace and defence industries because of its outstanding mechanical properties. It has a high strength-to-weight ratio, good fatigue resistance, and excellent corrosion resistance.

Machining is a common process used to shape an aluminum 7075 part into its final form. However, due to its high strength and low thermal conductivity, the machining process can be challenging. This is because it can cause tool wear, built-up edge formation, and rough surface finishes. Therefore, understanding the machinability of aluminum 7075 is essential to optimize the machining process and improve the final quality of the product.

Numerous researchers (Bhushan, Kumar and Das 2010, Kaya, Uçar et al. 2012, Yeganefar, Niknam and Songmene 2019, Luo, Wang and Zhang 2020, Magabe and Gupta 2023) have explored the influence of diverse cutting parameters, heat treatments, and cooling modes on machinability criteria in the context of machining aluminum 7075 series alloys. (Verma and Saha 2023) conducted experiments to evaluate the effects of cutting parameters on tool wear and surface roughness of aluminum 7075-T6 alloy when subjected to turning.

The results showed that higher cutting speeds and lower feed rates led to lower tool wear and better surface finish.

To enhance the machinability of aluminum 7075 series alloys, the use of advanced cutting tools, including coated carbide, ceramic, and diamond tools, which offer higher wear resistance and can endure high temperatures and cutting forces, is suggested. For example, (Aslantas, Hascelik and Çiçek 2022) evaluated the performance of diamond-coated and uncoated carbide tools in milling of aluminum 7075 alloy.

The results showed that the diamond-coated tool had lower tool wear and better surface finish than the uncoated carbide tool.

The machinability of Al 7075 can be significantly affected by different heat treatments, primarily because of its hardness variation. The hardness of the material affects the cutting forces required to machine it, and as a result, different heat treatments can lead to different machinability characteristics.

Typically, aged, and hardened aluminum alloys require greater cutting forces during machining. However, there are instances where this trend is not true. For example, in a study conducted by (Kaya, Uçar et al. 2012), it was observed that the cutting force required to machine aged Al 7075 was lower compared to the non-aged alloy. This phenomenon could be attributed to the increased brittleness of the hardened material, resulting in decreased sticking properties and reduced built-up edge (BUE) formation. These factors together lead to reduced cutting forces during machining. Furthermore, this study demonstrated that precipitation hardening had a positive effect on the surface quality of the 7075 alloy.
They found that aged alloys had lower surface roughness compared to non-aged alloys.
This improvement in surface quality would result from the reduced BUE formation, which is a common cause of surface roughness during machining.

The use of cutting fluid during the machining of Aluminum 7075 has its advantages and disadvantages. While the use of lubrication can improve part quality and reduce cutting forces, its effectiveness decreases at high cutting speeds. At very high cutting speeds, the heat generated during machining is efficiently evacuated by the chip, making the use of cutting fluid less effective. Additionally, increasing the flow rate of the cutting fluid can lead to higher dust emissions in terms of particle emissions.

Therefore, the use of cutting fluid during the machining of Al 7075 should be carefully evaluated to balance its advantages and disadvantages, particularly at high cutting speeds where its effectiveness may be reduced (Khettabi, Nouioua et al. 2017).

1.4 Conclusion

This chapter aimed to discuss the properties of aluminum alloys that make them widely applicable in the industry. The focus was on exploring the aspects and methods by which aluminum properties are enhanced, such as alloying and heat treatment.

One key indicator of aluminum's mechanical properties was hardness. While higher hardness generally signified better mechanical properties, it was essential to consider how variations in mechanical properties affected material machinability, a factor that required in-depth study.

In the second part of the chapter, concepts of machining and machinability were discussed, with an emphasis on roughness, cutting force, and dust emissions. In addition to introducing these machinability criteria, the methods and procedures for measurement and data acquisition were reviewed and discussed.

Lastly, research and studies related to aluminum, particularly aluminum 7075 machinability, were reviewed. Generally, highlighted insights from the reviewed aluminum machinability studies suggested that, despite aluminum's low shear strengths making it easy to machine, machinability relatively decreased in hardened cases.

In terms of the effect of cutting parameters on the machinability of aluminum alloys, the rate showed a significant impact on surface roughness and cutting force. A higher feed rate led to a significant increase in both surface roughness and cutting force. Although a higher cutting speed generally resulted in lower cutting force requirements for aluminum machining, it did not show a significant effect on surface roughness.

The use of cutting fluid during the machining of Aluminum 7075 had both advantages and disadvantages. While lubrication could improve part quality and reduce cutting forces, its effectiveness decreased at high cutting speed.

CHAPTER 2

METHODOLOGY

2.1 Introduction

The objective of this chapter is to describe and explain the methodology and experimental procedures that were employed in this research. The research study employed a multi-level full factorial design to investigate the machinability of three distinct compositions of Al 7075, each subjected to two separate heat treatments. This involved conducting six distinct heat treatments on three different alloys and measuring their respective micro-hardness values. From these experiments, the two heat treatments resulting in the highest and lowest micro-hardness values were then selected to investigate their effect on the machinability of the specific aluminum 7075 alloy workpiece. Machining experiments were conducted to investigate the impacts of the selected heat treatments, the addition of Sc and Sc+Li to the base Al 7075 alloy, and machining parameters (cutting speed, feed rate) on the machinability. These experiments involved measuring various machinability criteria, including cutting forces, surface roughness, and particle emission. The data obtained from these experiments were statistically analyzed to determine the optimal heat treatment and cutting parameters for improving the machinability of the aluminum 7075 alloy workpiece investigated.

2.2 Experimental procedures

The methodology of this study involves the use of a multi-level full factorial design of experiment. The study aims to investigate the effect of various factors on the machining of three Al 7075 alloys, namely, Al 7075, Al 7075-Sc, and Al 7075-Li -Sc. The alloys were subjected to solution heat treatment at 8h @ 47°C, followed by two distinct aging heat treatments at 8h @ 280°C and 24h @ 120°C, respectively. The experiments were conducted under dry and wet milling conditions.

Table 2.1 shows the machining experimental factors and their corresponding levels. Workpiece materials and cooling mode were treated as qualitative factors, while the remaining factors were considered quantitative.

Table 2.1 Experimental variables and their levels

Experimental variables	Level 1	Level 2	Level 3
Cutting speed (m/min)	200	400	600
Feed per tooth (mm/z)	0.05	0.1	0.15
Cooling mode	Dry	-	Wet
Material	Al 7075	Al 7075-Sc	Al 7075-Li-Sc
Heat treatment	8h @ 280 °C	-	24h @ 120

The study investigated 12 different conditions. These conditions were obtained by using a Cartesian multiplication of three distinct variables, namely, material, heat treatments, and dry or wet conditions, resulting in $3 \times 2 \times 2 = 12$ unique combinations. For each of 12 conditions, nine tool paths were implemented, determined by varying the cutting speed and feed rate parameters, resulting in 3 x 3 = 9 unique tool paths for each condition shown in Figure 2.1.

Therefore, a total of 108 experiments were conducted. Table 2.2 provides the test parameters for the nine tool paths which were repeated for each of the 12 conditions.

The cutting speed and feed rate were determined based on the values recommended by the tool manufacturer as displayed in Figure 2.2, where the acronym SFM stands for Surface Feet per Minute.

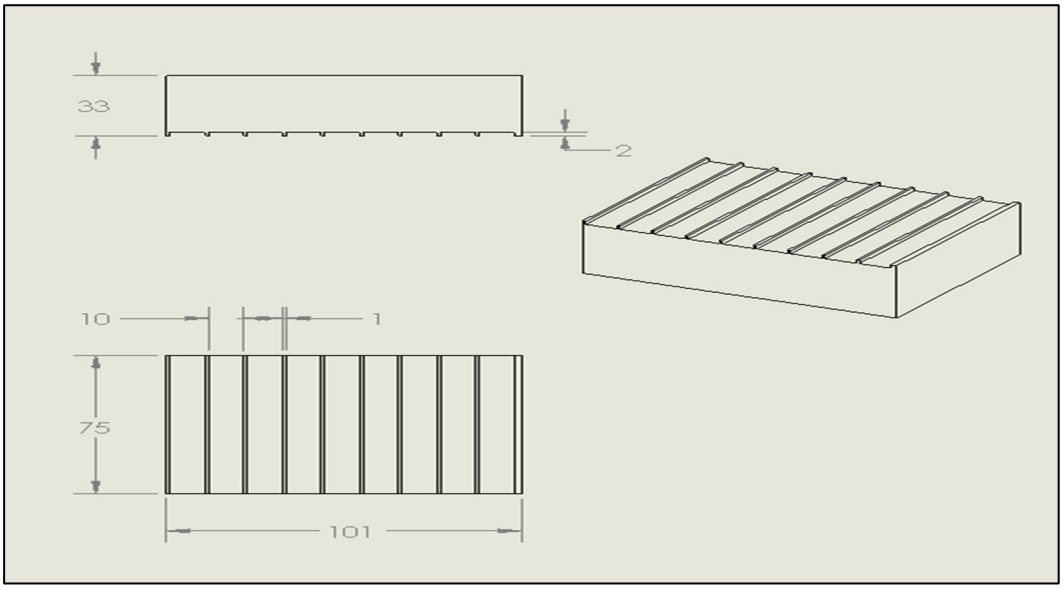

Figure 2.1 The tests layout during the experiments

Table 2.2 Cutting Parameters of Each Condition

Test (Tool Path)	Cutting speed (m/min)	Rotating Speed (rpm)	Feed rate (mm/tooth)	Feed rate (mm/second)	Cutting time (seconds)
1	200	6369	0.05	15.9	4.71
2	400	12739	0.05	31.8	2.36
3	600	19107	0.05	47.8	1.57
4	200	6369	0.1	31.8	2.36
5	400	12739	0.1	63.7	1.18
6	600	19107	0.1	95.5	0.79
7	200	6369	0.15	47.8	1.57
8	400	12739	0.15	95.5	0.79
9	600	19107	0.15	143.3	0.52

The recommended feed rates based on the cutting speed range are shown in the Table 2.3.

Table 2.3 Feed rates based on the cutting speed range

Cutting speed (m/min)	Feed rate (mm/tooth)
850 – 1400 SFM = 259 – 426 m/min	0.0762
1700 – 2000 SFM = 518 – 609 m/min	0.1524

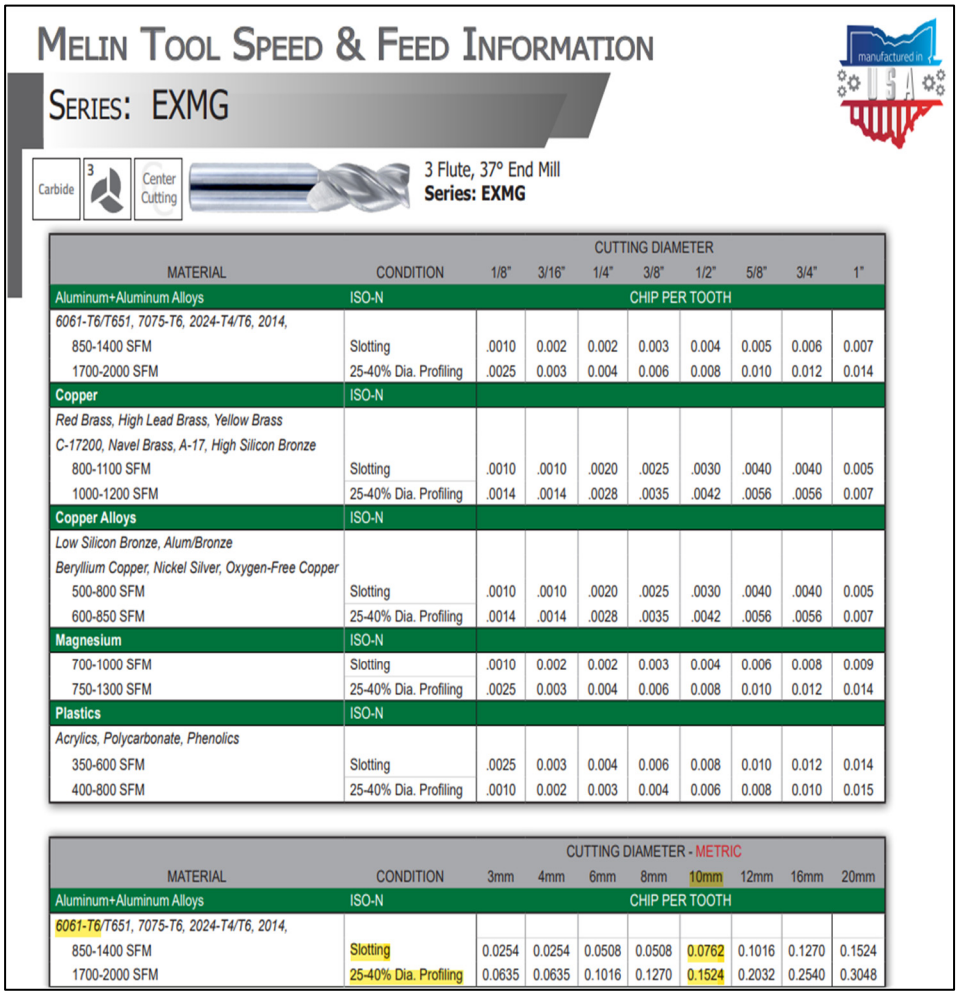

MELIN TOOL SPEED & FEED INFORMATION

SERIES: EXMG

Carbide | 3 | Center Cutting

3 Flute, 37° End Mill
Series: EXMG

MATERIAL	CONDITION	CUTTING DIAMETER 1/8"	3/16"	1/4"	3/8"	1/2"	5/8"	3/4"	1"
Aluminum+Aluminum Alloys	ISO-N	CHIP PER TOOTH							
6061-T6/T651, 7075-T6, 2024-T4/T6, 2014,									
850-1400 SFM	Slotting	.0010	0.002	0.002	0.003	0.004	0.005	0.006	0.007
1700-2000 SFM	25-40% Dia. Profiling	.0025	0.003	0.004	0.006	0.008	0.010	0.012	0.014
Copper	ISO-N								
Red Brass, High Lead Brass, Yellow Brass									
C-17200, Navel Brass, A-17, High Silicon Bronze									
800-1100 SFM	Slotting	.0010	.0010	.0020	.0025	.0030	.0040	.0040	0.005
1000-1200 SFM	25-40% Dia. Profiling	.0014	.0014	.0028	.0035	.0042	.0056	.0056	0.007
Copper Alloys	ISO-N								
Low Silicon Bronze, Alum/Bronze									
Beryllium Copper, Nickel Silver, Oxygen-Free Copper									
500-800 SFM	Slotting	.0010	.0010	.0020	.0025	.0030	.0040	.0040	0.005
600-850 SFM	25-40% Dia. Profiling	.0014	.0014	.0028	.0035	.0042	.0056	.0056	0.007
Magnesium	ISO-N								
700-1000 SFM	Slotting	.0010	0.002	0.002	0.003	0.004	0.006	0.008	0.009
750-1300 SFM	25-40% Dia. Profiling	.0025	0.003	0.004	0.006	0.008	0.010	0.012	0.014
Plastics	ISO-N								
Acrylics, Polycarbonate, Phenolics									
350-600 SFM	Slotting	.0025	0.003	0.004	0.006	0.008	0.010	0.012	0.014
400-800 SFM	25-40% Dia. Profiling	.0010	0.002	0.003	0.004	0.006	0.008	0.010	0.015

MATERIAL	CONDITION	CUTTING DIAMETER - METRIC 3mm	4mm	6mm	8mm	10mm	12mm	16mm	20mm
Aluminum+Aluminum Alloys	ISO-N	CHIP PER TOOTH							
6061-T6/T651, 7075-T6, 2024-T4/T6, 2014,									
850-1400 SFM	Slotting	0.0254	0.0254	0.0508	0.0508	0.0762	0.1016	0.1270	0.1524
1700-2000 SFM	25-40% Dia. Profiling	0.0635	0.0635	0.1016	0.1270	0.1524	0.2032	0.2540	0.3048

Figure 2.2 Cutting speed and feed rate recommended by the tool manufacturer (taken from the manufacturer's catalog)

2.3 Workpiece material

For the conducted experimentation, a pair of commercial Al7075 plates, measuring 160×75×16, were employed. Additionally, two Al7075-Sc blocks and two Al 7075-Li-Sc blocks, each measuring 101×75×33, were utilized.

The material composition of the workpieces is presented in Table 2.4. To ensure standardized testing conditions, the machining process was executed in a unidirectional manner along a path length of 75 mm. This approach ensured that all toolpaths were consistently maintained at a uniform length of 75 mm.

Table 2.4 Chemical composition (wt%) of Al 7075 workpiece materials

Elements	Si	Mg	Cr	Mn	Fe	Cu	Zn	Ni	Ti	V	Li	Sc
Al 7075	0.21	2.15	0.19	0.035	0.16	1.45	5.62	-	0.027	-	-	-
Al7075-Sc	0.11	2.8	0.16	<.003	0.053	1.5	6.6	0.003	0.094	0.006	0.060	0.11
Al 7075-Li-Sc	0.16	2.2	0.14	<.003	0.099	1.3	6.5	0.003	0.080	0.007	2.2	0.12

2.4 Sample preparation and heat treatment

In the characterization phase of the study, the aim was to perform a comparative analysis of six distinct heat treatments, as outlined in Table 2.5, regarding their respective hardness outcomes.

Table 2.5 Applied heat treatment process

Number	Solution heat treatment	Quenching	Artificial aging
1	(8h @ 470°C)	Quenched at the water at room temper-ature	None
2			Single aging (24h @ 120°C)
3			Single aging (8h @ 280°C)
4			Double aging (24h @ 120°C + 8h @ 180°C)
5			Double aging (8h @ 180°C + 24h @ 120°C)
6			Double aging (8h @ 280°C + 24h @ 120°C)

The primary objective was to determine which heat treatments provided the maximum and minimum microhardness values. To accomplish this, first, a tabletop manual cut-off machine (Struers Labotom-5) shown in Figure 2.3a, was used to prepare six samples with a size of 10×10 ×15mm. After sample preparation, solution heat treatment was conducted on these samples at a temperature of 470°C for a duration of 8 hours, which was then immediately followed by quenching in water at room temperature. Subsequently, artificial aging of five samples of each material was carried out at distinct temperatures and for varying times, as detailed in Table 2.5. The furnace employed for the solution heat treatment and aging is displayed in Figure 2.3b.

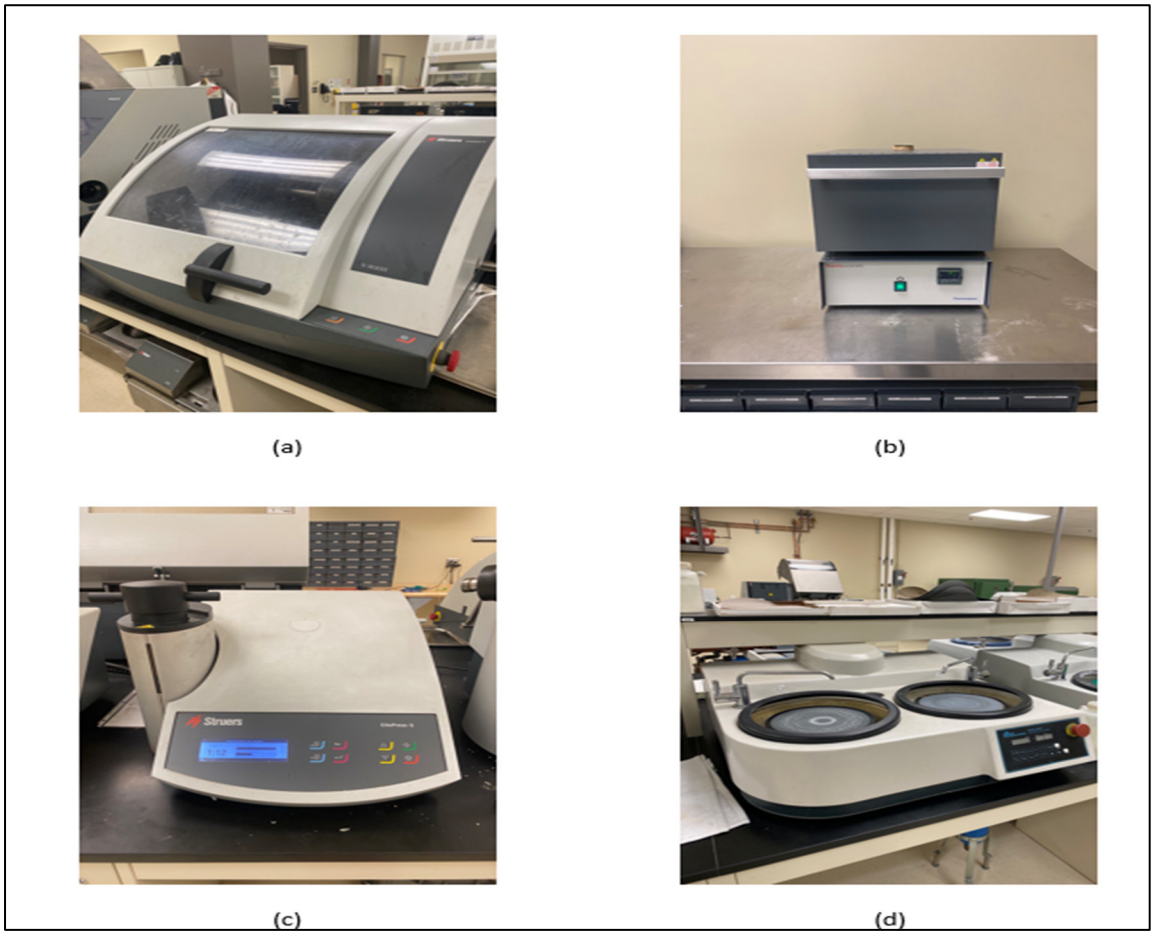

Figure 2.3 Equipements used for preparing heat treatment samples: (a) Struers Labotom-5 manual cutter, (b) Thermo Fisher Scientific F48015-60 furnace, (c) Struers CitoPress-5 automatic mounting press, and (d) Pace Technologies Nano 2000T grinder – polisher

Following heat treatment, the samples were mounted using an automatic mounting press (Struers CitoPress-5), as shown in Figure 2.3, c. The mounted samples were then subjected to grinding (sanding) using Silicon Carbide Waterproof papers. The order of grit sizes was 120/P120, 240/P280, 320/P400, 400/P800, and 600/P1200. The Pace Technologies Nano 2000T grinder – polisher shown in Figure 2.3d was used for polishing. Subsequently, 3 µm and 1µm diamond suspension monocrystalline Met Lab Corporation were utilized to polish the samples, followed by a finishing step using 0.06 µm Colloidal Silica Blue (10 pH) Met Lab Corporation.

2.5 Microhardness measurement

A Future-Tech FM-1 micro-hardness tester (Figure 2.4) was used to measure the microhardness of the samples.

Figure 2.4 Future-Tech FM-1 microhardness tester

In this machine, based on the measured sample material, the load (force) is adjusted from 10 grams to 1 kilogram.

A load of 100 grams (0.9807 N) was applied to all samples during the measurement. Each sample was measured at ten different points and the average was calculated as the final microhardness value for that sample.

A quadrangular depression (indentation) remains on the sample surface after running the device. By inserting the average value of the diagonals of this quadrilateral in Equation 2.1, the hardness of the sample at that point is obtained.

$$HV = 0.1891 \frac{F}{d^2} \tag{2.1}$$

Where F is the force (in N), and d is the average value of the diagonals (in mm).

2.6 Machining process

In total 108 experimental tests were conducted in the context of dry and wet milling, utilizing a 3-axis CNC machine tool featuring the following specifications: Power output of 50 kW, rotational speed of 28000 rpm, and torque of 50 Nm. The CNC machine is illustrated in Figure 2.5.

Milling was performed using uncoated carbide end milling cutting tools with a three-flute design (with z = 3) and a 10 mm diameter.

Figure 2.6 illustrates the specific details of the cutting tool employed in the experiment.

To ensure uniformity in the test conditions, the tools were systematically altered for every nine toolpaths, leading to the utilization of a total of twelve distinct tools throughout the experimental procedure.

Figure 2.5 Three-axis CNC HURON K2X10 machine tool
Taken from Slamani, Gauthier and Chatelain (2016)

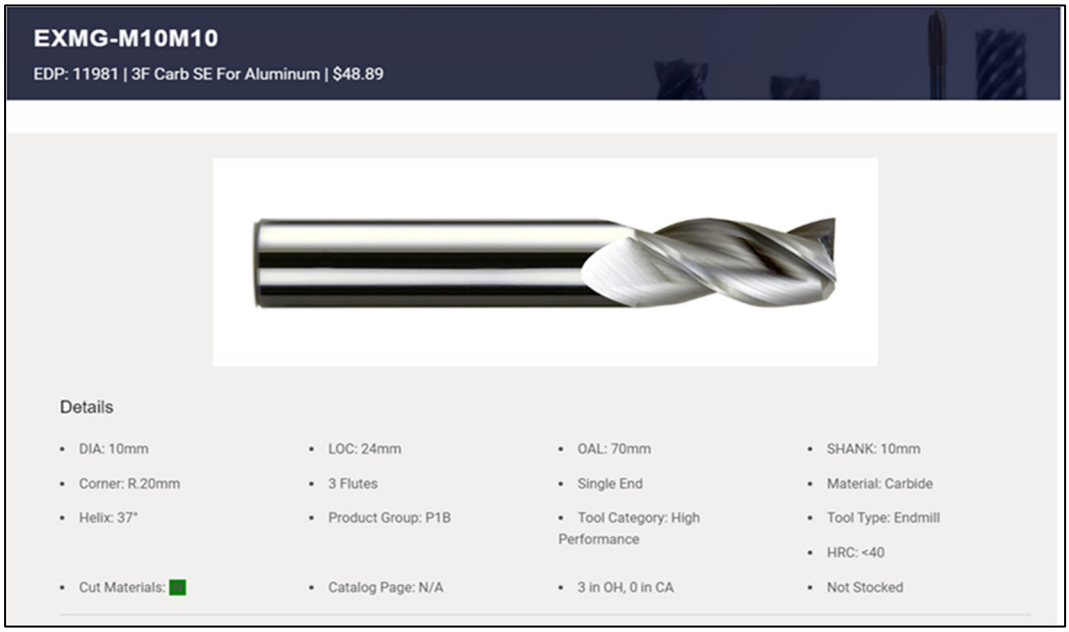

Figure 2.6 Cutting tool specifications (taken from a manufacturer's catalog)

2.7 Cutting force measurement

Cutting force is a critical parameter in many machining operations. Cutting force influences several important aspects of the machining process, such as tool wear, surface finish, and dimensional accuracy. Furthermore, understanding the relationship between cutting force and other process parameters, such as cutting speed and feed rate, can be useful to optimize the machining process. Therefore, for optimizing the machining process, it is crucial to accurately measure and control the cutting force.

In this investigation, the measurement of the three cutting force components (Fx, Fy, and Fz), was carried out during the machining process utilizing a 3-axis dynamometer (Kistler, model 9255-B), which was mounted in the milling machine. A sampling frequency of 12 kHz was used to acquire the cutting force signals. In the cutting plane, the Kistler 9255B three-axis dynamometer (see Figure 2.7) can measure forces ranging from -20 KN to 200 KN, and in the vertical plane, it can measure forces from -10 KN to 40 KN.

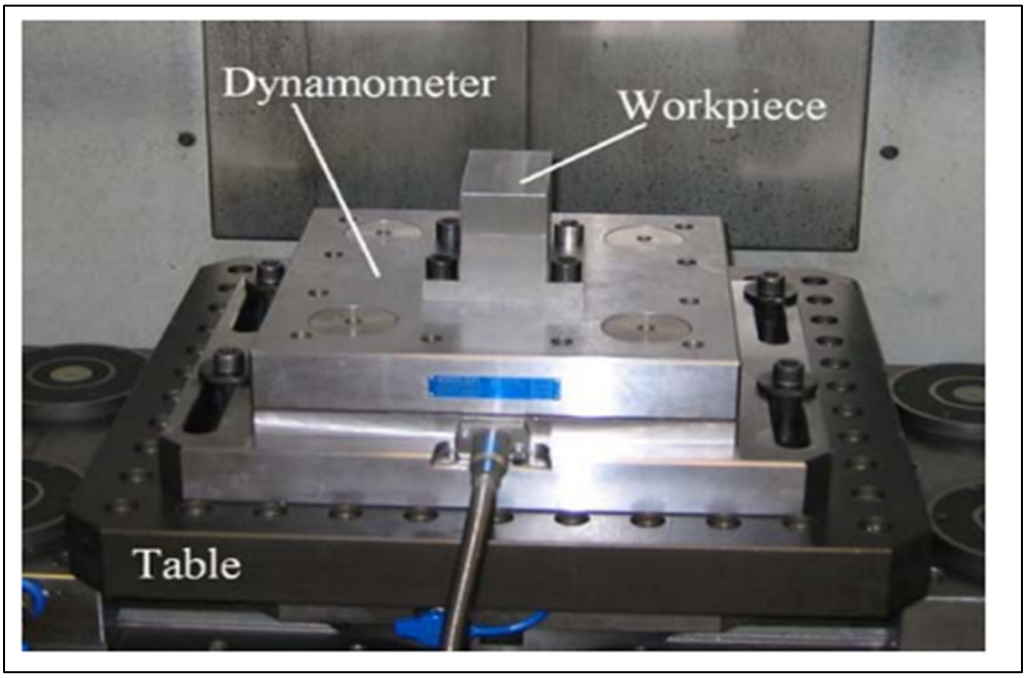

Figure 2.7 Workpiece mounted on the Kistler 9255B three-axis dynamometer
Taken from Rivière-Lorphèvre and Filippi (2009)

2.8 Surface roughness measurement

Surface roughness measurement is an essential process for ensuring the quality and performance of manufactured parts. Because of this, it is considered one of the most important machinability criteria. In this study, the Mitutoyo SJ-410 surface roughness tester shown in Figure 2.8 was used to measure the surface roughness of the machined surfaces. The SJ-410 uses a stylus tip to traverse the surface of the sample, measuring the height variations and producing a numerical representation of the surface roughness. To ensure accurate readings, the device was first calibrated using a standard reference sample. The sample surface was cleaned to remove any pollutants that could affect the measurements. Then the stylus was positioned at a starting point on the sample, and the traverse length and speed were set according to the sample specifications. Multiple roughness parameters, including Ra, Rz, and Rq, were measured and recorded for each sample. Each toolpath was measured in three sections (first, middle, and end) and the average of the three measurements was taken as the final roughness of that sample.

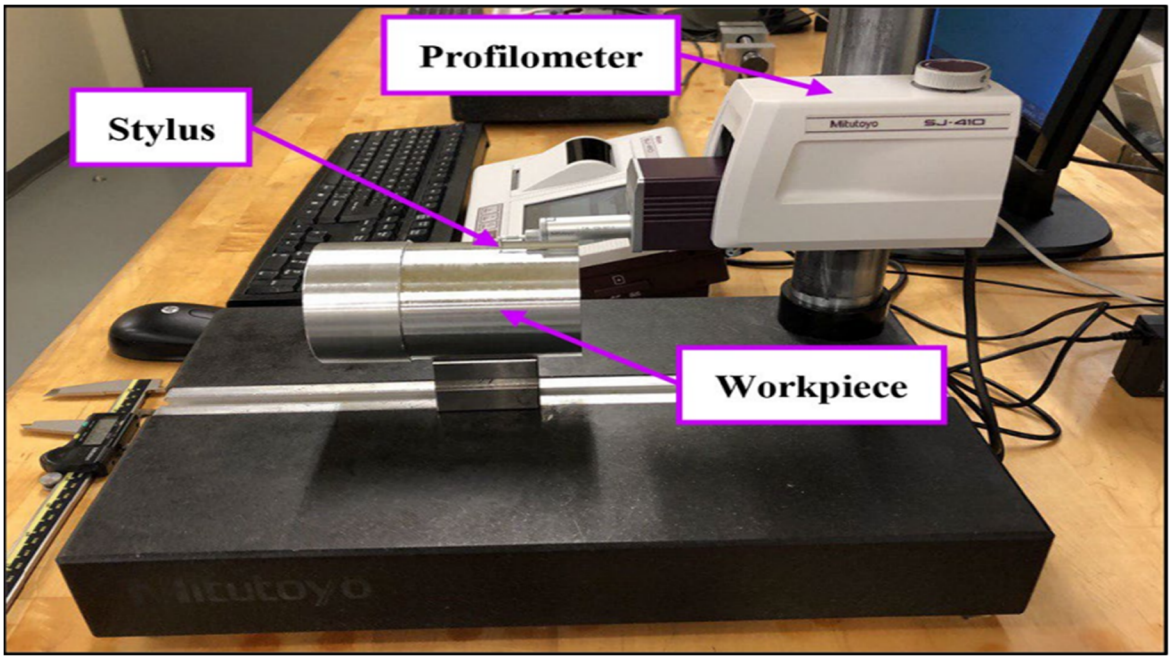

Figure 2.8 Mitutoyo SJ-410 surface roughness tester used for surface roughness measurement
Taken from Sadeghifar, Javidikia et al. (2022)

2.9 Particle emission measurement

The emission of metallic particles during machining operations was measured using an aerosol particle sizer (APS) and a scanning mobility particle sizer (SMPS).

A laser photometer was used to measure particle concentration, especially for particles with an aerodynamic diameter of less than 2.5 µm. The APS was used for particle size distribution measurements. It measures aerodynamic size distributions between 0.5 and 20 µm. In order to improve both the effectiveness and precision of the outcomes, the APS was combined with an SMPS to investigate the distribution of particles during the machining operation. Through an electrical mobility detection technique, the SMPS spectrometer is capable of assessing the size range of aerosols from 2.5 to 1000 nm. This instrument employs a bipolar charger within the electrostatic classifier to charge particles according to a predetermined distribution.

Subsequently, the particles are sorted based on their ability to traverse an electric field and are quantified via a condensation particle counter (CPC) (Khettabi, Songmene and Masounave 2010). The aerosol particle sizer (APS) and the condensation particle counter (CPC) are shown in Figure 2.9.

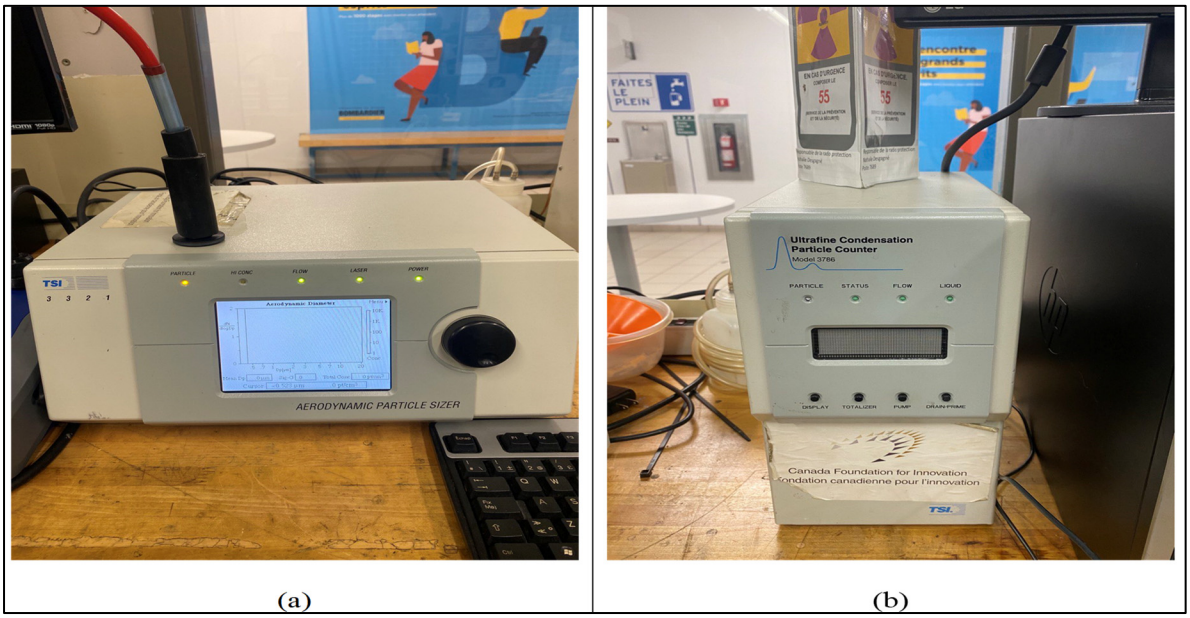

Figure 2.9 Particle emission analysis instruments: (a) Aerosol Particle Sizer (APS), and (b) Condensation Particle Counter (CPC)

2.10 Conclusion

In the first part of this chapter, the experimental procedures utilized in the study were introduced. This section included the presentation of the material's chemical composition and the dimensions of the workpieces. Detailed discussions covered all processes and steps undertaken for sample preparation, encompassing cutting, heat treatment, mounting, and polishing.

Subsequently, the process of micro-hardness measurement was explained. Shifting to the second part of the chapter, the methods employed during the machining process were presented. This section not only outlined the machining procedures but also introduced and elucidated the functionality of the data acquisition devices utilized in this research study.

CHAPTER 3

RESULTS AND DISCUSSION OF HEAT TREATMENT

3.1 Introduction

In recent years, the quest for improved mechanical properties and enhanced performance of aluminum alloys has led to significant research efforts in alloying and heat treatment of aluminum alloys. The Aluminum 7075 alloy, renowned for its high strength-to-weight ratio, is widely employed in the aerospace and automotive industries. However, the inherent strength and toughness of the alloy can be further optimized through the incorporation of specific alloying elements, such as Scandium (Sc) and Lithium (Li), coupled with appropriate heat treatment processes (Prasad, Gokhale and Wanhill 2013). The objective of this chapter is to investigate the influence of scandium (Sc) and lithium (Li) additions, in combination with different heat treatment conditions, on the microhardness of the Al 7075 alloy. This has been carried out using scanning electron microscopy (SEM) and energy dispersive spectroscopy (EDS) techniques which provide valuable insights into the microstructural variations and elemental composition of the alloy subjected to these different conditions.

The second goal pursued in this chapter is to determine the highest and lowest hardness values obtained from the five heat treatments used for the studied alloys. To achieve this objective, three aluminum alloys including Aluminum 7075, Aluminum 7075-Sc (with 0.1% Sc addition), and Aluminum 7075-Li -Sc (with 0.1% Sc and 2.2% Li addition) were solutionized at 470°C for 8 hours, following which they were rapidly quenched in water at room temperature, and subsequently subjected to aging using five distinct regimes. Table 3.1 presents a detailed overview of the distinct heat treatment procedures performed on the alloys and the corresponding hardness values achieved as a result of these treatments. The subsequent analysis, in the second part of the study, will also investigate the machinability of these two identified conditions: the hardest and softest states. The objective is to examine the influence of hardness achieved by heat treating and alloying on the machinability of Al 7075.

Table 3.1 Microhardness of alloys subjected to different heat treatments

Heat Treat-ment	Solution Heat Treatment	Artificial Aging	Alloy Type	Micro-hardness (VHN)
1	(8h @ 470°C)	-	Al 7075	113.7
			Al 7075-Sc	149.6
			Al 7075-Li-Sc	155.4
2		Single aging (24h @ 120°C)	Al 7075	176
			Al 7075-Sc	185
			Al 7075-Li-Sc	198
3		Single aging (8h @ 280°C)	Al 7075	62.6
			Al 7075-Sc	79.2
			Al 7075-Li-Sc	80.8
4		Double aging (24h @ 120°C + 8h @ 180°C)	Al 7075	142.7
			Al 7075-Sc	167.4
			Al 7075-Li-Sc	174.8
5		Double aging (8h @ 180°C + 24h @ 120°C)	Al 7075	144.8
			Al 7075-Sc	171.9
			Al 7075-Li-Sc	174
6		Double aging (8h @ 280°C + 24h @ 120°C)	Al 7075	65.9
			Al 7075-Sc	78.8
			Al 7075-Li-Sc	78.7

3.2 Influence of heat treatment type on alloy hardness

In this section, the hardness (i.e. strength) of the alloy material resulting from the heat treatment regime applied to it will be discussed for the three Al 7075 alloy types studied, namely alloys Al 7075, Al 7075-Sc, and Al 7075-Li-Sc. The effect of the alloying elements Sc and Li added to the base Al 7075 alloy would be automatically included together with that of the heat treatment: the additions will affect the precipitates formed during each of the heat treatments applied, which, in turn, will affect the hardness exhibited by the alloy in question. As the precipitates formed are microscopic in size, the strength/hardness will be appropriately measured in terms of microhardness, using a Vickers microhardness tester.

3.2.1 Effect of the heat treatments on microhardness of Al 7075 alloy

The measured microhardness results for Al 7075 alloy summarized in Table 3.1 are presented in Figure 3.1. Based on the findings, it was observed that subjecting the Al 7075 alloy to the heat treatment #2, where the alloy was aged at a temperature of 120°C for a duration of 24 hours resulted in the highest microhardness level, viz. 176 VHN. In contrast, employing a heat treatment process at a temperature of 280°C for a period of 8 hours (heat treatment #3) resulted in the lowest microhardness level for this alloy among the investigated heat treatment processes, measuring approximately 62.6 VHN. Solution heat treatment had a notable effect on enhancing the microhardness of the as-cast alloy. The initial microhardness of the as-cast alloy, measured at 58.7 VHN, was improved considerably, giving a microhardness of 113.7 VHN This represents a significant improvement of 55 VHN units compared to the as-cast condition. This demonstrates the positive impact of solution heat treatment on increasing the microhardness of the Al 7075 alloy.

To examine the impact of double aging on microhardness, three distinct double aging processes were tried on the alloy. In one of these processes, the sample was initially aged at 280°C for 8 hours, followed by a subsequent aging at 120°C for 24 hours (heat treatment #6). The resulting microhardness measurement showed a value of 65.9 VHN, displaying a value comparable to that obtained through single aging at 280°C for 8 hours, namely, 62.6 VHN (heat treatment #3).

With respect to the other two double aging treatments, the microhardness value obtained from double aging for 24 hours at 120°C and 8 hours at 180°C (heat treatment #4) was very close to the microhardness value obtained when the sequence of the double aging process was reversed, viz., using 8 hours at 180°C, followed by 24 hours at 120°C (heat treatment #5).
The microhardness values in these two cases were 142.7 VHN and 144.8 VHN, respectively.

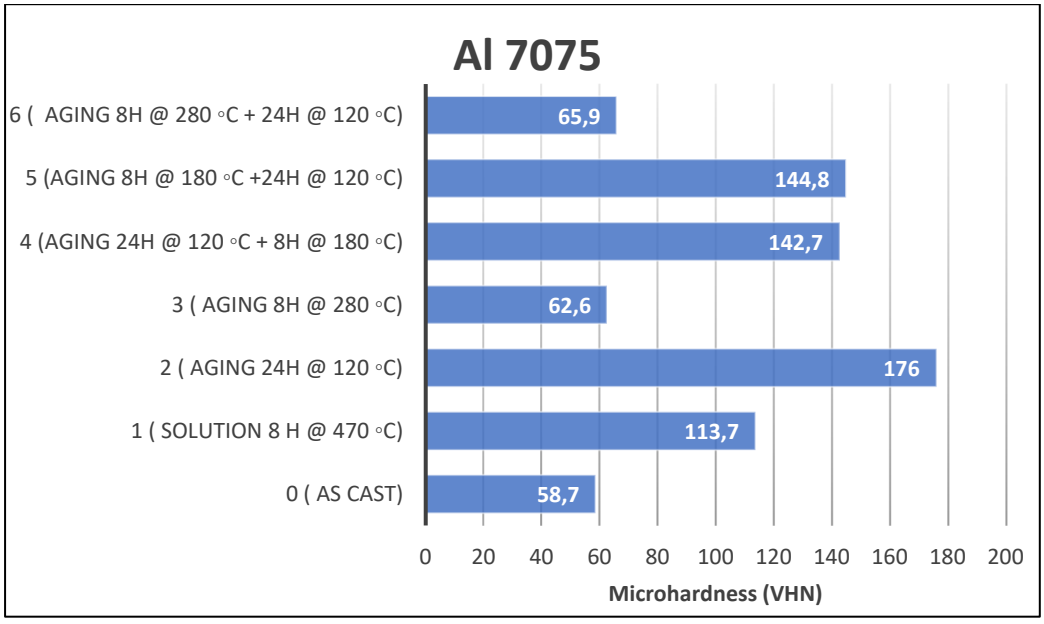

Figure 3.1 Microhardness of Al 7075 subjected to different heat treatments

Overall, from the results obtained for the three double aging treatments, it is reasonable to conclude that the aging temperature is the factor that controls the resulting microhardness, rather than the aging time. In addition, aging at 180°C is more effective in increasing the alloy strength than 120°C. Using a temperature as high as 280°C drastically reduces the alloy strength, with either a single aging or double aging treatment. This suggests that the precipitates are affected to different extents at these different temperatures. An examination and analysis of the corresponding microstructures using SEM/EDS as will be discussed in subsequent sections would shed further light on how and why the observed microhardness values result.

3.2.2 Effect of the heat treatments on microhardness of Al 7075-Sc alloy

In this section, the microhardness of the Al 7075-Sc alloy will be presented and discussed. The microhardness of Al 7075-Sc alloy in the as-cast condition was significantly higher than that of the Al 7075 sample. The reason for this phenomenon is due to the distinct compositions of the two alloys.

Table 2.4 illustrates that Al 7075-Sc contains 0.11% Sc in addition to 6.6% Zn, which is almost one percent higher than Al 7075 which has 5.62% Zn. The results of the study carried out by Pruthvi and Shennoy (Pruthvi and Shenoy 2022) also indicated that the weight percentage of Zn has the most significant contribution to hardness, accounting for approximately 47.05% of the variations observed. Therefore, it is crucial to precisely control and take into consideration the amount of Zn added to the alloy to achieve the desired hardness value in the material.

In another study, researchers Li and coworkers (Li, Pan et al. 2009) discovered that the addition of a small amount of Sc leads to the formation of Al_3(Sc, Zr) particles, which play a crucial role in refining the cast microstructures of Al-Zn-Mg-Cu-Zr based alloys. Their findings indicated that the most optimal and practical amount of Sc addition in such alloys is 0.21 wt.%. Therefore, by adding 0.21 wt.% Sc, they were able to achieve the desired microstructural refinement in the Al-Zn-Mg-Cu-Zr based alloys investigated in their work.

In the present study, although the microhardness was higher in the as-cast Al 7075-Sc alloy sample in comparison to the as-cast Al 7075 alloy, the Al 7075-Sc alloy reacted similarly to the different heat treatment processes in each case.

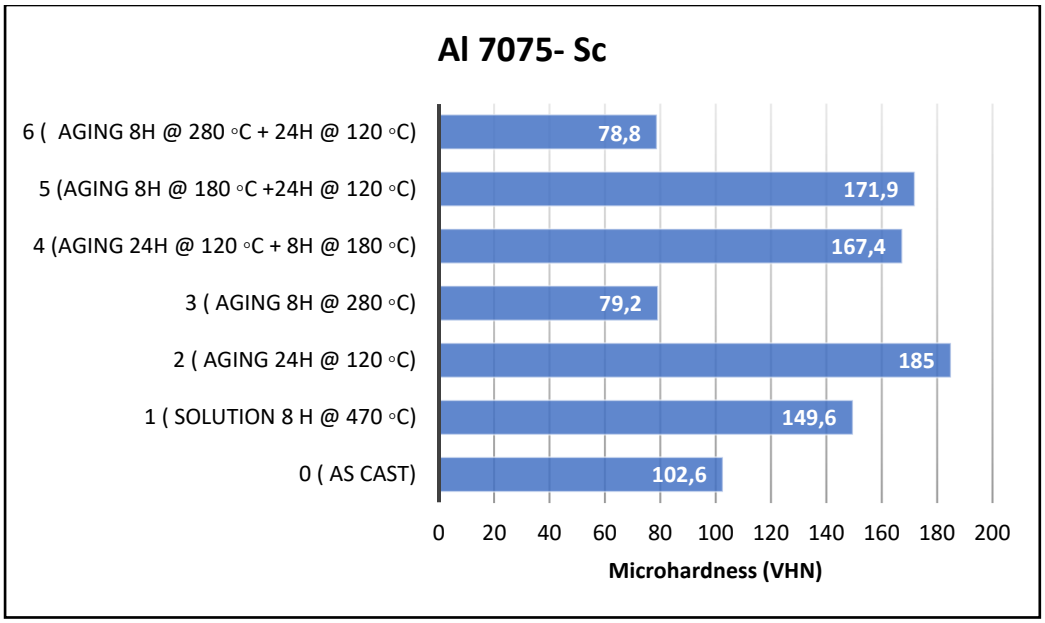

Figure 3.2 Microhardness of Al 7075-Sc samples obtained with different heat treatments

The Al 7075-Sc alloy exhibited the highest microhardness value of 185 VHN when subjected to a single aging process for 24 hours at 120°C. This aging treatment matches the widely recognized T6 temper, which is known to render 7075 aluminum alloys very hard. The T6 heat treatment involves a solution heat treatment within the temperature range of 450-480°C, followed by aging at 120-185°C. During artificial aging, precipitates such as Al_2CuMg and $MgZn_2$ form, contributing to the increased hardness (Darsono and Koin 2021).

However, it is important to note that higher aging temperatures can lead to the formation of larger precipitates resulting in a decrease in alloy hardness. This observation was also evident in our study, where the microhardness decreased to 79.5 VHN after aging for 8 hours at 280°C.

Interestingly, despite achieving the highest microhardness through single aging at 120°C for 24 hours, it was unable to compensate for the hardness reduction. Even this condition resulted in a slightly lower microhardness of 78.8 VHN, though this difference is negligible. In this sample, the microhardness resulting from the double aging treatment of 24 hours at 120°C followed by 8 hours at 180°C was equal to 167.4 VHN.

The reverse process (8 hours at 180°C and then 24 hours at 120°C) also did not show a meaningful difference since the resulting microhardness was 171.9 VHN, close to the former.

This interesting observation again reinforces the fact that the temperature is the main factor controlling the hardness obtained, as discussed in the previous section.

3.2.3 Effect of the heat treatments on microhardness of Al 7075-Li-Sc alloy

The importance that aluminum-lithium (Al-Li) alloys have gained in the aerospace industry stems from such valuable properties as their low density, high stiffness, and an excellent strength-to-weight ratio.

When Li is added to high-strength alloys, it brings about a reduction in the material density and an increase in the elastic modulus. As a result, Al-Li alloys offer enhanced performance for aerospace applications where lightweight *and* strong materials are essential (ud Din, Kamran et al. 2016).

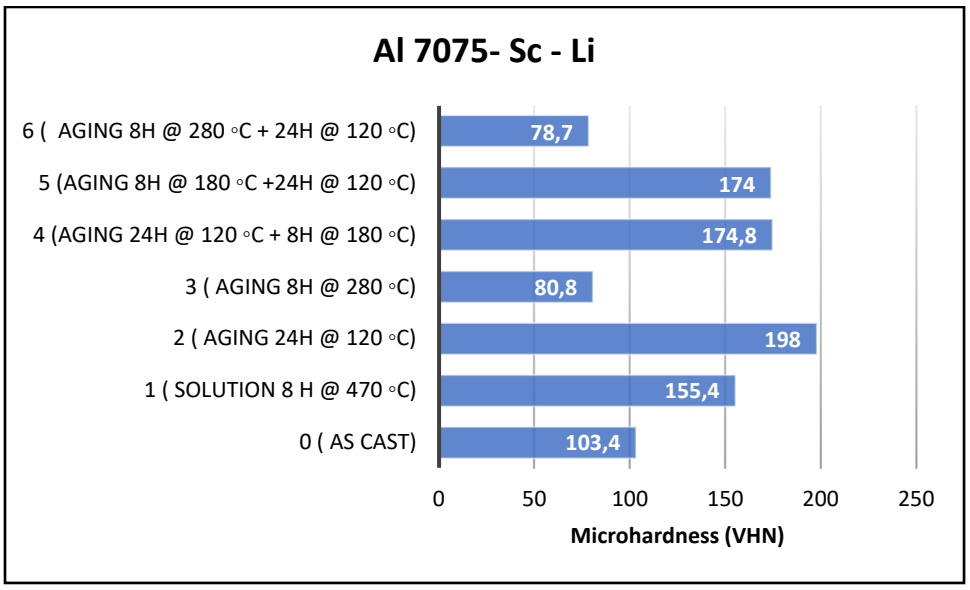

Figure 3.3 Microhardness of Al 7075-Li-Sc samples obtained with different heat treatments

To investigate the influence of alloying Al-7075 alloy with Li on the microhardness as a mechanical property criterion, 2.2 wt.% Li was added to Al 7075-Sc alloy. The microhardness

results, as shown in Figure 3.3, revealed that this addition did not significantly affect the microhardness of the alloy in the as-cast condition, since the microhardness of the Al 7075-Li-Sc alloy, measured at 103.4 VHN, was only slightly higher than that of Al 7075-Sc (102.6 VHN).

Furthermore, during the conducted heat treatment processes, both alloys exhibited almost no difference in their microhardness. For instance, at the almost lowest microhardness obtained after aging for 8 hours at 280°C, both alloys exhibited approximately 80 VHN. Double aging of 8 hours at 280°C followed by 24 hours at 120°C resulted in identical microhardness values of 78 VHN for both alloys. Similarly, aging at 180°C for 8 hours followed by 24 hours also yielded the same results, with only a slight variation, measured at 174 VHN. The reverse process produced the same outcome. While the addition of Li did not play a significant role in altering microhardness under most heat treatment conditions, it became more notable when aiming for the highest microhardness achieved by aging at 120°C for 24 hours. In this condition, the microhardness reached 198 VHN, nearly 13 units higher than that of the Al 7075-Sc alloy sample alone. This finding suggests that lithium is highly effective in the formation of small, uniformly dispersed precipitates, contributing to the enhanced microhardness of the Al 7075-Li-Sc alloy.

3.3 SEM/EDS investigations of Al 7075-Li-Sc alloys

After the heat treatment process of the solid solution at 120°C for 24 hours, the precipitated phases in the alloy consisted mainly of $Al_3(Sc, Zr)$, η’ ($MgZn_2$), and θ’(Al_2Cu) phases (Xia, Wang et al. 2021). The η’ phase is the most abundant metastable phase in artificially aged alloy and is the primary strengthening precipitate, typically appears as small, spherical particles. These particles are uniformly distributed throughout the aluminum matrix and can be observed in SEM images as small spots (see Figure 3.4) Comparing Figure 3.4 and 3.5, show that the precipitates are more uniform and smaller in 3.4 that is the obvious cause of increase in hardness in Al 7075-Li- Sc alloy aged 24 hours at 120°C.

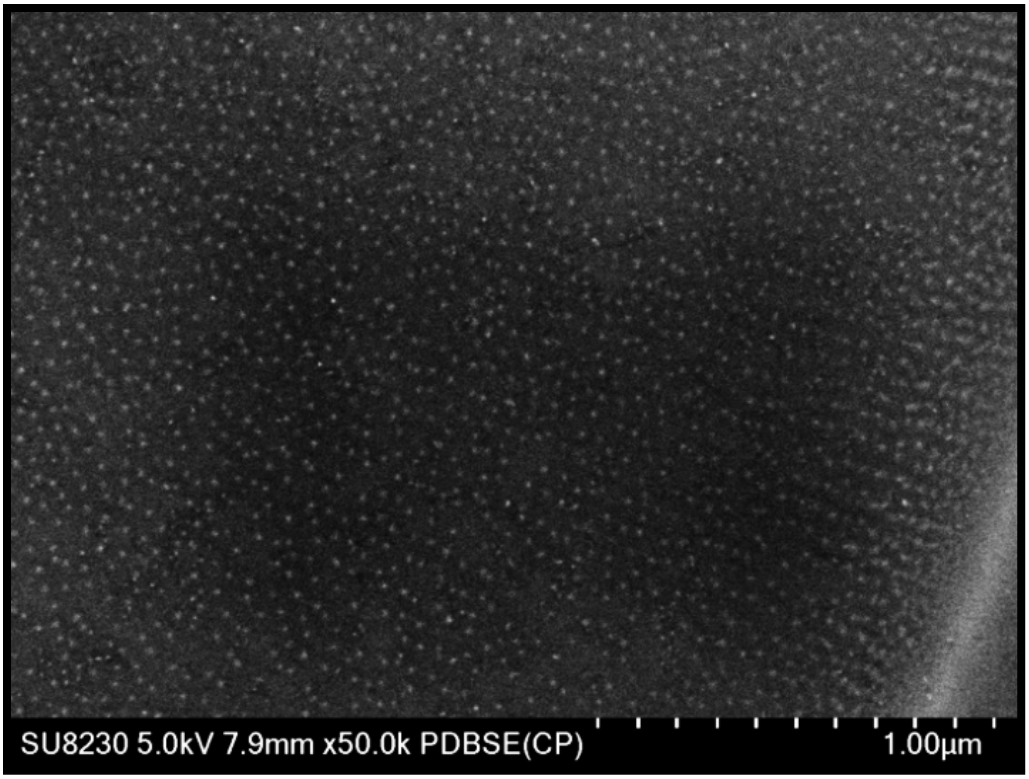

Figure 3.4 Backscattered electron image obtained from an Al 7075-Li- Sc alloy sample aged at 120 ◦C for 24 h

The application of heat treatment to the aluminum alloy can result in the creation of distinct precipitates and phases characterized by diverse shapes and microstructures. The exact nature of the microstructure will depend on the specific heat treatment process used.
The addition of alloying elements plays a vital role in enhancing the characteristics of Al-Zn-Mg-Cu alloys, and the control of the types and amounts of these added elements has been implemented during the alloys' evolution.

The precipitates that form in 7075 alloy include the η' (eta-prime), η (eta), and S' (S-prime) phases. The η' phase is the primary strengthening precipitate in 7075 alloy. It forms at around 120°C-160°C and reaches peak strength at around 120°C. The η phase forms at higher temperatures of around 160°C-200°C and has a lower strengthening effect than the η' phase. The S' phase forms at even higher temperatures of around 200°C-250°C and is less common in 7075 alloy (X.-M. and Starink 2001).

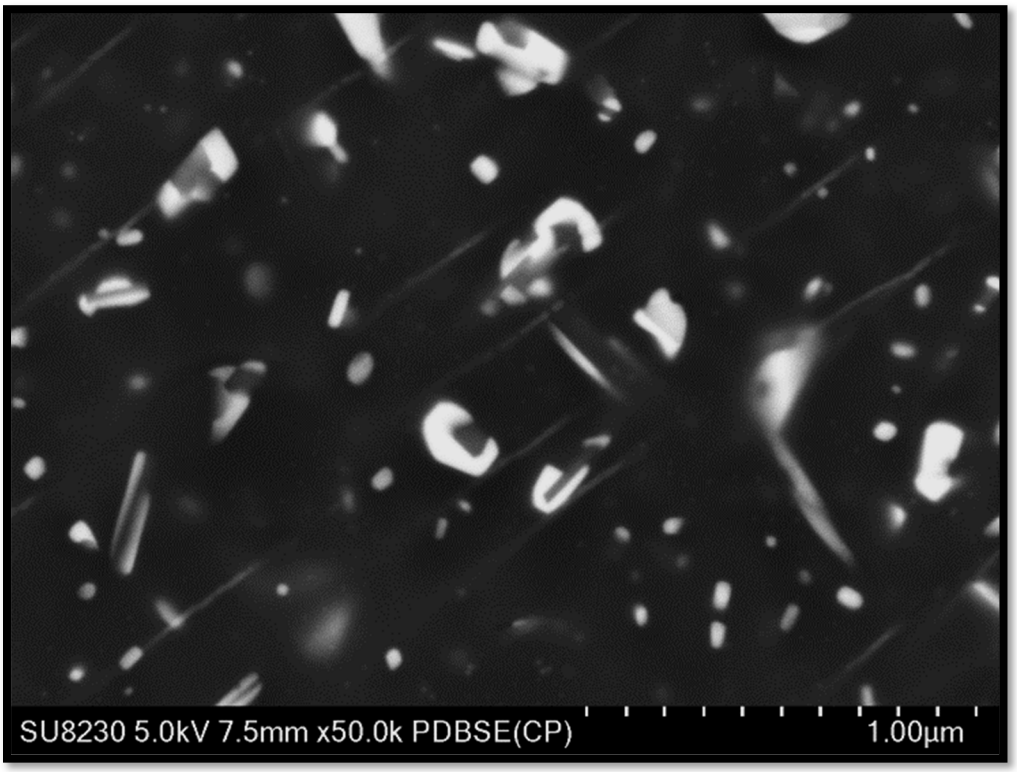

Figure 3.5 Backscattered electron image obtained from an Al 7075-Li- Sc alloy sample aged at 280°C for 8 h

The addition of lithium to the 7000 series aluminum alloys can significantly alter the precipitation behaviour during artificial aging.

The Li modifies the alloy microstructure by reducing the solubility of Cu in aluminum, promoting the formation of a new strengthening phase, called the T1 phase or theta phase. The T1 phase typically forms between 100°C and 160°C, while the η' phase forms at around 120°C-160°C in standard 7075 alloy. The T1 phase has a similar strengthening effect as the η' phase but is smaller in size and more homogeneously distributed in the matrix. The combination of T1 and η' phases leads to a synergistic strengthening effect in these alloys (Wei, Chen et al. 2000). The addition of bo'h Li and Sc to 7000 series aluminum alloys can further modify the precipitation behaviour during artificial aging.

Scandium is known to enhance the precipitation kinetics of aluminum alloys and promote the

formation of fine and homogeneously distributed precipitates. When both Li and Sc are added to the alloy, it can exhibit even higher strength and toughness than with Li alone. The addition of Sc promotes the formation of a new intermediate precipitate, called the β″ (beta double prime) phase, which acts as a nucleation site for the T1 and η' phases. The β″ phase forms at lower temperatures than the T1 phase, typically between 60°C-100°C (Huang, Loretto and White 1993).

The 7075-aluminum alloy contains a range of alloying elements in significant quantities, and segregation takes place during the solidification process. This segregation contributes to the development of a coarse non-equilibrium eutectic phase located at the grain boundary.

SEM and EDS images of the as-cast eutectic structure of Al 7075-Sc alloy are shown in Figure 3.6. (a) and (b).

The small needle-like particles observed around the non-equilibrium eutectic phase (see the high magnification image to the right in Figure 3.6. (a)), are generally considered to be the $MgZn_2$ phase, separated by the precipitate free zone (PFZ) from the eutectic AlMgCuZn phase.

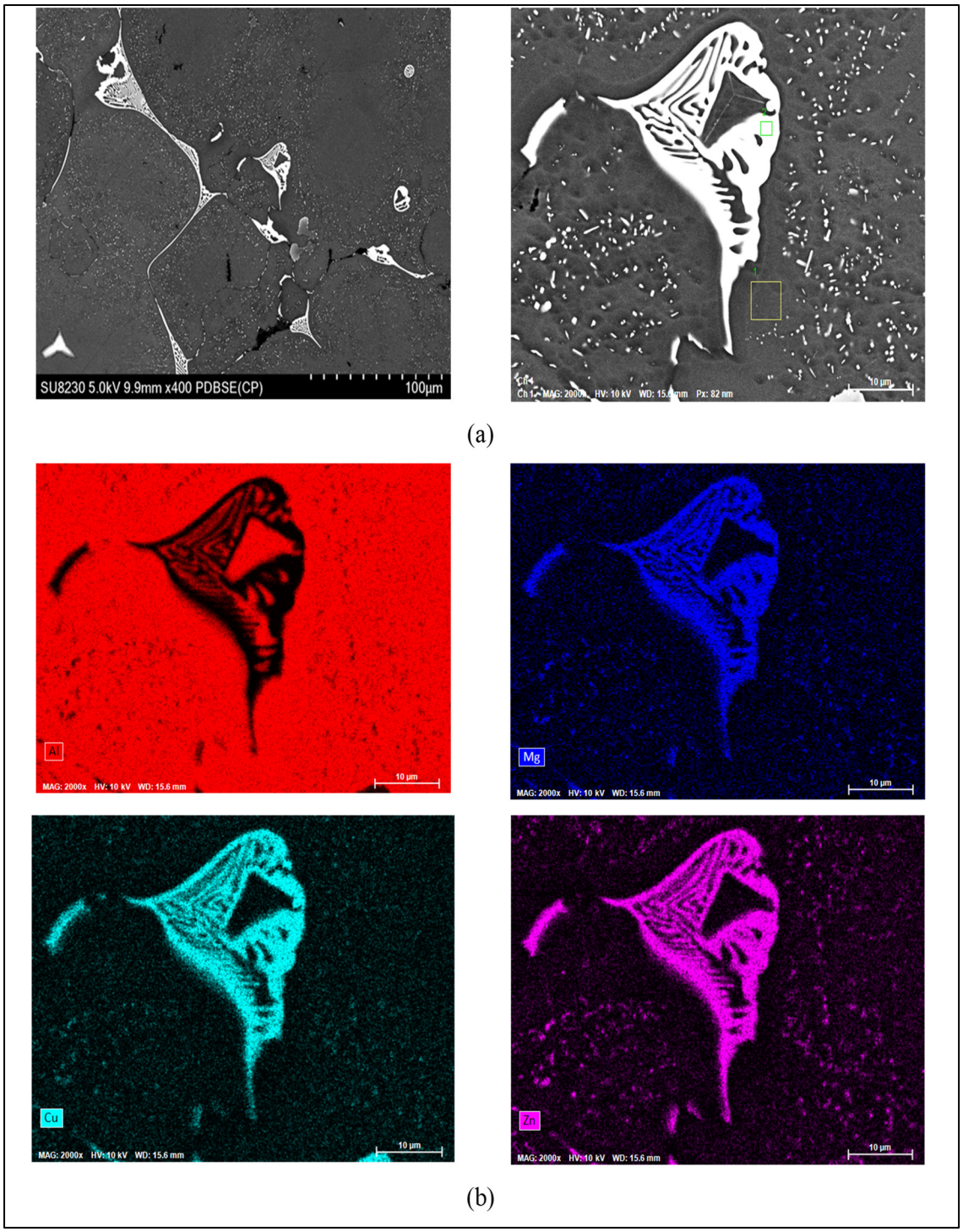

Figure 3.6 (a) SEM images and (b) X-ray images showing the distribution of Al, Mg, Cu and Zn in the AlMgCuZn eutectic phase

3.4 Conclusion

Based on the data derived from this chapter investigations, the following observations can be made.

- The highest level of hardness was consistently achieved for all alloys when subjected to a 24-hour heat treatment at 120°C across the different conditions explored.
- Conversely, the lowest hardness values were observed in both single aging (8 hours at 280°C) and double aging (8 hours at 280°C followed by 24 hours at 120°C). This observation underscores the primary role of aging temperature in influencing alloy hardness and strength, regardless of whether the aging process is single or double.
- The presence of η-phase particles was found to coincide with the development of regions devoid of precipitates around existing phases. This suggests a complex interplay between phase transformations and precipitation phenomena during heat treatment.
- The coarsening and spheroidization of η-phase particles were observed to occur through the Ostwald ripening mechanism, wherein smaller particles in solution dissolved and subsequently deposited onto larger particles. This mechanism plays a pivotal role in the evolution of the microstructure in these alloys.

CHAPTER 4

MACHINING RESULTS AND DISCUSSION

4.1 Introduction

The purpose of this chapter is to investigate the impact of various factors, including mechanical properties attained through the heat treatment process, cutting parameters (feed rate and cutting speed), and machining conditions (wet and dry machining), on machinability criteria. The machinability criteria explored in this study comprise surface roughness, cutting force, and particle emission.

A separate statistical analysis has been conducted for each alloy to gain a comprehensive understanding of how the input variables influence the variation in the mentioned outputs.

This approach allows for a thorough examination of the intricate relationships between the selected mechanical properties, cutting parameters, machining conditions, and the corresponding machinability criteria.

4.2 Surface roughness analysis

Surface roughness is undeniably one of the most crucial criteria in assessing machinability. Not only does it profoundly impact part quality, precision, and overall performance, but it also has a significant influence on various mechanical properties, including corrosion resistance, creep life, wear resistance, ductility, tensile strength, fatigue life, and overall material strength (Rawangwong, Chatthong et al. 2012).

When investigating the variables that affect surface roughness, we can categorize them into three main groups. The first category is related to machining variables, which commonly includes cutting speed, feed rate, and depth of cut.

Among these variables, the feed rate stands out as the most significant factor influencing surface roughness, as supported by the findings of numerous studies(Mathew, Hamzehlouia and Mears 2010), (Nimase and Khodke 2015).

The second category includes factors that are more related to machining conditions, such as tool material, tool geometry, and the cooling method employed during the machining process, which can include dry, wet, and Minimum Quantity Lubrication (MQL) methods.

The third fundamental category revolves around the characteristics of the workpiece, particularly its material composition. For instance, different alloys yield varying roughness results. Consequently, alloying plays a pivotal role in influencing the machined surface roughness. Moreover, the mechanical properties of the workpiece significantly impact surface roughness. For example, distinct levels of hardness resulting from various heat treatment processes can lead to a wide array of surface roughness outcomes.

Understanding and quantifying the influence of these various categories of factors on surface roughness is essential for optimizing the machining process, achieving superior surface quality, and ensuring the mechanical integrity of the final product. By examining and comprehending the interactions between these variables, manufacturers can make knowledgeable decisions to enhance their machining strategies, thereby leading to improved product performance and increased efficiency.

To facilitate the statistical analysis of the obtained results and to distinguish the primary influential variables affecting surface roughness, an Analysis of Variance (ANOVA) was executed.

ANOVA is a powerful tool used to assess the impacts of independent variables, including both main and interaction effects, on responses.

The following set of terms and expressions have been utilized in the ANOVA process of this study.

P-value: In the ANOVA method, the P-value, which falls between zero and one, quantifies the probability that the observed outcome could have arisen randomly. If the P-value associated with an independent variable is more than 0.1, it indicates an insignificant effect on the de-

pendent variable. When the P-value ranges between 0.05 and 0.1, the input variable demonstrates a moderately significant impact on the response. An input parameter with a P-value lower than 0.05 signifies a substantial effect on the examined outcome.

Coefficient of determination (R^2): The coefficient of determination (R^2) quantifies the proportion of variation in response values that can be explained by the controllable factors and their interactions. To put it more simply, R-squared indicates the percentage by which the response variable is predicted by the examined cutting variables, considering their specific level. When R^2 exceeds 75%, the predictive model becomes responsive to variations in variables. In other words when R-squared is more than 75% the output is statistically significant to the variation of cutting parameters.

Three distinct diagrams are employed to investigate and compare the most influential input variables on the output:

Pareto chart: The Pareto chart offers a visual representation that enables a clear comparison of the relative importance and statistical significance of both the primary effects and the interaction effects of process parameters.

Main effect plot: This plot is a vital tool for assessing the influence of each parameter on the response variable while keeping other variables constant, aiding in understanding their relative importance.

Interaction plot: This type of plot serves to illustrate the interaction effects between independent parameters on the output. In fact, an interaction plot illustrates how one independent variable influences the response while another independent variable is varying, highlighting the dynamic relationship between these variables.

4.2.1 Statistical analysis of Al 7075 machined surface roughness

In the statistical analysis of Al 7075 surface roughness results shown in Table AI.1, the R-squared value is approximately 94.7%. This value signifies that the analytical model and output are highly responsive to the variations in the process parameters.

P-value for feed rate, cooling mode, and hardness is zero. For the interaction of hardness and cooling mode as well as the interaction of feed rate and hardness p-values are 0.0001 and

0.0003 respectively. As well as cutting speed p – value equals with 0.0031. Consequently, the confidence level of the mentioned variables is more than 95%. The ANOVA table is show in Table AII.1.

The Pareto chart depicted in Figure 4.1 illustrates that the feed rate exhibits the most significant influence on surface roughness. This observation is supported by the main effect plot (Figure 4.2, a), where the Ra value transitions from 0.92 µm at the lowest feed rate level (0.05 mm/th) to nearly 1.79 µm at the highest feed rate of 0.15 mm/th. In the context of machining Al 7075 within this study, the impact of cutting speed on roughness is not highly significant. As indicated in Figure 4.2, b, the variation in cutting speed ranging from 200 to 600 m/min results in an increase of less than 0.2 µm in surface roughness.

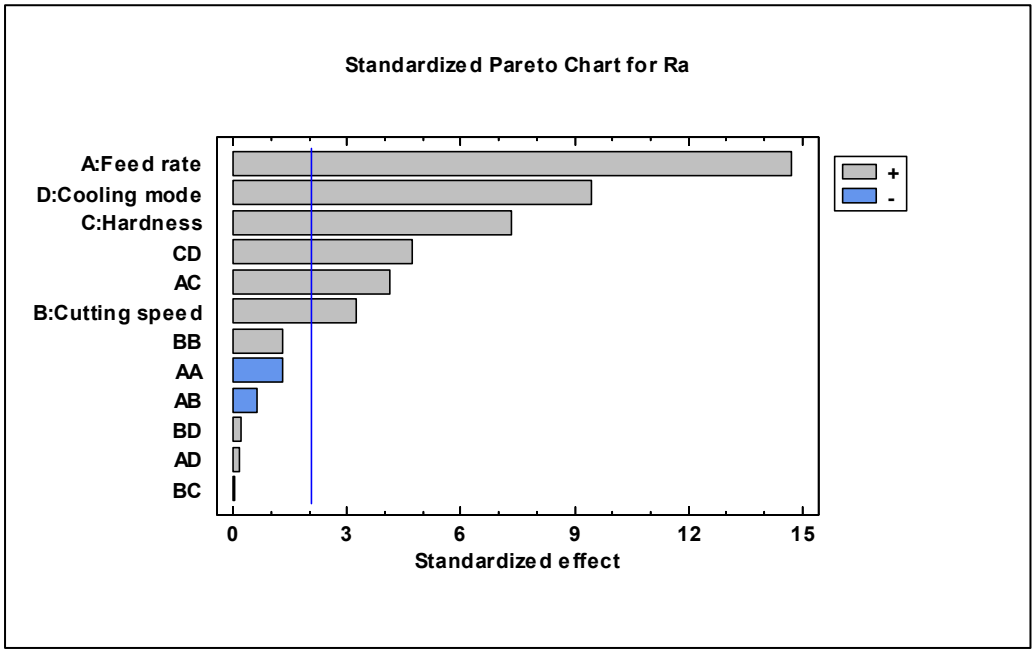

Figure 4.1 Pareto chart of Ra for Al 7075 machining

Following the feed rate, which exhibited the most impact on surface roughness, as indicated by the Pareto chart (Figure 4.1) the cooling mode and subsequently the hardness emerge as the variables with the greatest influence on Ra in the machining of Al 7075. It's a very interesting result that shows the wet cooling condition and using high flow of cutting fluid in high-speed

machining of Al 7075 not only doesn't have positive effect on surface quality, but it also leads to roughness enhancement.

As shown in Figure 4.2, c the roughness in wet machining is almost 0.45 µm higher than dry machining. This finding aligns with the results of the study conducted by (Khettabi, Nouioua et al. 2017). Their investigation into the effect of various cutting fluid flow rates on surface quality yielded comparable conclusions. Specifically, their findings indicated that elevated flow rates of cutting fluid only result in a reduction of surface roughness when applied to low cutting speeds. From these observations, it can be concluded that dry machining has more advantageous than wet machining in the context of high-speed machining of Al 7075.

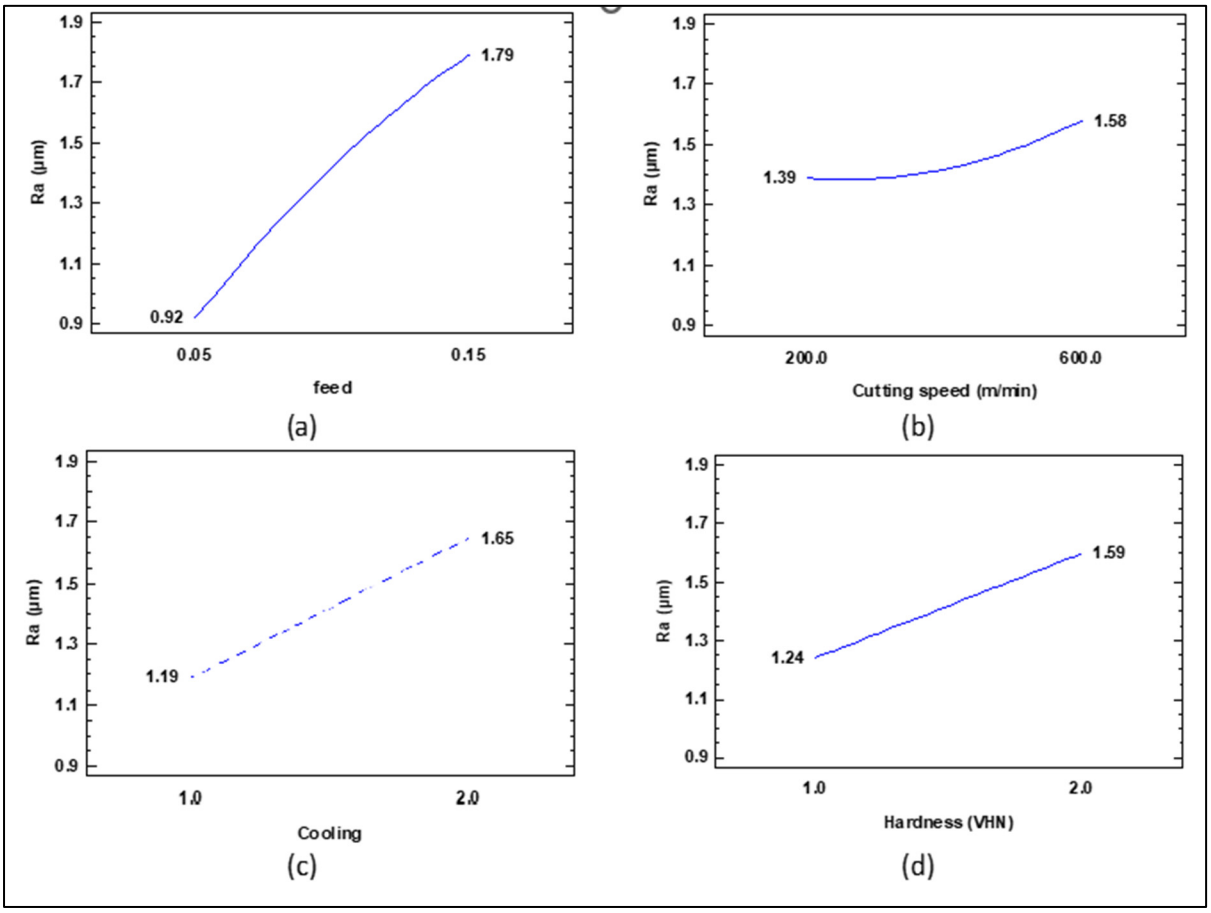

Figure 4.2 Main effects plot for Ra in machining of Al 7075

To validate and confirm the detrimental impact of fully wet machining on surface quality, we extended our investigation to include the analysis of Rt results. The Pareto chart (Figure 4.3) highlights a similar negative effect on Rt when employing cooling mode and wet machining.

These findings prove negative effect of wet machining on both arithmetic (Ra) and physical roughness (Rt) parameters.

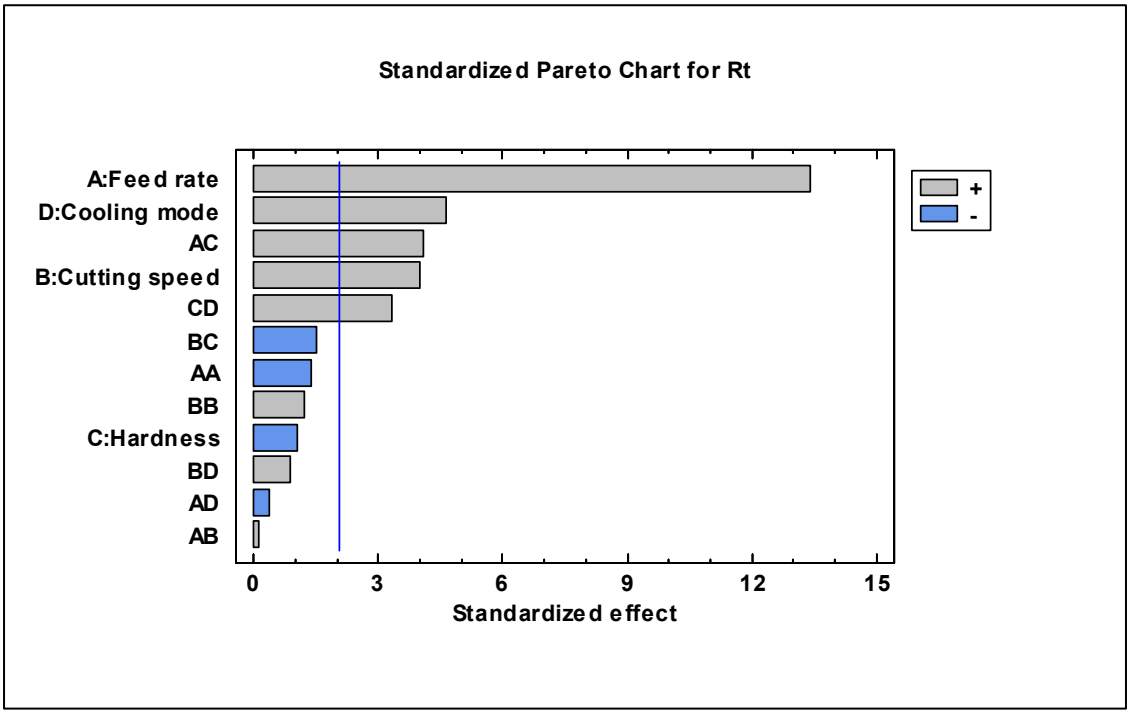

Figure 4.3 Pareto chart of Rt for Al 7075 machining

According to Pareto charts shown as Figures 4.1 and 4.3, a notable distinction emerges between Ra and Rt, especially regarding the influence of hardness. While the impact of hardness on Ra is significant, it has an insignificant negative effect on Rt. This behaviour can be attributed to the machining process, where the hardness of the workpiece may hinder the separation of large particles from the surface. Consequently, Rt, which represents the highest peaks and lowest valleys, becomes lower.

The third significant effective parameter on Ra is the hardness attained through distinct heat treatments discussed in advance. The main effect plot (Figure 4.2, d), which displays the consequences of varying individual independent variables on the dependent variable, reveals that the machined surface roughness of the hardest specimen, characterized by a Vickers hardness number (VHN) of 176, shows an increase of nearly 0.35 µm when compared to the softest work piece with 62 VHN.

Following feed rate, cooling mode, and hardness, the interaction between cooling mode and hardness emerges as a significant factor affecting Ra (Figure 4.4). In the machining of soft alloys, the roughness in wet conditions is only 0.2 µm greater than in dry conditions.
However, for hard alloy machining, the roughness in wet mode is approximately 0.8 micrometers higher than in dry mode.

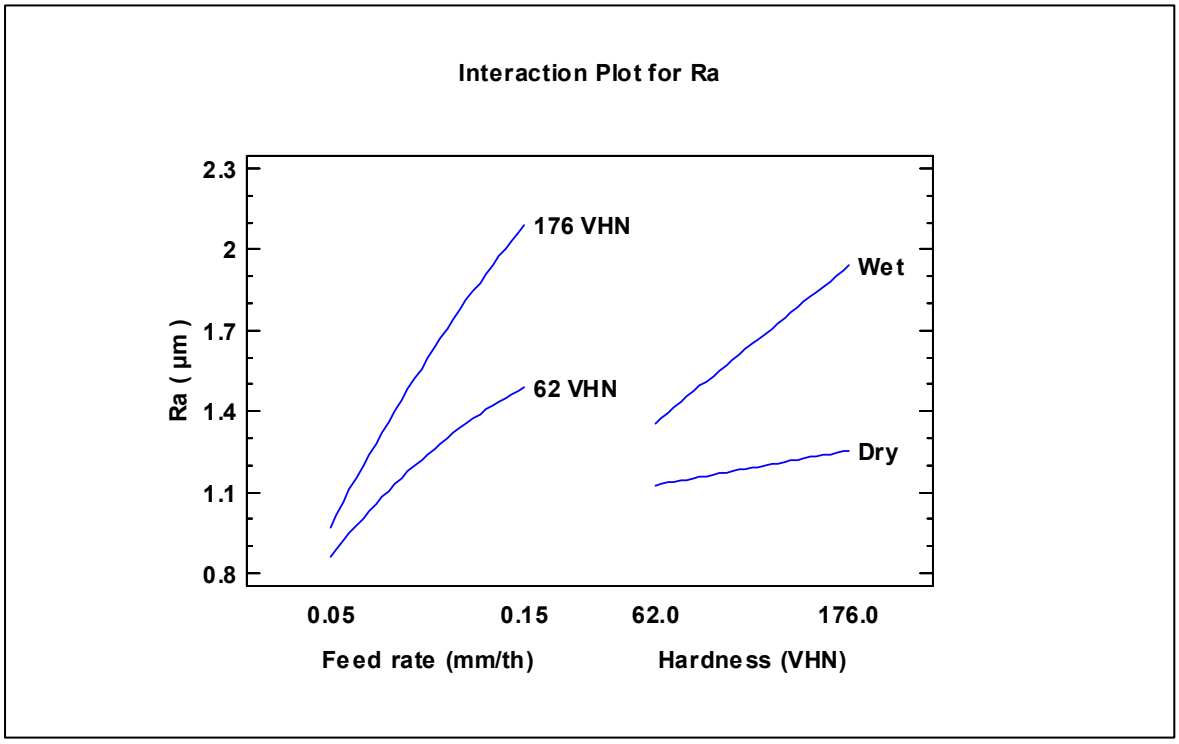

Figure 4.4 Interaction plot for Ra in machining of Al 7075

The interaction between hardness and feed rate also has a significant effect on Ra.
This significance is highlighted in the interaction effect plot (Figure 4.4), where alterations in hardness, ranging from 62 to 176 VHN, are examined within the context of two feed rate levels: 0.05 mm/th and 0.15 mm/th. At the initial feed rate level of 0.05 mm/th, the roughness experiences only a slight change as hardness varies, with an approximate difference of 0.1 µm. However, when considering the highest feed rate level of 0.15 mm/th, a more substantial impact becomes apparent. The roughest surface, belonging to the hardest Al 7075 (176 VHN), exhibits an increase of nearly 0.6 µm compared to the smoothest surface, attributed to the softest block with a VHN of 62. While the increase in feed rate has led to an elevation of surface roughness in the soft sample, the rise in roughness is notably greater in the case of the hard sample. In other words, when both the feed rate and the work piece hardness are elevated, the surface quality experiences a substantial reduction.

3D surface plots illustrated in Figure 4.5 depict the interaction effects between cutting parameters (cutting speed and feed rate), the distinguished machining condition (cooling mode), and the workpiece material property (hardness). As demonstrated in Figures 4.5, a, and 4.5, c, the best surface roughness, regardless of the hardness of the workpiece and the cooling mode, is achieved at a lower feed rate and cutting speed, almost near 0.5 µm. However, as the feed rate increases, the influence of hardness becomes significant, with Ra approaching 2 µm in higher hardness (176 VHN), while for soft workpieces (62 VHN), the roughness remains below 1.5 µm. Wet machining had a detrimental effect on the surface quality of Al 7075 in this study. Although this effect was not significant in soft samples, it exhibited a pronounced negative influence on the surface roughness of hard workpiece. As illustrated in Figure 4.5, d, the highest Ra values were observed in hard workpieces machined with high feed rates and cutting speeds under wet condition.

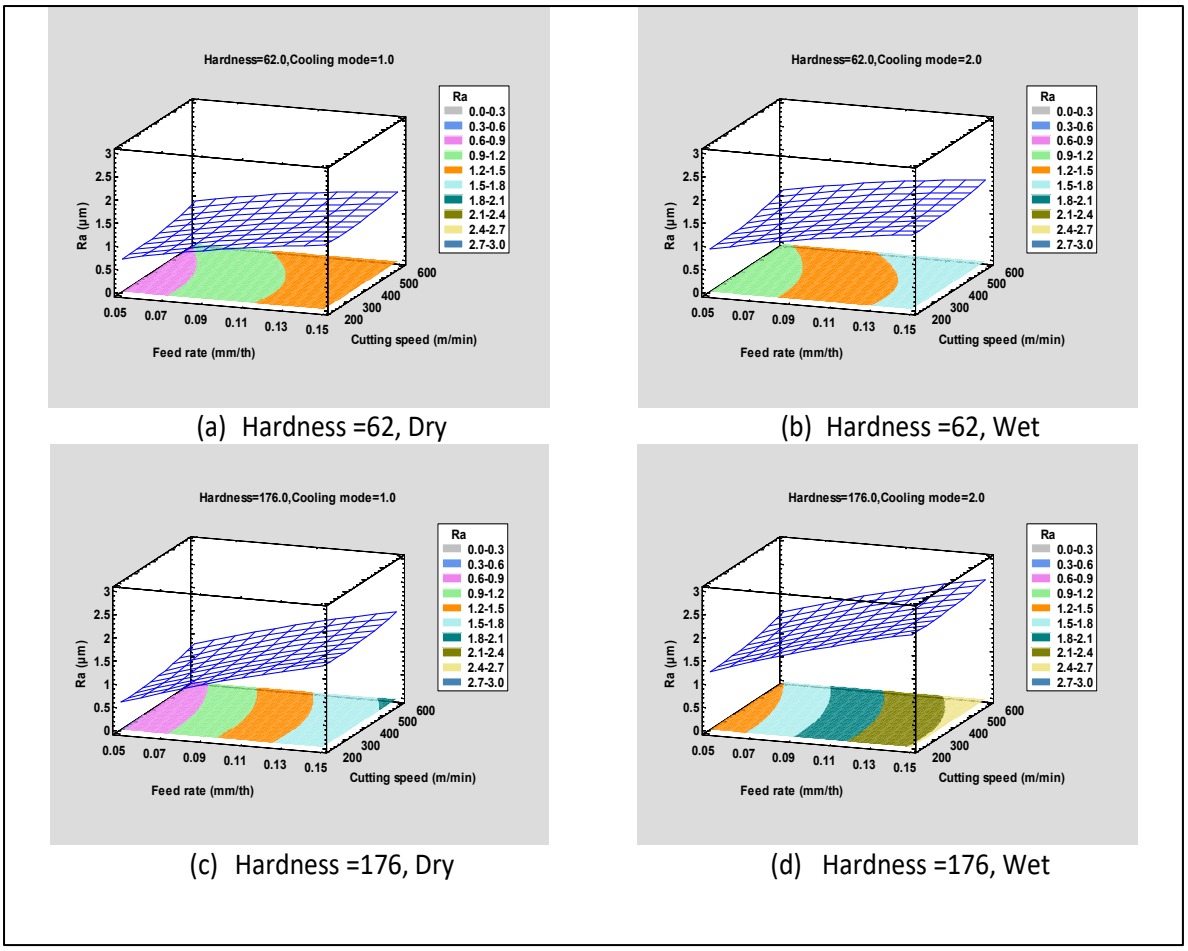

Figure 4.5 3D surface plots of Ra in different hardness and cooling mode for Al 7075

4.2.2 Statistical analysis of Al 7075 - Sc machined surface roughness

The obtained results for the machined surface roughness of Al 7075 - Sc are presented in Table AI.2. Like the machining of Al 7075, this alloy exhibits statistically significant sensitivity to variations in cutting parameters, as evidenced by a R-squared value of approximately 86.9%.

In this experimental study as shown in the ANOVA table (Table AII.1), the p-values for feed rate, cutting speed, and hardness are all zero, indicating their substantial influence on surface roughness.

The interaction between feed rate and hardness resulted in a p-value of 0.0369. Therefore, the mentioned parameters achieved a confidence level more than 95%, confirming their statistical

significance. In contrast, cooling mode demonstrated a negligible impact on roughness, as evidenced by its p-value of 0.65.

Our analysis, as indicated in the Pareto chart (Figure 4.6), challenges our initial expectation. We anticipated that feed rate would be the primary factor influencing surface roughness. However, our findings have revealed a different scenario.

In this specific case, hardness emerges as the leading factor affecting surface roughness (Figure 4.7, a).

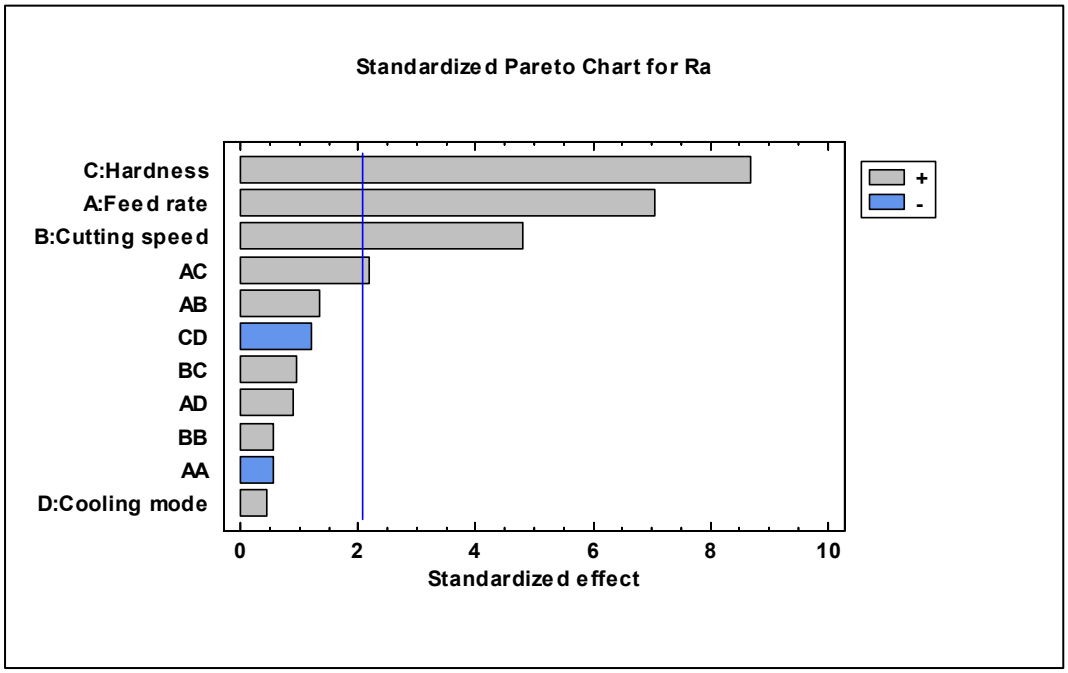

Figure 4.6 Pareto chart of Ra for Al 7075 - Sc machining

While according to the Pareto chart, the feed rate may not be the first influential factor on surface roughness, the main effect plot (Figure 4.7, b) reveals an almost similar impact compared to hardness. When we increased the feed rate from 0.05 to 0.15 mm/th, a significant change in surface roughness was observed. The roughness increased by 0.64 µm, rising from an initial value of 1.1 µm to nearly 1.74 µm. This increase is approximately similar to the effect

seen with variations in hardness, where the roughness also increased by 0.65 µm, from 1.14 µm to 1.79 µm.

As revealed by the Pareto chart analysis, the third crucial cutting parameter affecting Al 7075 - Sc surface roughness is the cutting speed. An increase in cutting speed is associated with a decline in the quality of the machined surface. When we operated at the lowest cutting speed of 200 m/min, surface roughness was 1.29 µm.

However, as the cutting speed was increased up to 600 m/min, we observed a growth in roughness, reaching around 1.72 µm (see Figure 4.7, c). This finding highlights the need for consideration and optimization of cutting speed in machining processes of Al 7075 - Sc alloy to achieve the desired surface quality.

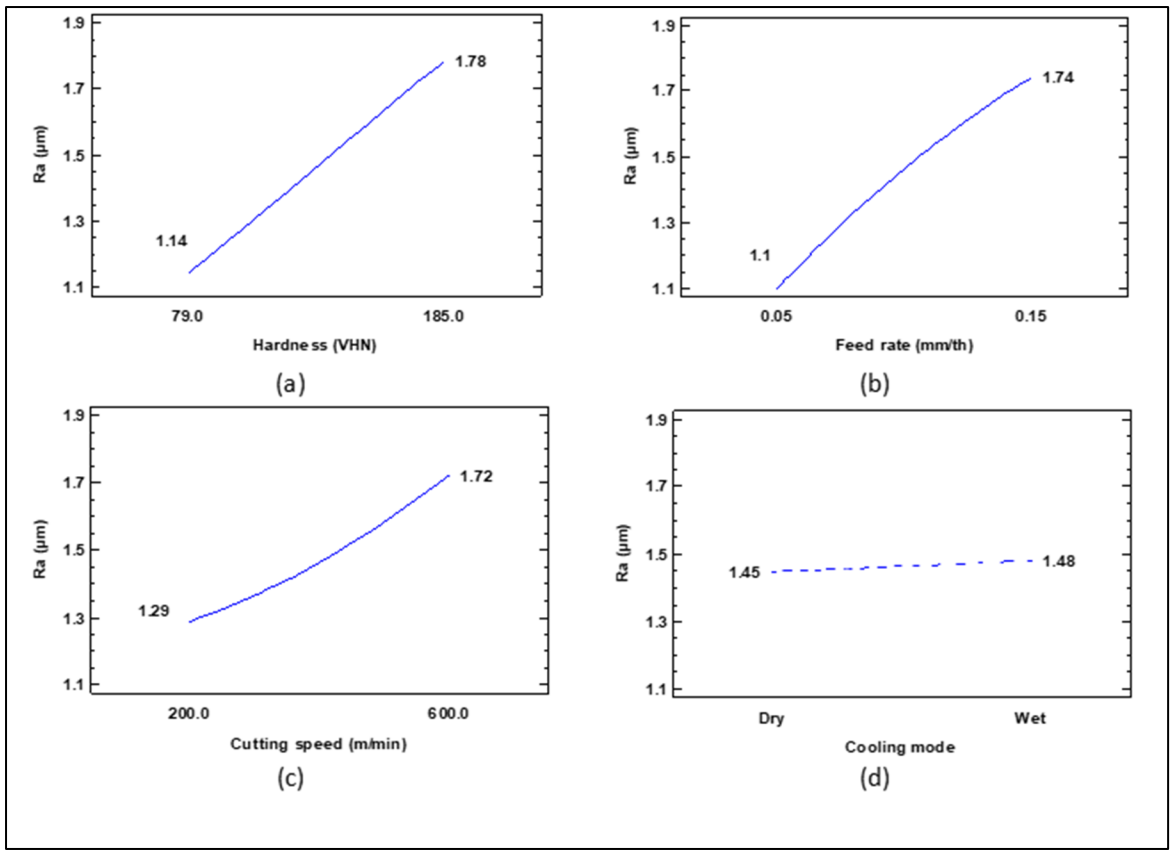

Figure 4.7 Main effects plot for Ra in machining of Al 7075 – Sc

In this case, the influence of the cooling mode on surface roughness (Ra) is insignificant. This is evident in the Pareto chart and the main effect plot, where the cooling mode is shown to have a negligible positive effect on Ra during the machining of Al 7075 – Sc.

The interaction between hardness and feed rate is ranked fourth in terms of its impact on surface roughness. This relationship is further clarified by the interaction plot presented in Figure 4.8. Notably, the plot highlights a substantial difference in surface roughness, specifically, when we compare the softest machined block with a hardness of 79 VHN, at the lowest feed rate, to the hardest machined specimen with a hardness of 185 VHV, at the highest feed rate, we observe a considerable difference of approximately 1.3 units. This difference shows the significant effect of the interaction between hardness and feed rate on surface roughness in our machining experiments.

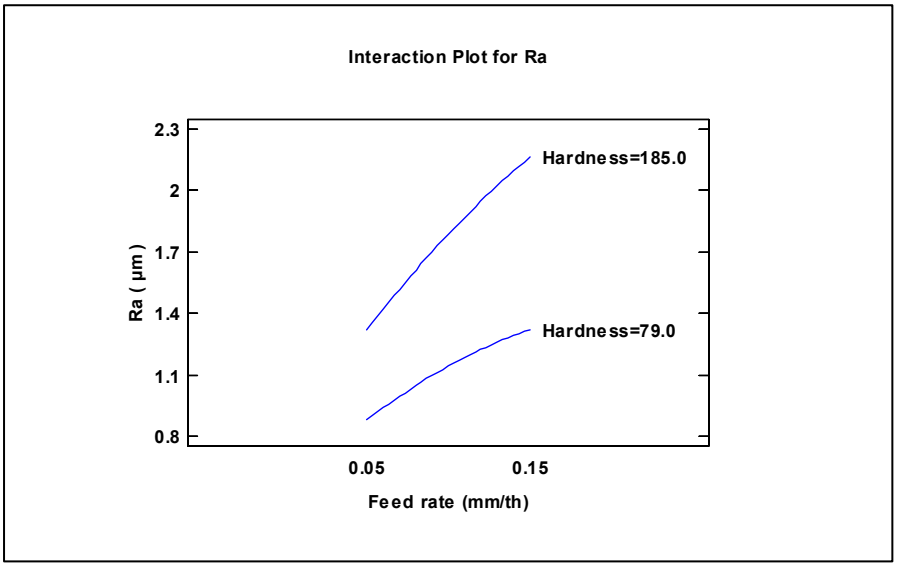

Figure 4.8 Interaction plot for Ra in machining of Al 7075 – Sc

Based on the 3D surface plots shown in Figures 4.9, a, and 4.9, b, at a low hardness level of 79 VHN, roughness varies from approximately 0.75 to 1.5 µm in dry machining condition and from 0.9 to 1.7 µm in wet machining condition as feed rate and cutting speed increase. These findings demonstrate the significant influence of feed rate and cutting speed on surface roughness, while the cooling mode appears to have a negligible effect. Figures 4.9, c, and 4.9, d, also highlight the significant influence of cutting speed on the machining process. However, the

most notable observation is the pronounced impact of hardness, with the particularly detrimental effect of the feed rate on the machined surface quality of hard Al 7075 – Sc. Here, the roughness increases significantly, jumping from approximately 1.2 to 2.5 µm as the feed rate and cutting speed increase to 0.15 mm/th and 600 mm/min, respectively.

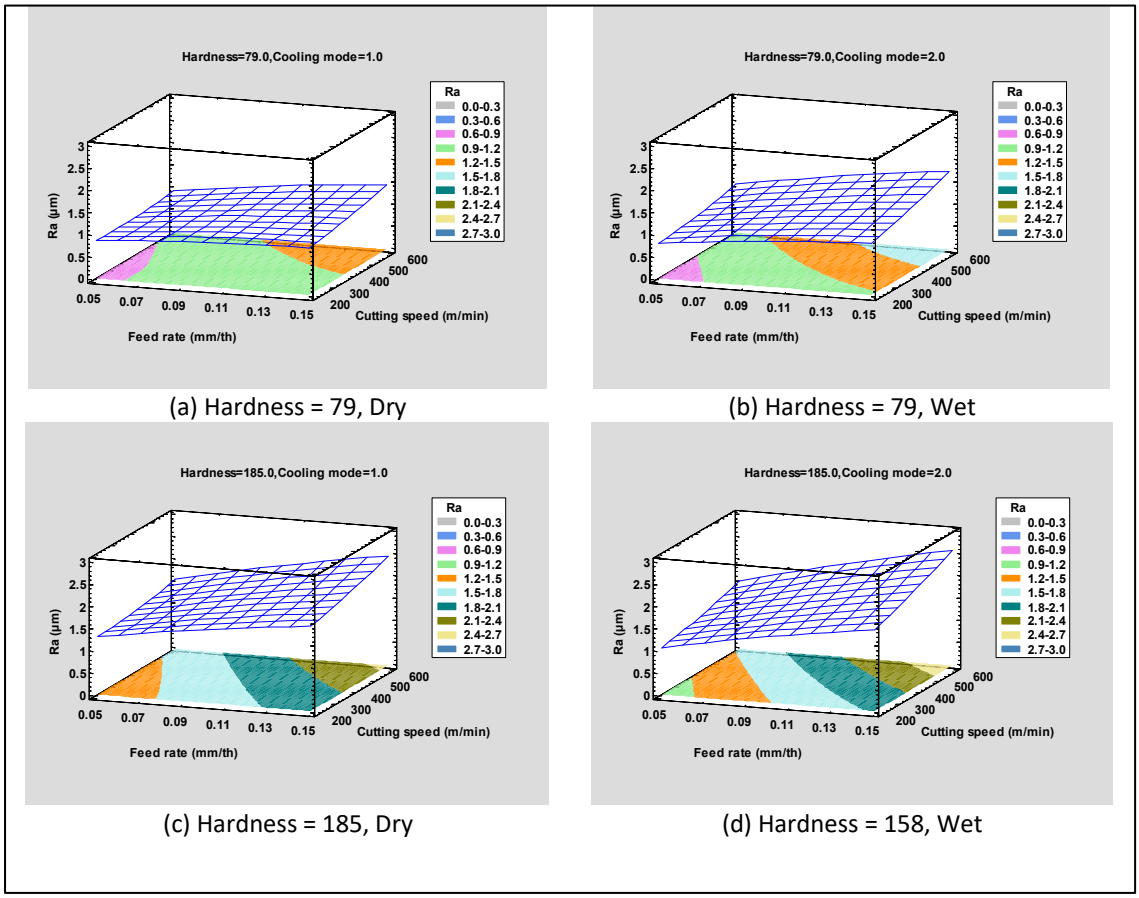

Figure 4.9 3D surface plots of Ra in different hardness and cooling mode for Al 7075 – Sc

4.2.3 Statistical analysis of Al 7075-Li-Sc machined surface roughness.

Table AI.3 presents the roughness data obtained from machined surfaces of Al 7075-Li-Sc for reference and analysis. The machining process of Al 7075-Li-Sc demonstrates a noteworthy sensitivity to variations in cutting parameters, supported by a high R-squared value of 96.86%. In simpler terms, the fitted model effectively accounts for 96.86% of the variability observed

in Ra, indicating a strong correlation between the chosen cutting parameters and the surface roughness outcome.

In this context, it is notable that eight effects exhibit P-values less than 0.05, signifying their significant deviation from zero at the 95.0% confidence level. The ANOVA table for the statistical analysis of Al 7075-Li-Sc is presented in Table AII.3. As illustrated in the Pareto chart (Figure 4.10), which captures all independent variables and their interactions, it is evident that only hardness fails to pass the threshold indicated by the blue line. This result shows the low confidence level associated with hardness and its insignificance in influencing Ra during the machining of this alloy.

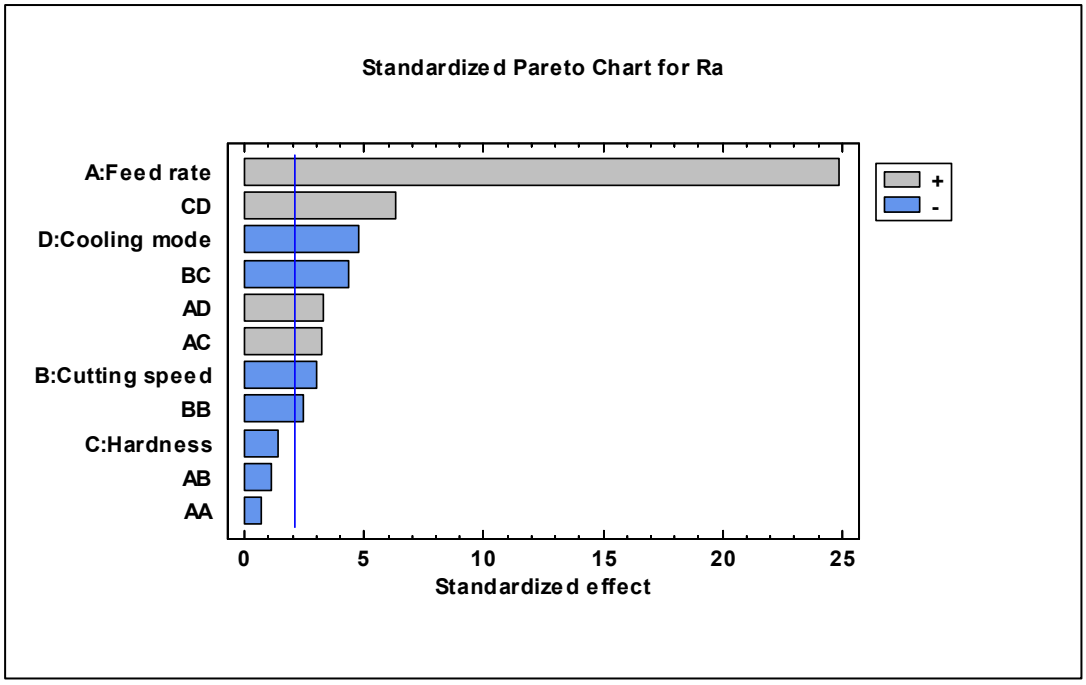

Figure 4.10 Pareto chart of Ra for Al 7075-Li-Sc machining

According to the Pareto chart (Figure 4.10) and the main effect plot (Figure 4.11, a), it is evident that variations in feed rate have the most substantial impact on Ra in machining of Al Al 7075-Li-Sc. As depicted in the main effect plot, the roughness increases significantly, jumping from 0.71 µm at low feed rates to nearly 1.48 µm at high feed rate. This observation underscores the notable influence of feed rate on the surface roughness outcome.

Unlike the other two alloys, where the cooling mode did not have positive effect on surface quality, in this case, wet machining played a positive role in enhancing surface quality by reducing roughness. While the individual alteration of the cooling mode resulted in a relatively modest reduction of approximately 0.15 µm in roughness when comparing wet machining to dry operation (as seen in Figure 4.11, b), it's crucial to emphasize its interaction with hardness, which has a more significant impact on roughness variation, as will be discussed in the following paragraph.

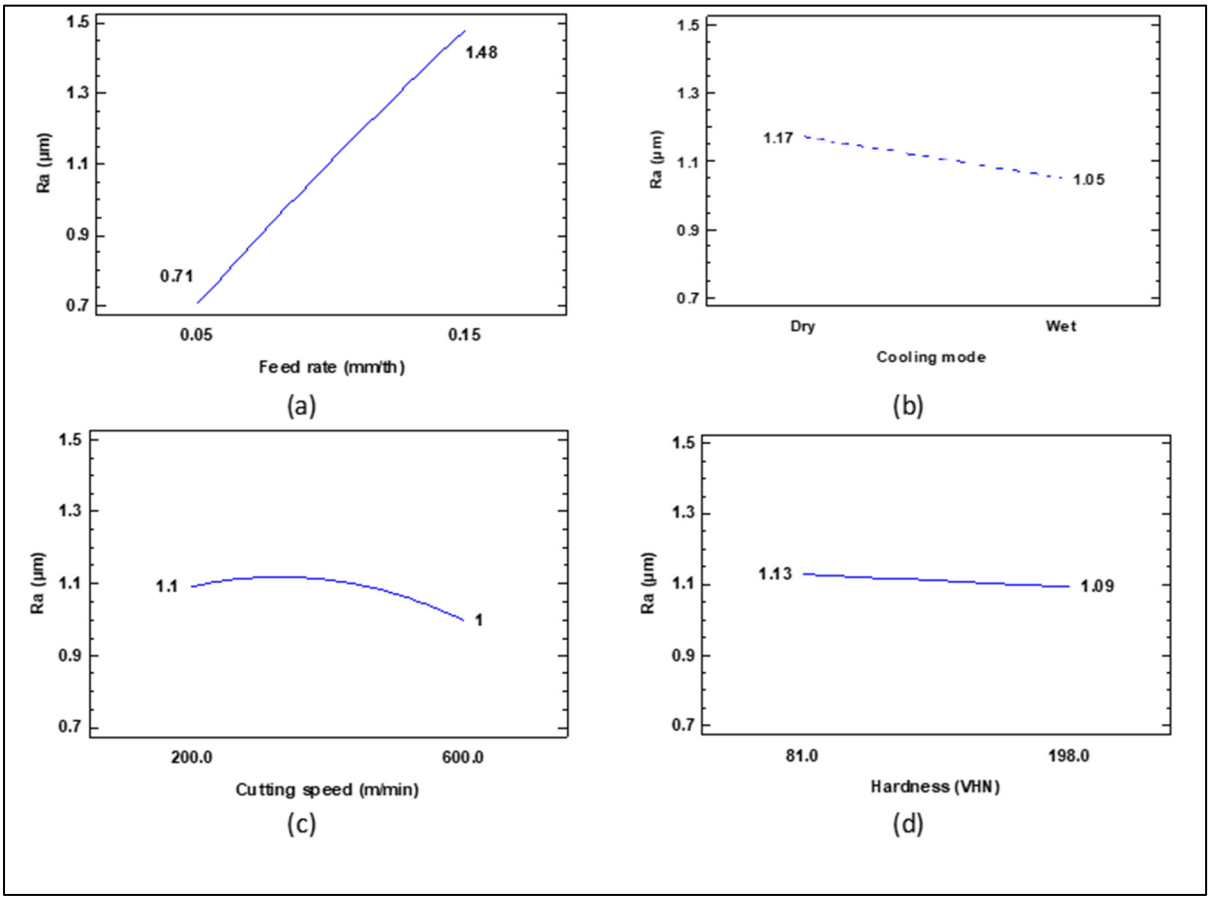

Figure 4.11 Main effects plot for Ra in machining of Al 7075-Li-Sc

Despite the hardness does not have significant statistical effect on the roughness its interaction with other parameters plays much more notable role in affecting the roughness. As seen in Pareto chart (Figure 4.10) the interaction of hardness with the cooling mode emerges as the

second most notable effect among the variables. As depicted in the interaction plot of hardness and cooling mode in Figure 4.12, the lowest roughness value, at 0.99 µm, is attributed to the softest block with a hardness of 81 VHN machined in a wet condition. In contrast, the highest surface roughness, at 1.27 µm, is observed for the lowest hardness when machined in a dry condition. interestingly, machining the hardest alloy in both wet and dry conditions yield similar roughness results, approximately 1.12 and 1.07 µm, respectively. The results reveal that employing a high level of cutting fluid reduced roughness in soft workpiece. However, it is important to note that it did not yield a positive effect on roughness in hard workpiece; instead, it slightly increased Ra.

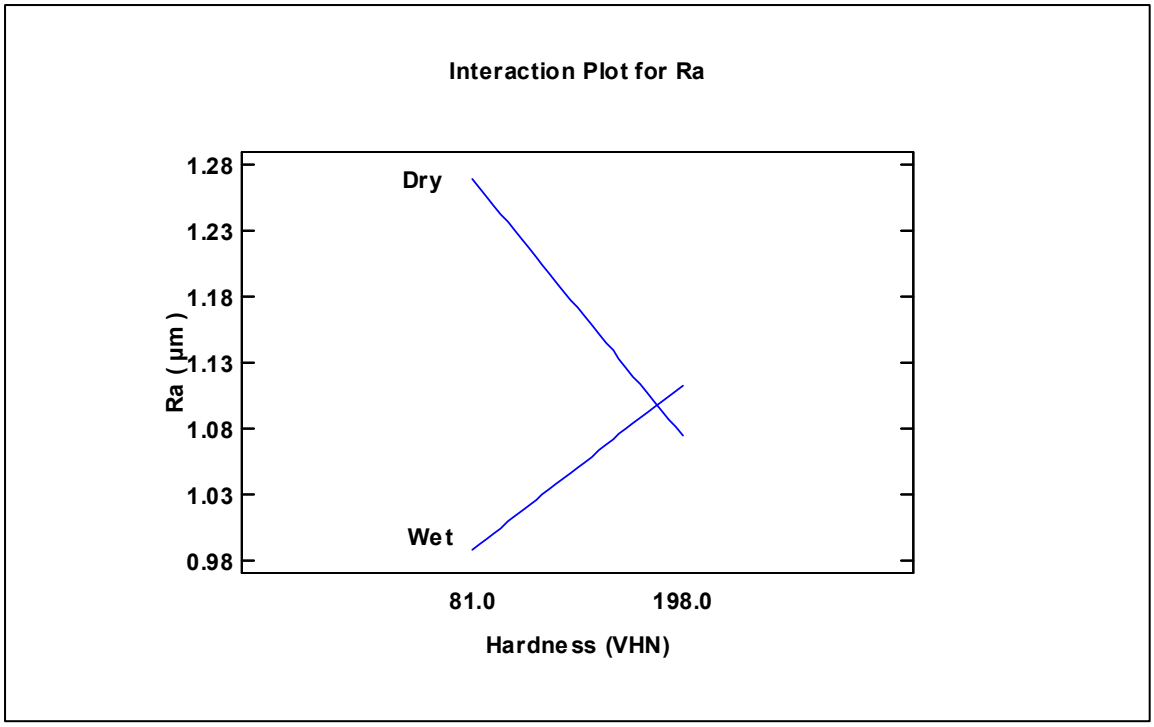

Figure 4.12 Interaction plot for Ra in machining of Al 7075-Li-Sc

Main effect plots and interaction plots provide valuable insights into how variables and their interactions affect the response variable, while other independent variables are typically held constant at their mid-levels. These plots are instrumental in gaining a comprehensive understanding of how variations in independent variables impact the outcomes.

For instance, as illustrated in Figure 4.12, the minimum roughness value of 0.99 μm is observed for the surface of the softest workpiece when machined under wet conditions. It's important to note that this roughness value is associated with a mid-level feed rate, and it does not represent the absolute lowest roughness among the series of tests conducted on this alloy. To achieve a complete understanding of the roughness levels under different conditions, including both the highest and lowest roughness values, 3D surface plots become invaluable. These plots not only provide a visualization of the data but also offer crucial insights into the optimal parameter settings for achieving desired outcomes.

As demonstrated in Figure 4.13, b, the lowest roughness value achieved is 0.5 μm. This level of roughness is attained under the lowest feed rate and cutting speed settings (0.05 mm/th and 200 m/min) for the 81 VHN workpiece when machined under wet conditions.

As depicted in Figure 4.13, d, when machining the hardest Al 7075-Li-Sc material with a hardness of 198 VHN under wet conditions, a roughness level of nearly 1.7 μm is attained. This outcome is achieved by utilizing a high feed rate (0.15 mm/th) and a low cutting speed (200 mm/min).

Another interesting conclusion that can be drawn from the 3D surface plot is that, given the relatively insignificant impact of cutting speed and its potentially positive effect on surface quality, it becomes possible to reduce the feed rate, which significantly influences roughness variation, while simultaneously increasing the cutting speed.

As a result, it is feasible to achieve lower roughness levels while maintaining a high enough chip removal rate, a crucial criterion for meeting industry standards.

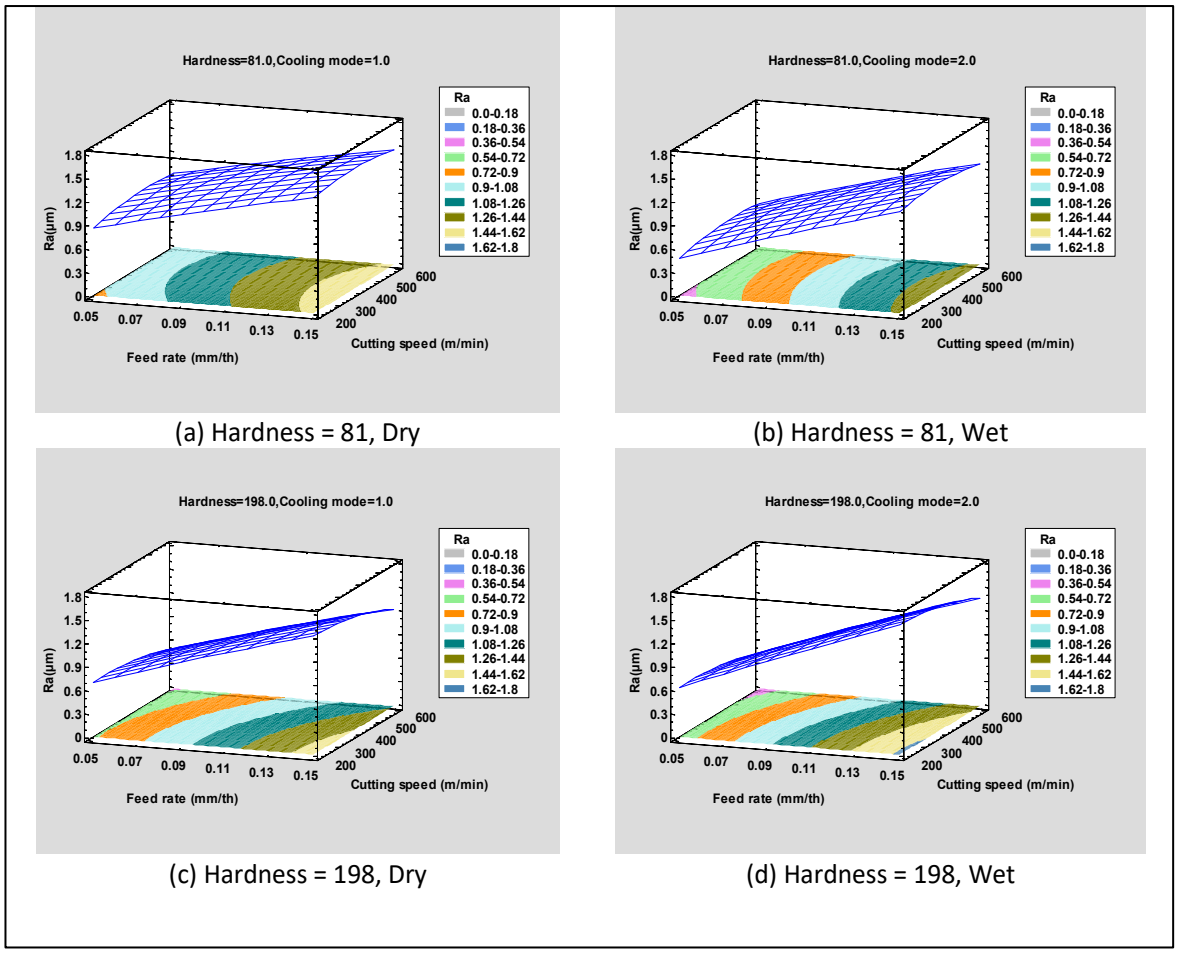

Figure 4.13 3D surface plots of Ra in different hardness and cooling mode for Al 7075– Sc – Li

4.2.4 Effect of alloying on surface roughness

To facilitate a comparison among these three alloys and to examine the influence of alloying on machined surface roughness, we conducted an additional statistical analysis.

Since the hardness levels were not uniform across these alloys, we made the decision to investigate the impact of two different heat treatments, categorized as heat treatment number 2 (24 hours @ 120°C) for achieving the highest hardness and heat treatment number 3 (8 hours @ 280°C) for the lowest hardness, as factors affecting roughness.

The model explains 89.67% of the variability in Ra based on variations in three categorical factors, including Cooling mode, Material, and heat treatment, and two quantitative factors, feed rate, and cutting speed.

The ANOVA table for this analysis is presented in Table AII.4 in Appendix II. As observed in the Pareto chart (Figure 4.14) and the main effect plot (Figure 4.15), feed rate, material, and the type of heat treatment exhibit the most significant effects on Ra when considering all alloys.

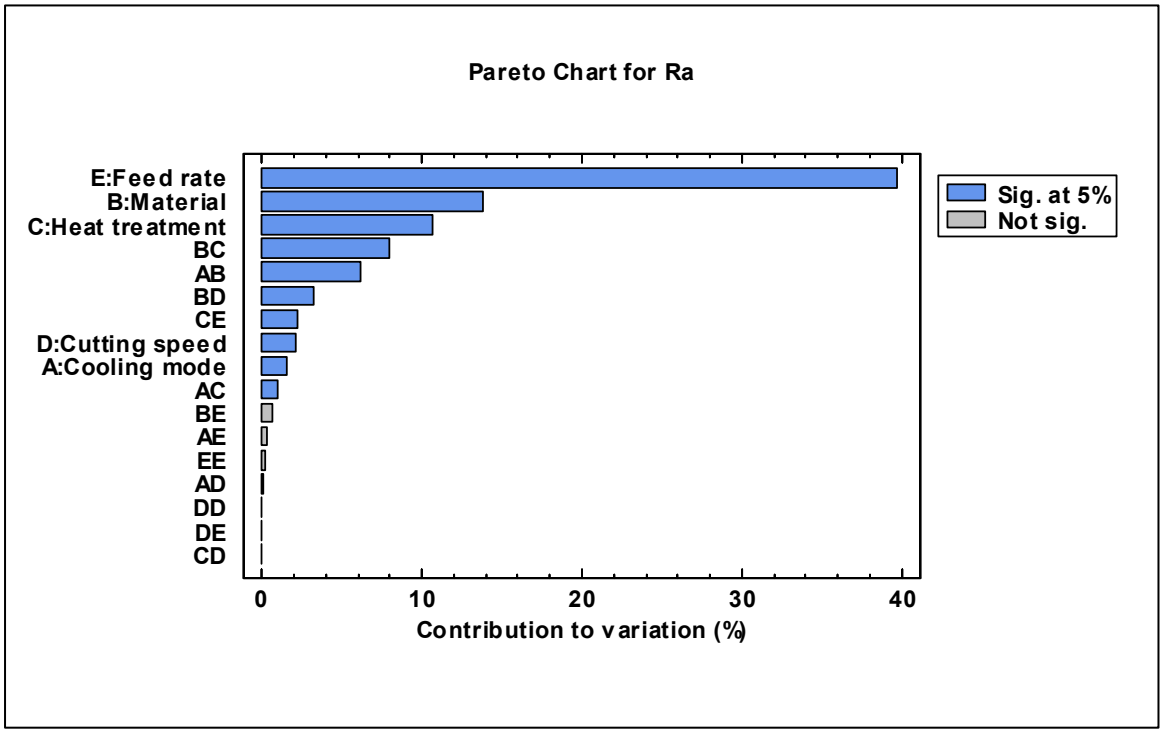

Figure 4.14 Pareto chart of Ra for regarding to all three alloys

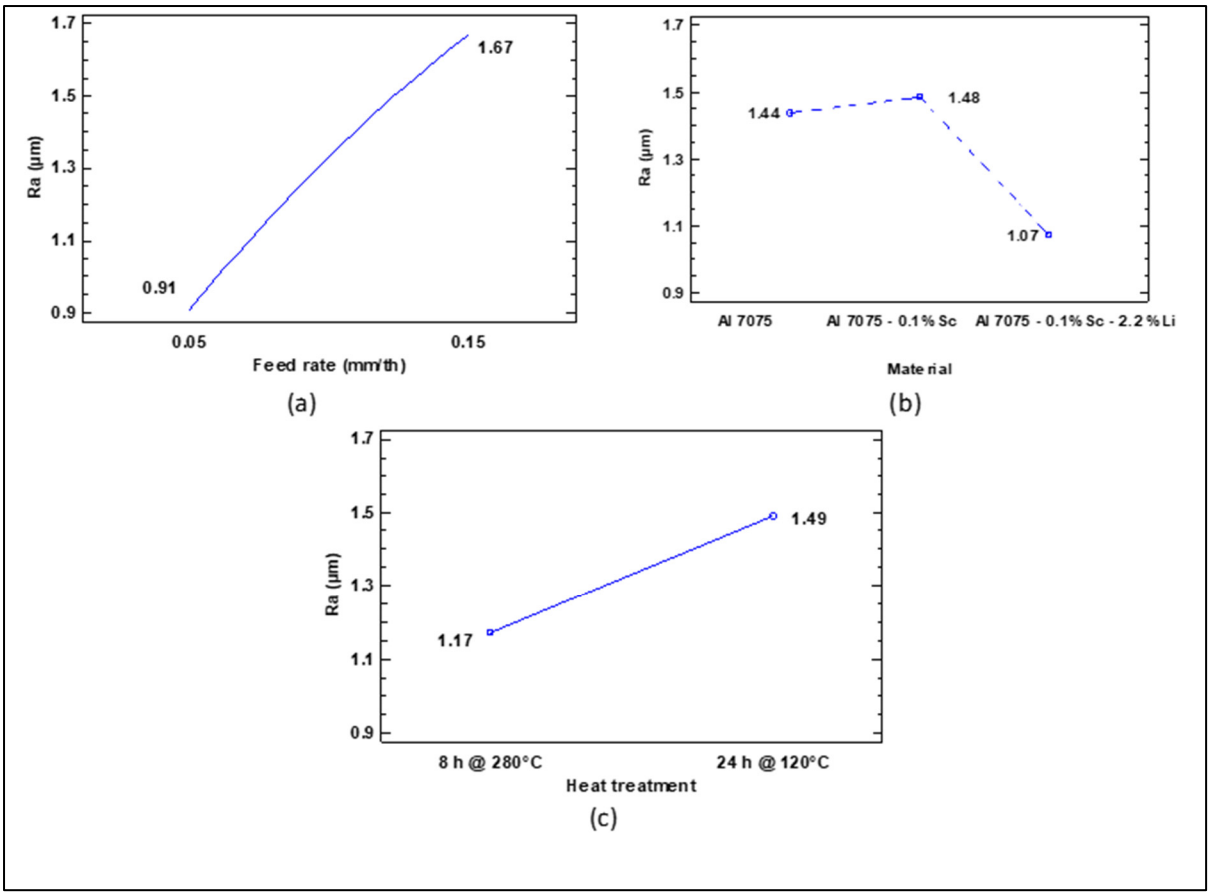

Figure 4.15 Main effects plot for Ra in machining of all three alloys

Based on the main effect plot illustrated in Figure 4.15(b), when other independent parameters are held constant at their mid-levels, the machined surface roughness of Al 7075 and Al 7075 - Sc doesn't show notable differences.

However, in the case of Al 7075-Li-Sc, the addition of 2.2% Li to Al 7075 - Sc leads to a significantly improved surface quality, with Ra decreasing from 1.48 to 1.07 micrometers.

The effect of alloying on roughness becomes much more significant when the alloys undergo different heat treatments.

As demonstrated in the interaction plot (Figure 4.16), when the alloys are subjected to an 8-hour heat treatment at 280°C, which results in the lowest hardness for all alloys, the impact of alloying is not significant.

However, after precipitation hardening for 24 hours at 120°C, the story changes dramatically. It's worth noting that the sample Al 7075 - Sc contained almost 1% more Zn, in addition to 0.1% Sc. Consequently, after heat treatment for 24 hours at 120°C, the machined surface roughness of Al 7075 - Sc is approximately 0.4 micrometers higher than that of Al 7075.

However, this extra hardness is offset by the addition of 2.2% Li, resulting in a roughness decrease of nearly 0.6 micrometers, reaching approximately 1.2 micrometers.

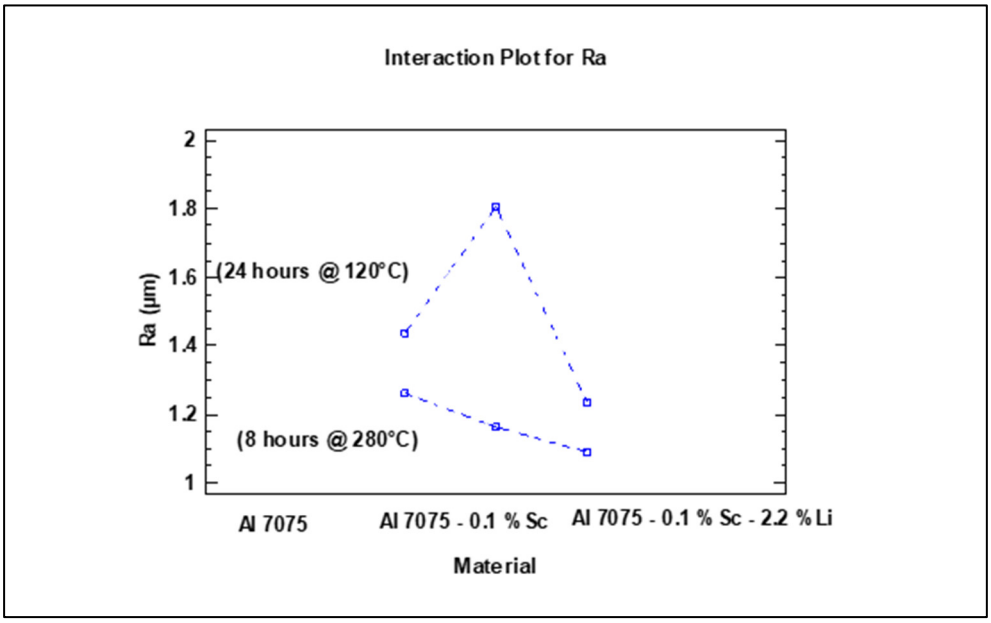

Figure 4.16 Interaction effect of material and hardness on surface roughness

4.3 Cutting force analysis

The evaluation of machinability often revolves around two primary criteria: cutting force and surface roughness. Among these, cutting force stands out as a pivotal parameter for optimizing machining performance. The reduction of cutting force under specific cutting conditions can enhance machinability significantly. Notably, a decrease in cutting force correlates with improved dimensional accuracy and reduced tool wear rates throughout the machining process (Marani, Songmene et al. 2020).

Furthermore, it is essential to consider that the periodically varying cutting force has a direct impact on cutting heat, thereby exerting a critical influence on tool wear and the overall quality of the machined surface. This phenomenon is particularly relevant in milling processes, which are characterized by multi-tooth discontinuous cutting (Meng, Lin and Mi 2021).

There are many factors affecting cutting force. some of these factors include alloying elements, impurities, casting process, heat treatment, machine tool rigidity, and cut-ting tool geometry. through the cutting parameters depth of cut and feed rate have the most significant effect on the cutting force enhancement since the effective area of shear per tooth increases with increase in depth of cut and feed rate. An increase in cutting speed, associated with elevated temperatures, leads to a reduction in shear strength, ultimately resulting in a decrease in cutting force (Pathak, Sahoo and Mishra 2013).

Hardness, a factor influenced by hardening precipitation, serves as a key determinant of mechanical properties. It's worth noting that higher hardness levels are associated with increased cutting forces. totally When processing materials with high mechanical properties, it is common to encounter elevated cutting forces, which, in turn, can lead to higher temperatures (Gupta, Korkmaz et al. 2022). The incorporation of lubricants into the machining process improves tribological performance by lowering the coefficient of friction, diminishing cutting forces, and mitigating tool wear. This decrease in cutting force necessitates a reduced demand for specific cutting energy, consequently lowering production costs (Shankar, Mohanraj and Ponappa 2017).

In the upcoming section, we will perform a statistical analysis of the cutting force results. This analysis will explore the influence of workpiece properties, specifically microhardness, as well as various process parameters, such as feed rate, cutting speed, and cooling mode, on machining conditions.

4.3.1 The statistical analysis of cutting force in machining of Al 7075

An ANOVA analysis has been conducted on cutting force results presented in Table AI.4, to investigate the effects of independent variables, including feed rate, cutting speed, microhardness, and cooling mode, on cutting force during the milling of Al 7075. The model accounts for 89.9% of the variation in cutting force based on the mentioned inputs. Further details of the ANOVA analysis are provided in Table AII.5. In the machining of Al 7075, as depicted in Figure 4.14 and 4.18a, the feed rate exhibits the most significant positive influence on cutting force, showing an impressive enhancement of approximately 65 N across the range of 0.05 to 0.15 mm/th.

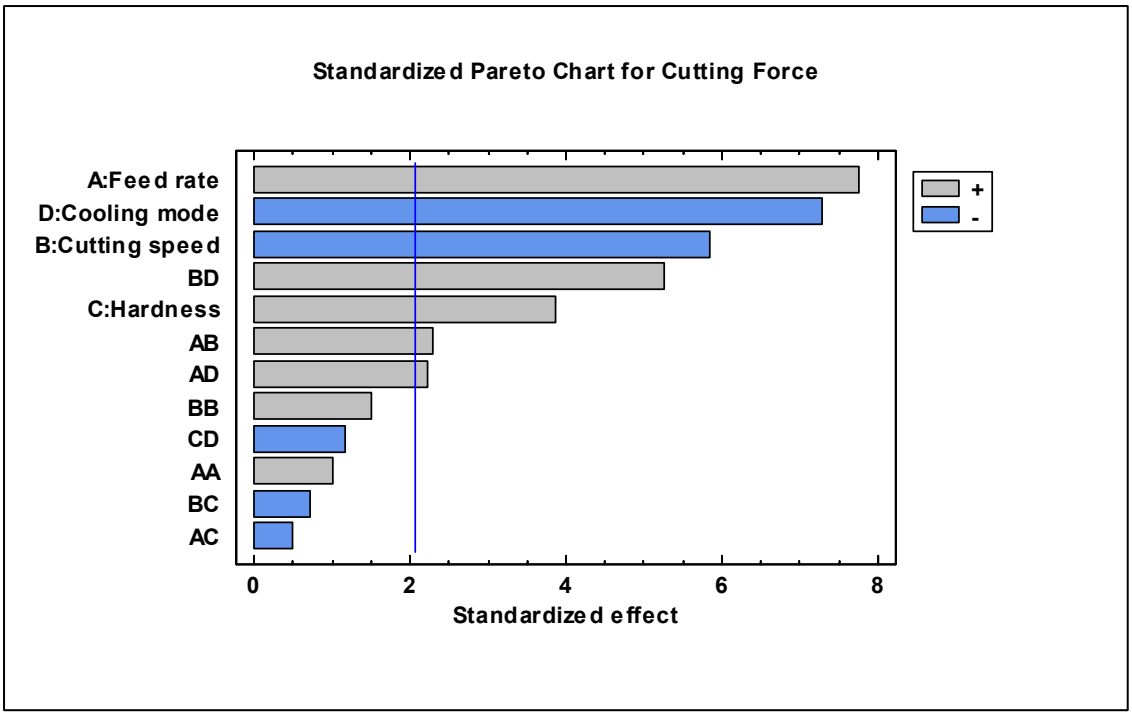

Figure 4.17 Pareto chart of cutting force for Al 7075

When machining under wet conditions, there is a notable reduction in cutting force by approximately 50 N, with all other parameters held constant, as illustrated in Figure 4.18b.

The use of cutting fluid in the machining process leads to a decrease in the coefficient of friction, resulting in a reduction in cutting force. The third parameter significantly affecting cutting force in Al 7075 machining is cutting speed.

As depicted in Figure 4.18, c, when the cutting speed increased from 200 to 600 m/min, the cutting force decreased from 156.7 to 108 N. Two primary reasons can be mentioned to justify this phenomenon. Firstly, the higher heat generated during machining at higher cutting speeds softens the workpiece in the cutting zone, reducing shear strength. Secondly, at higher cutting speeds, the chip length is shorter, resulting in a shorter actual contact length compared to the natural contact length (Pathak, Sahoo and Mishra 2013).

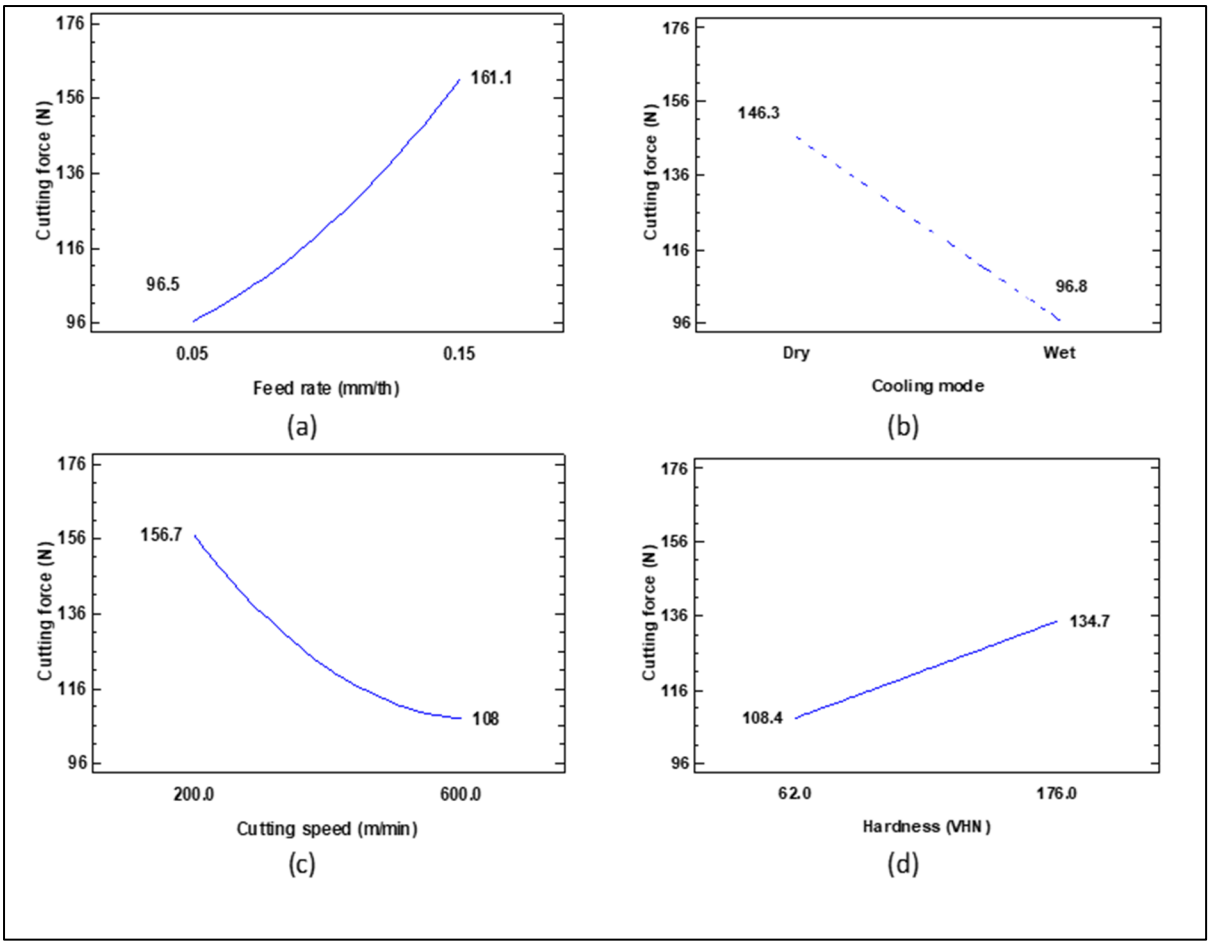

Figure 4.18 Main effects plot for cutting force in machining of Al 7075

The direct impact of hardening on cutting speed is also notable. In the case of hard Al 7075 with a hardness of 176 VHN, the cutting force is approximately 26 N higher compared to the soft condition with a hardness of 62 VHN (see Figure 4.18d).

In terms of the interaction effect between the independent variables, the interaction between cutting speed and cooling mode proved to be significant.

As illustrated in Figure 4.19, at low cutting speeds (200 m/min), the cutting force is approximately 100 N higher in dry machining compared to wet machining. However, at high cutting speeds (600 m/min), there is almost no difference in the cutting force observed between dry and wet machining conditions for Al 7075.

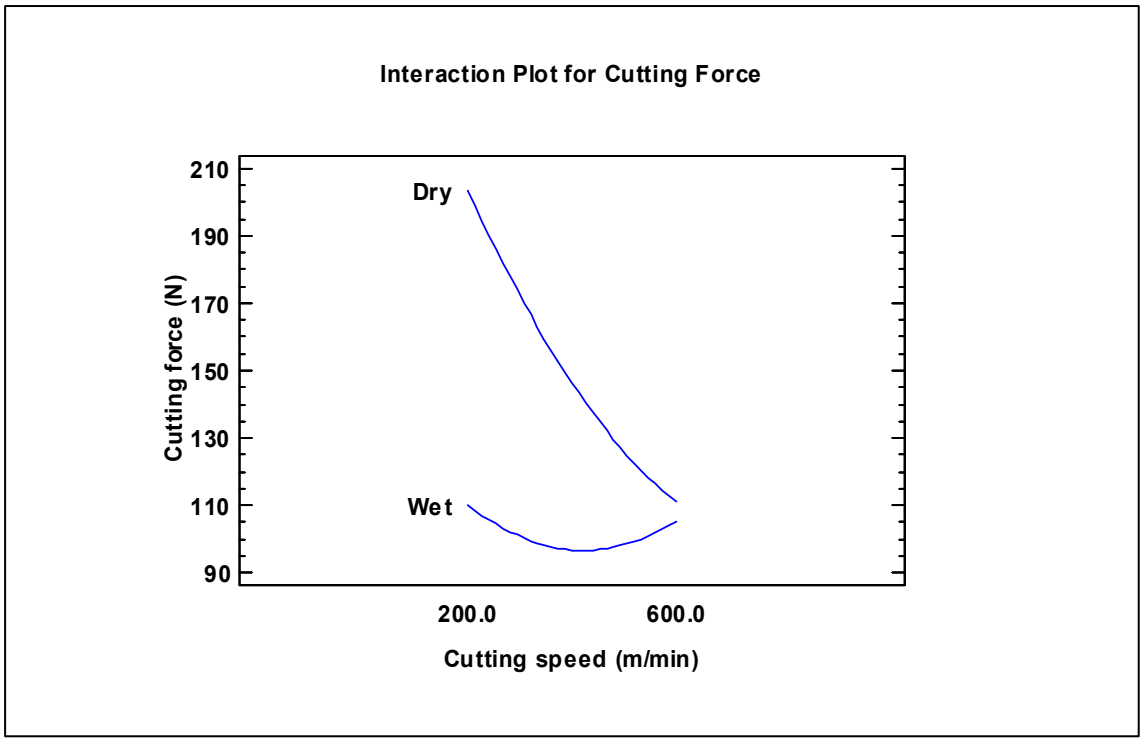

Figure 4.19 Interaction plot for cutting force in Al 7075 machining

This finding reveals that the use of cutting fluid at low speeds is beneficial and significantly reduces cutting forces. However, in high-speed machining, wet machining is nearly ineffective in reducing cutting forces. Figure 4.20 depicts a 3D surface plot illustrating the cutting force during the machining of Al 7075.

In dry machining, as observed in sections (a) and (c) of the figure, cutting force exhibits greater sensitivity to variations in cutting speed, while in wet machining, an increase in feed rate has a more significant impact on increasing the cutting force.

It can also be observed that, overall, the level of cutting force is significantly lower in wet conditions, particularly when machining harder alloy.

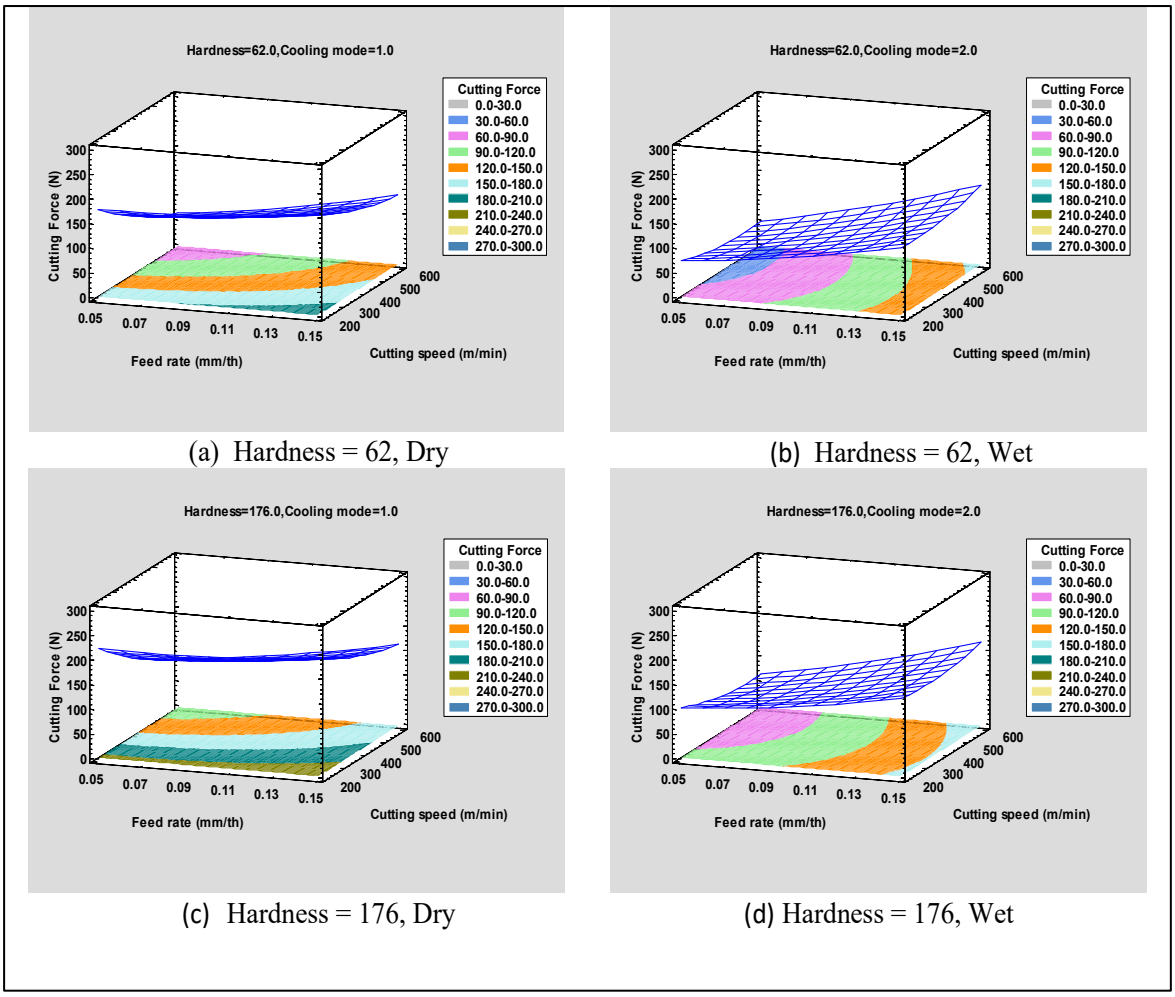

Figure 4.20 3D surface plots of cutting force in different hardness and cooling mode for Al 7075

From the visually illustrated results in Figure 4.20, the conditions associated with both the highest and lowest cutting forces can be observed.

In Al 7075 with a hardness of 62 VHN, the highest cutting force (almost 200 N) was recorded during machining with a feed rate of 0.15 mm/th and a cutting speed of 200 m/min in dry condition, and lowest force was almost 54 N achieved during wet machining with a feed rate of 0.05 mm/th and a cutting speed of 600 m/min. in terms of Al 7075 with hardness 176 VHN the highest and lowest amount of cutting force has been recorded in the exact same conditions with 73 and 233 N respectively.

4.3.2 The statistical analysis of cutting force in machining of Al 7075 – Sc

The cutting force results obtained from Al 7075 - Sc machining is presented in Table AI.5 in the APPENDIX section.

The R-squared value obtained from the statistical analysis on the cutting force results is 93.4%, indicating that the model explains nearly 93% of the variation in cutting force based on the examined variables.

The details of the ANOVA parameters are presented in Table AII.6.

In Al 7075 - Sc machining, the feed rate stands out as having the most significant impact on cutting force, as depicted in the Pareto chart (Figure 4.21). Following feed rate in order of significance are cooling mode, hardness, and cutting speed, that each one has approximately half the effect of feed rate.

The direct effect of increasing the feed rate on cutting force, as shown in Figure 4.22, resulted in nearly a 48 N increase in force when the feed rate was raised from 0.05 to 0.15 mm/th.

Both the Pareto chart and the main effect plot indicate that using a high level of cutting fluid in machining Al 7075 - Sc is beneficial for reducing cutting force. According to Figure 4.22, this reduction was approximately 20 N when machining under wet conditions compared to dry machining.

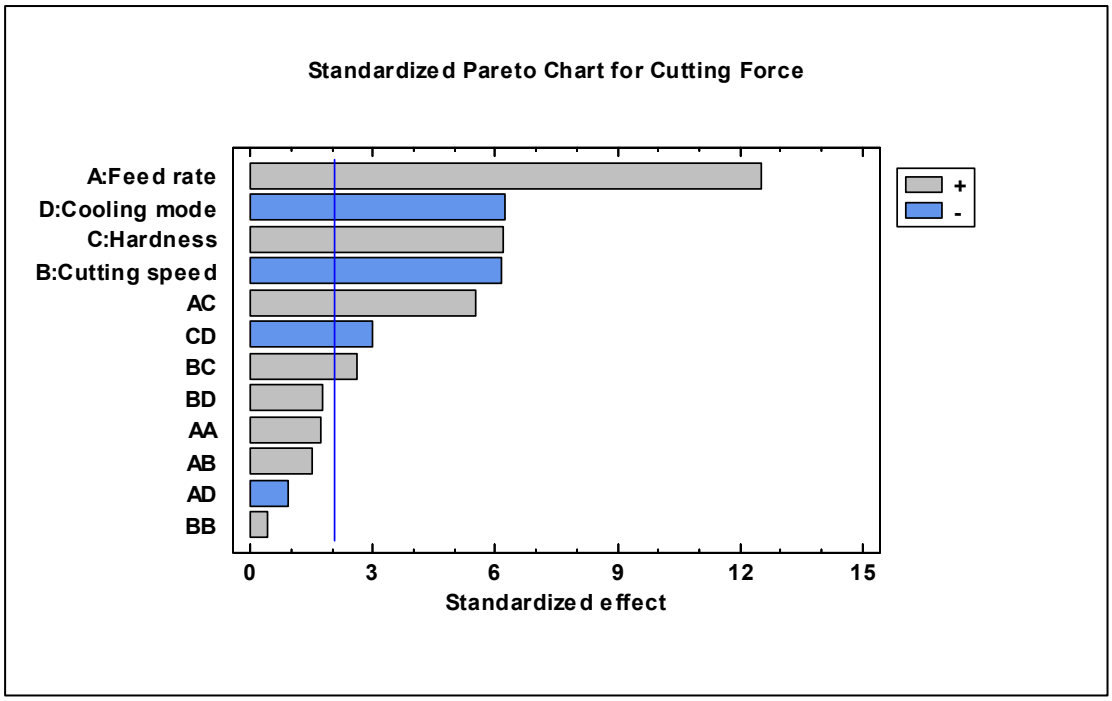

Figure 4.21 Pareto chart of cutting force for Al 7075 – Sc

Alloy hardness significantly affected cutting force, with machining the softest condition of Al 7075 - Sc (achieved by heat treating for 8 hours at 280°C) requiring nearly 20 N less cutting force compared to the hardest alloy (heat treated for 24 hours at 120°C) with a cutting force of 129 N.

As expected, cutting speed also had a significant impact on reducing cutting force. Increasing the cutting speed from 200 to 600 m/min resulted in a reduction in cutting force from 132.5 to 109 N.

The interaction plot in Figure 4.23 highlights the amplified impact of feed rate in high hardness condition of the alloy. As shown in the plot, machining both hardness levels at a low feed rate (0.05 mm/th) required approximately 100 N of cutting force.

However, when machining the hard alloy with the high feed rate (0.15 mm/th), it needed more than 40 N additional cutting force compared to machining the soft alloy, which required nearly 130 N of cutting force.

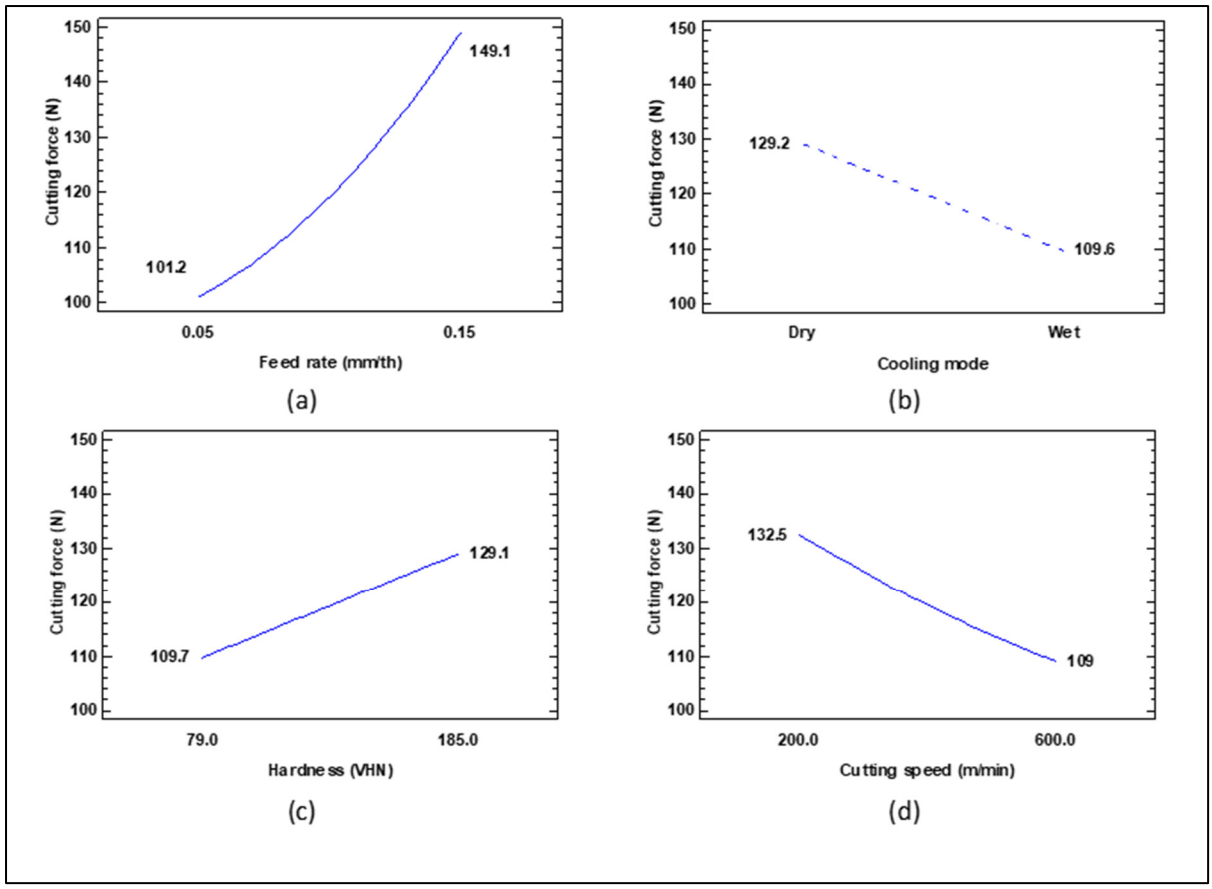

Figure 4.22 Main effects plot for cutting force in machining of Al 7075 - Sc

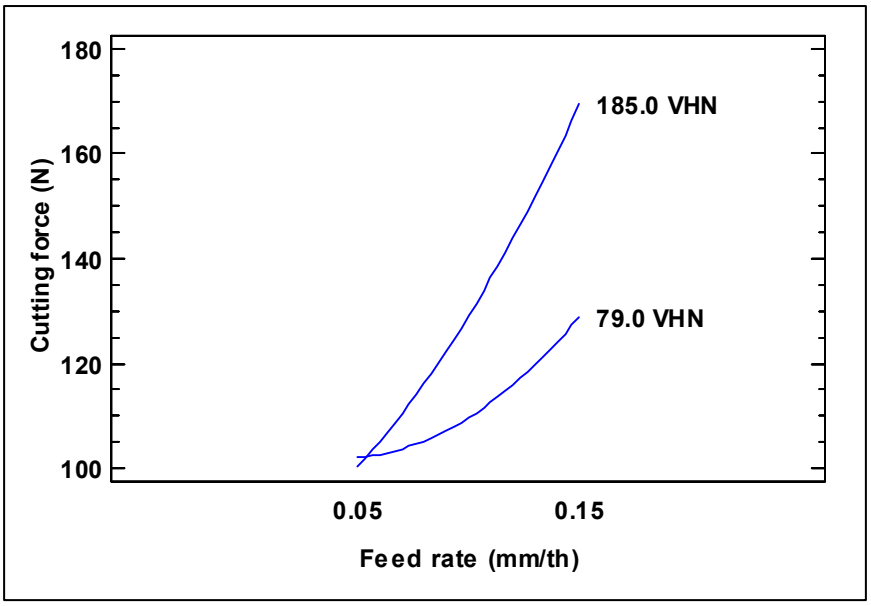

Figure 4.23 Interaction plot for cutting force in Al 7075 - Sc machining

One point that can be drawn from the 3D surface plots (Figure 4.24, (a) and (b)) is that the negative effect of cutting speed is more pronounced in the soft alloy, especially in dry condition. Although the effect of cutting speed is not as significant in hard alloy machining, its impact is still noticeable in dry machining.

The 3D surface plots (Figure 4.24, (a) and (b)) also shows that the negative effect of cutting speed is more pronounced in the soft alloy, especially in dry condition. Although the effect of cutting speed is not as significant in hard alloy machining, its impact is still noticeable in dry machining.

The heightened impact of feed rate on cutting force in hard Al 7075 - Sc is evident in the 3D surface plots (Figure 4.24, (c) and (d)), where the steep inclination of the plot sharply increases with an increase in feed rate.

The highest cutting force in the machining of soft Al 7075 - Sc with a hardness of 79 VHN was associated with the highest feed rate (0.15 mm/th) and the lowest cutting speed (200 m/min) in dry conditions, resulting in 163 N. Conversely, the lowest cutting force, approximately 80 N, was observed in both dry and wet machining with the lowest feed rate (0.05 mm/th) and the highest cutting speed (600 m/min).

The machining of the hardest Al 7075 - Sc alloy, with a hardness of 185 VHN, yielded the highest cutting force when using the highest feed rate (0.15 mm/th) and the lowest cutting speed (200 m/min) in dry conditions, resulting in a force of 191 N. In contrast, the lowest cutting force (81 N) was observed during wet machining with the lowest feed rate (0.05 mm/th) and the highest cutting speed (600 m/min). It's worth noting that using the same cutting parameters (cutting speed and feed rate) in dry machining resulted in a force of nearly 110 N. This highlights the remarkable impact of wet machining on the hard Al 7075 - Sc alloy.

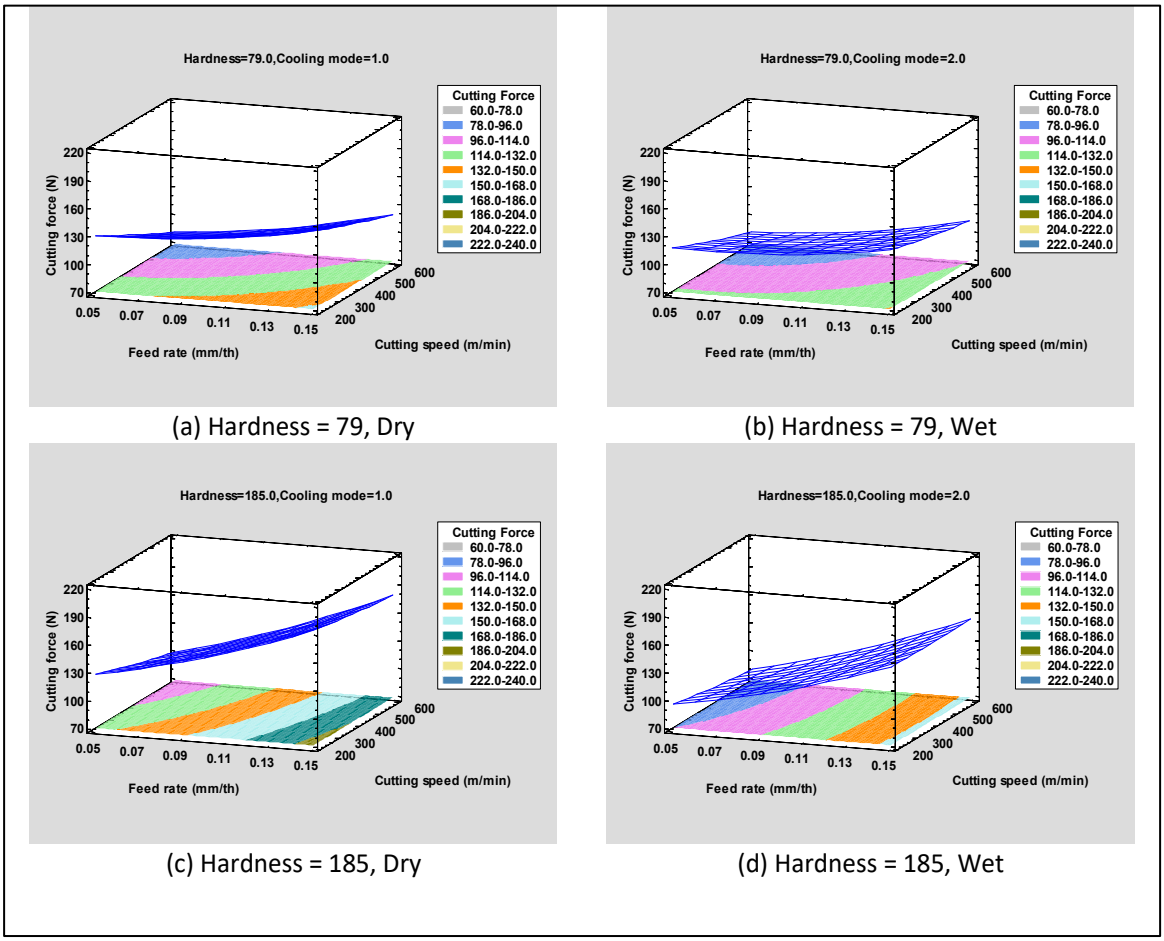

Figure 4.24 3D surface plots of cutting force in different hardness and cooling mode for Al 7075 - Sc

4.3.3 The statistical analysis of cutting force in machining of Al 7075-Li-Sc

An ANOVA analysis was conducted on the cutting force results obtained from the machining of Al 7075-Li-Sc, which are presented in Table AI.6. This analysis was carried out to investigate the impact of independent variables, including feed rate, cutting speed, microhardness, and cooling mode, on cutting force. The model successfully explains 94.8% of the variations in cutting force attributed to these input factors. Further details of the ANOVA analysis can be found in Table AII.7.

Like two other alloys in the machining of Al 7075-Li-Sc, feed rate emerges as the most significantly influential factor affecting the variation in cutting force. This observation is evident from the Pareto chart depicted in Figure 4.25. According to the main effect plot (Figure 4.26, a), machining with the high feed rate (0.15 mm/th) resulted in a cutting force approximately 54 N higher compared to machining with a low feed rate (0.05 mm/th), where the cutting force measured 101.2 N.

The hardness in machining of Al 7075-Li-Sc had more significant effect on the cutting force compared to machining of Al 7075 - Sc. as seen in figure 4.26, b the cutting force in the machining of soft alloy with 81 VHN and hard one with 198 VHN was 107.6 and 143.6 N respectively.

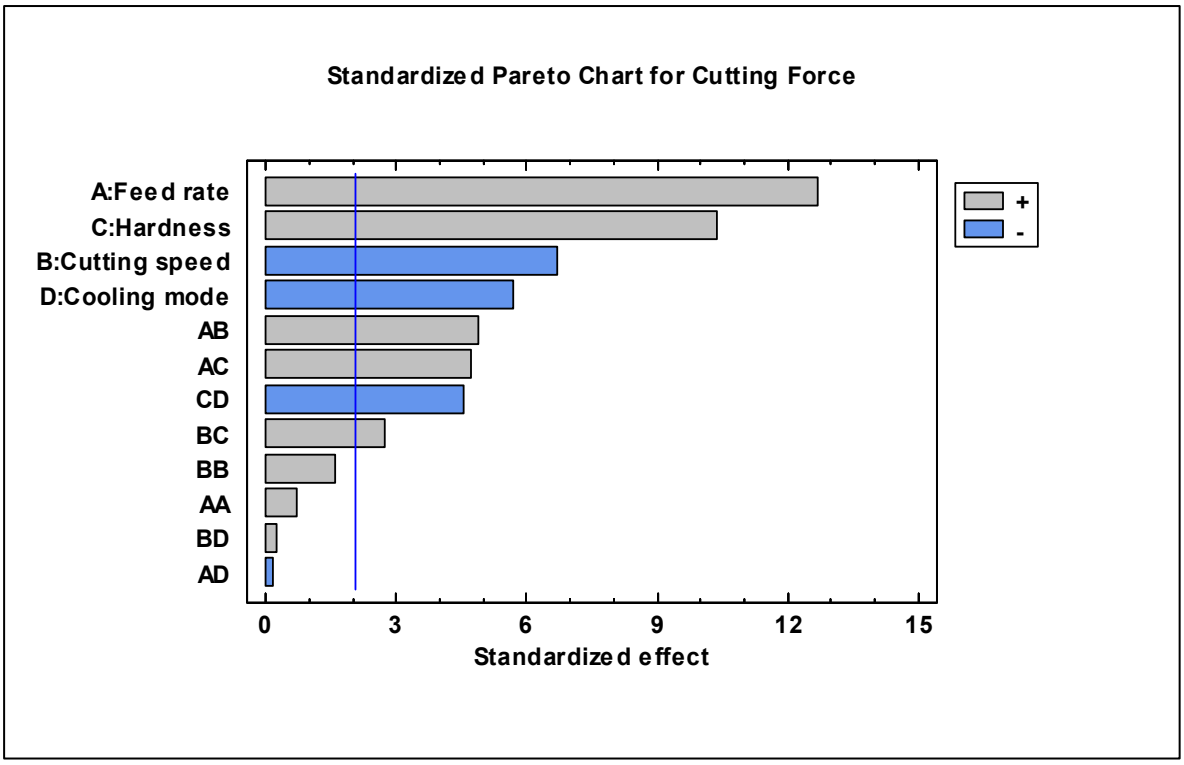

Figure 4.25 Pareto chart of cutting force for Al 7075-Li-Sc

When comparing the cutting forces in the machining of Al 7075 - Sc and Al 7075-Li-Sc, it becomes evident that the effect of hardness between the hard and soft conditions on cutting force is more pronounced in Al 7075– Li - Sc. This is attributed to the presence of lithium in the alloy's structure, which increases its hardness during heat treatment for 24 hours at 120°C. As shown in Figure 4.22, c and Figure 4.26, b, the cutting forces are nearly identical under soft conditions in both alloys, with Al 7075 - Sc and Al 7075-Li-Sc having similar hardness values of 81 VHN and 79 VHN, respectively. However, in the machining of hard alloys, the cutting force is approximately 14 N higher in Al 7075-Li-Sc (198 VHN) compared to Al 7075 - Sc (185 VHN).

Both cutting speed and the use of cutting fluid in machining had a significant impact on reducing cutting force. As depicted in Figure 4.26, c, machining this alloy at 600 m/min resulted in a cutting force of 117.2 N, while machining at 200 m/min led to a cutting force of 145.6 N. As

depicted in Figure 4.26, part d, employing wet machining for Al 7075-Li-Sc led to a reduced cutting force compared to dry machining, with cutting forces of 115.7 and 135.5, respectively.

Interestingly, feed rate, hardness, cutting speed, and cooling mode had a more significant impact on the variation of cutting force compared to their interactions.

The interaction between feed rate and cutting speed had a positive and significant effect on cutting force. This implies that increasing the feed rate had a more pronounced effect on variation of cutting force when the cutting speed was higher. As shown in Figure 4.27a, while the cutting force remained the same at high cutting speeds for both high and low feed rates, in the case of low feed rate, machining at 600 m/min resulted in a nearly 50 N lower cutting force compared to machining at 200 m/min.

In the context of the interaction between feed rate and hardness, as illustrated in Figure 4.27, b, the effect of feed rate on cutting force was more pronounced in harder workpieces. At a low feed rate (0.05 mm/th), the cutting force in machining the alloy with 198 VHN was approximately 20 N higher than that for the alloy with 81 VHN. However, this difference increased to 60 N when machining with a feed rate of 0.15 mm/th.

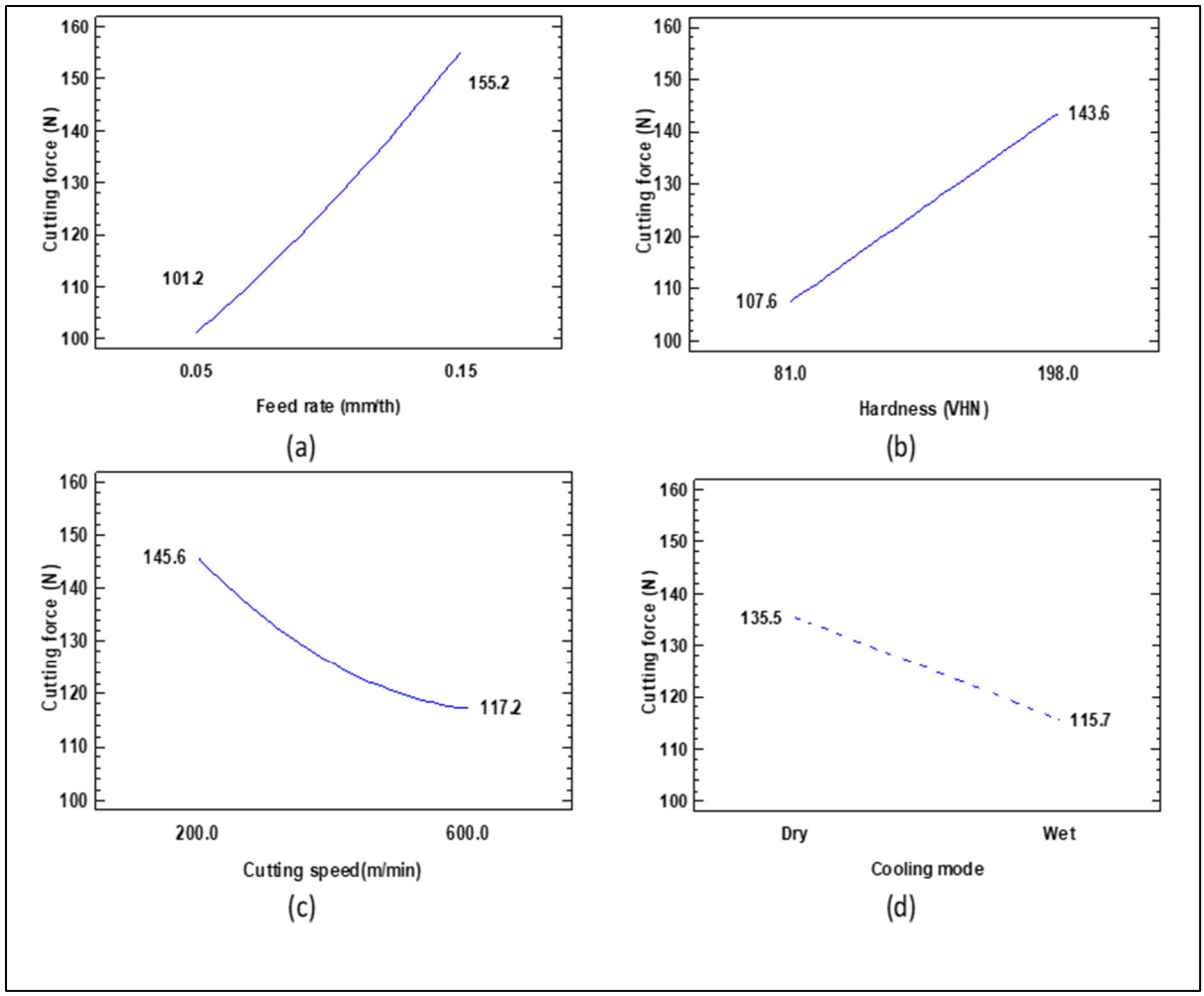

Figure 4.26 Main effects plot for cutting force in machining of Al 7075-Li-Sc

Although the cutting force was higher in the harder workpiece during machining of Al 7075-Li-Sc, machining in dry conditions intensified this effect compared to wet machining, as depicted in Figure 4.27c. High-speed machining of this alloy reduces cutting force in both hard and soft workpieces, with a more substantial reduction observed in the soft material.

In Figure 4.27d, it is evident that the cutting force decreased less than 20 N when cutting speed increased from 200 to 600 m/min in the hard alloy (198 VHN), while this decrease in the soft sample (81 VHN) was approximately 40 N. As observed in 3D Surface plots (Figure 4.28, a and b), the cooling mode's effect on cutting force was not significant in the soft workpiece of

Al 7075-Li-Sc. Alternatively, when comparing Figure 4.28, c and d, the importance of utilizing cooling fluid became apparent during the machining of the hard Al 7075-Li-Sc alloy.

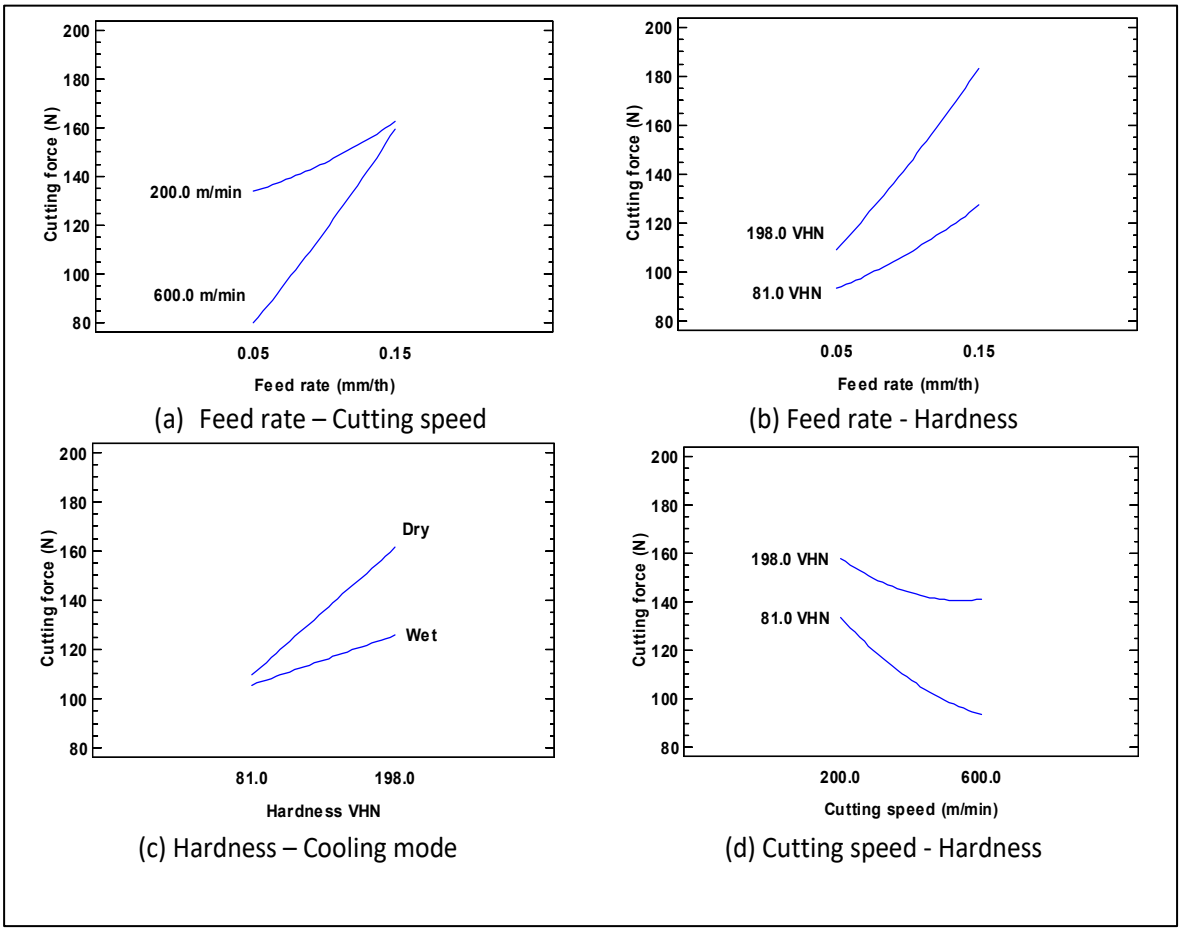

Figure 4.27 Interaction plot for cutting force in Al 7075-Li-Sc machining

Based on 3D surface plots, the effect of feed rate on cutting force in soft condition was minimal, but a significant reduction in cutting force occurred with an increase in cutting speed, especially at lower feed rates. This highlights the significant impact of the interaction between feed rate and cutting speed. While the feed rate had an insignificant effect on cutting force during the machining of the soft alloy, it displayed a much more pronounced impact on cutting force in the case of the hard Al 7075-Li-Sc alloy. This underscores the positive effect of the interaction between feed rate and hardness.

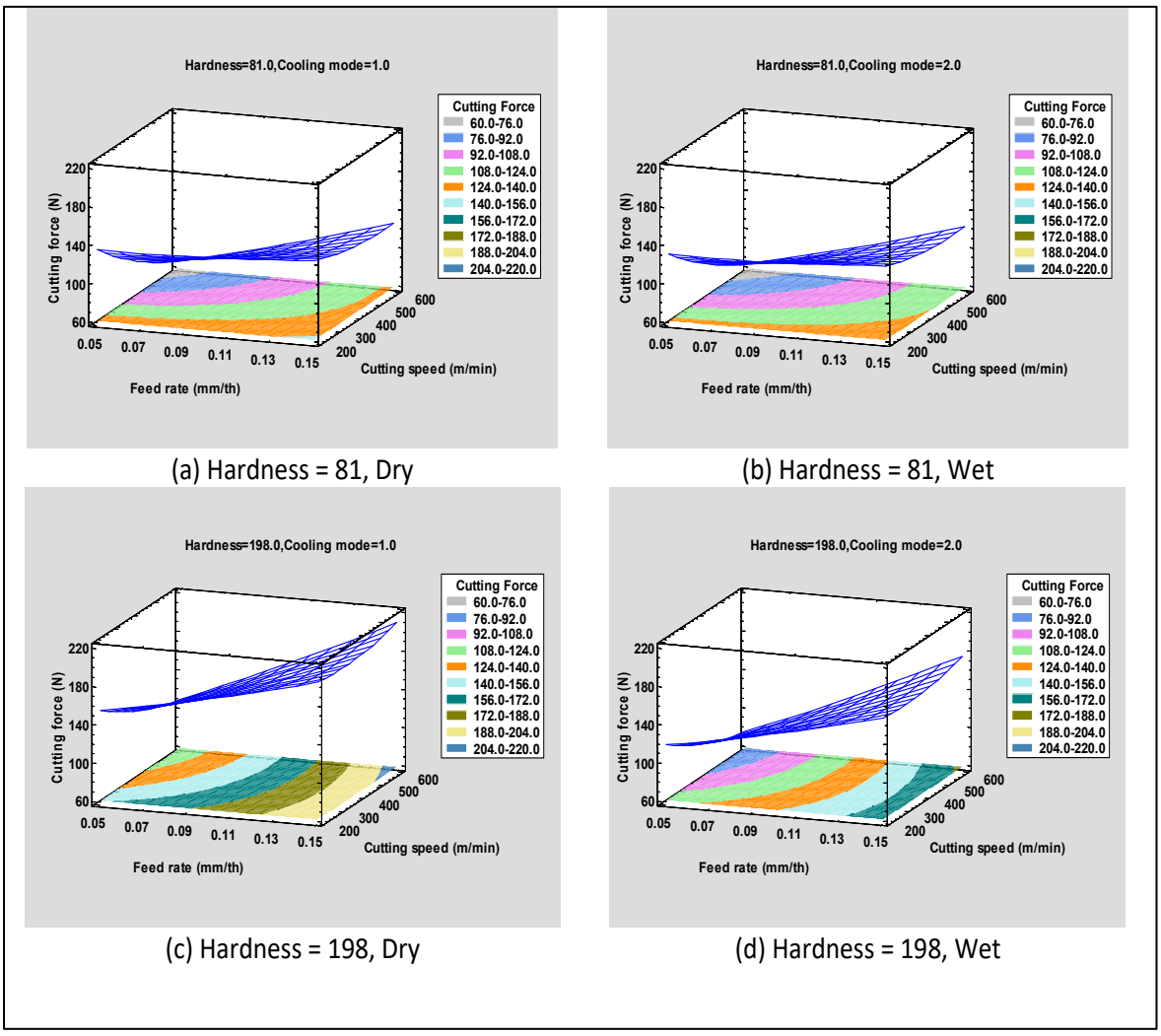

Figure 4.28 3D Surface plots of cutting force in different hardness and cooling mode for Al 7075-Li-Sc

The minimum cutting force level achieved during the machining of Al 7075-Li-Sc was observed when machining the soft alloy under both dry and wet conditions with the lowest feed rate (0.05 mm/th) and highest cutting speed (600 m/min), resulting in a cutting force of approximately 63 N. The maximum cutting force level achieved during the machining of Al 7075-Li-Sc was observed when machining the hard alloy under dry conditions with the highest feed rate (0.15 mm/th) and highest cutting speed (600 m/min), resulting in a cutting force of approximately 204 N. While Figure 4.28 c suggests that the maximum force occurred at a

cutting speed of 600 m/min, the results table (Table AI.6) reveals that the exact same cutting force was achieved with the highest feed rate and the lowest cutting speed (200 m/min). This is due to the insignificant effect of cutting speed on cutting force at high feed rates.

4.4 Particle emission analysis

The machining process, the interaction between cutting tools and workpiece materials generates a complex aerosol composed of fine particles, aerosols, and potentially harmful compounds. These emissions, often referred to as machining aerosols, have garnered increasing attention due to their potential impact on the environment, worker health, and product quality.

As depicted in the Pareto chart (Figure 4.29), the cooling mode, cutting speed, and their interaction had a notable impact on the mass concentration of particle emissions across all three alloys.

Just in the case of Al 7075 - Sc, there exists a slight discrepancy where hardness and its interaction with cutting speed and cooling mode exhibit a minor significance regarding the mass concentration of particle emissions during the machining process. This minor influence of hardness is visually depicted in Figure 4.30b, where the variation of mass concentration for hard Al 7075 - Sc remained below 15 mg/m³, suggesting that this effect may be negligible and could be attributed to other factors such as noise factors.

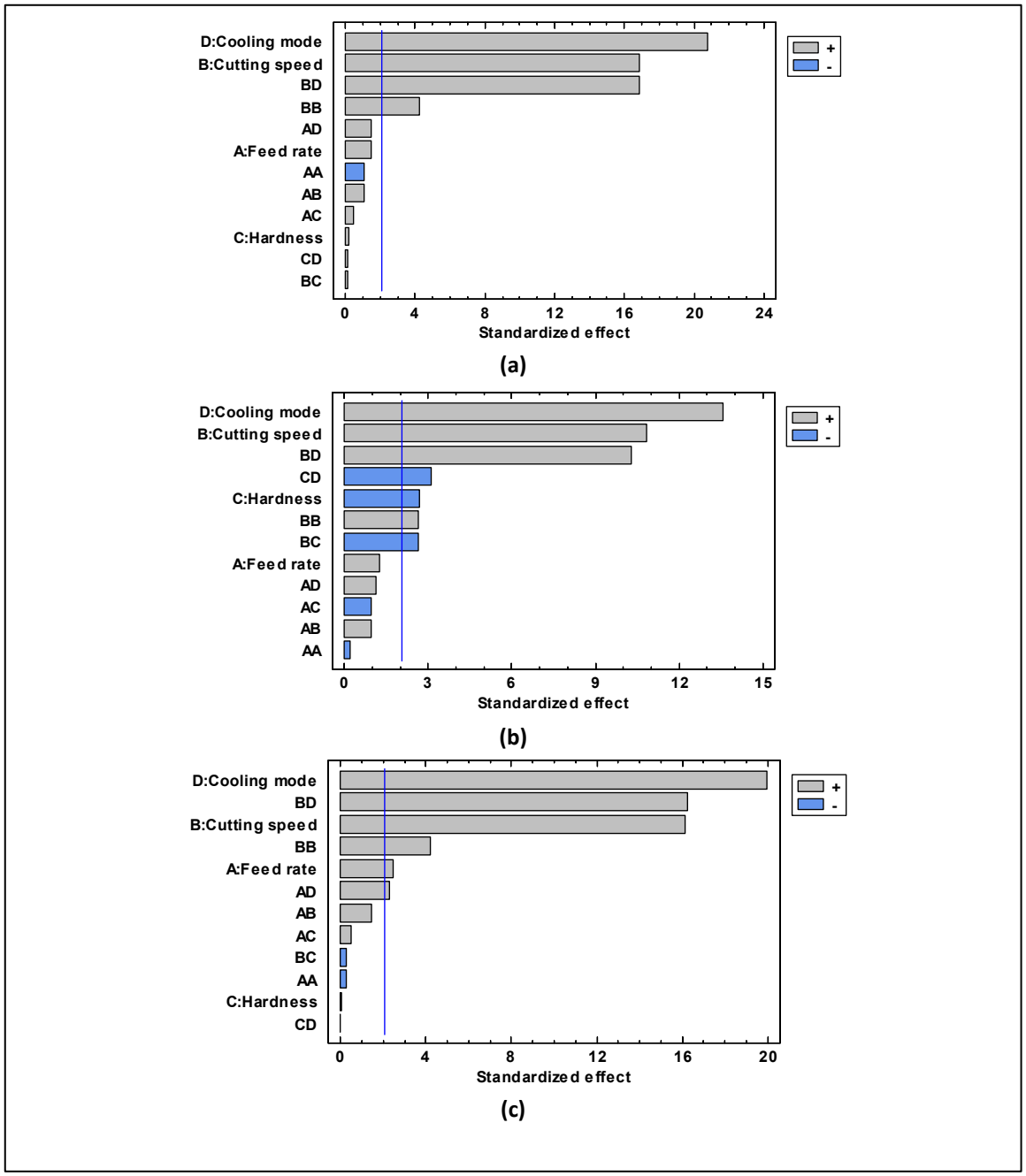

Figure 4.29 Pareto charts of mass concentration for (a) Al7075, (b) Al7075-Sc, (c) Al 7075-Li-Sc

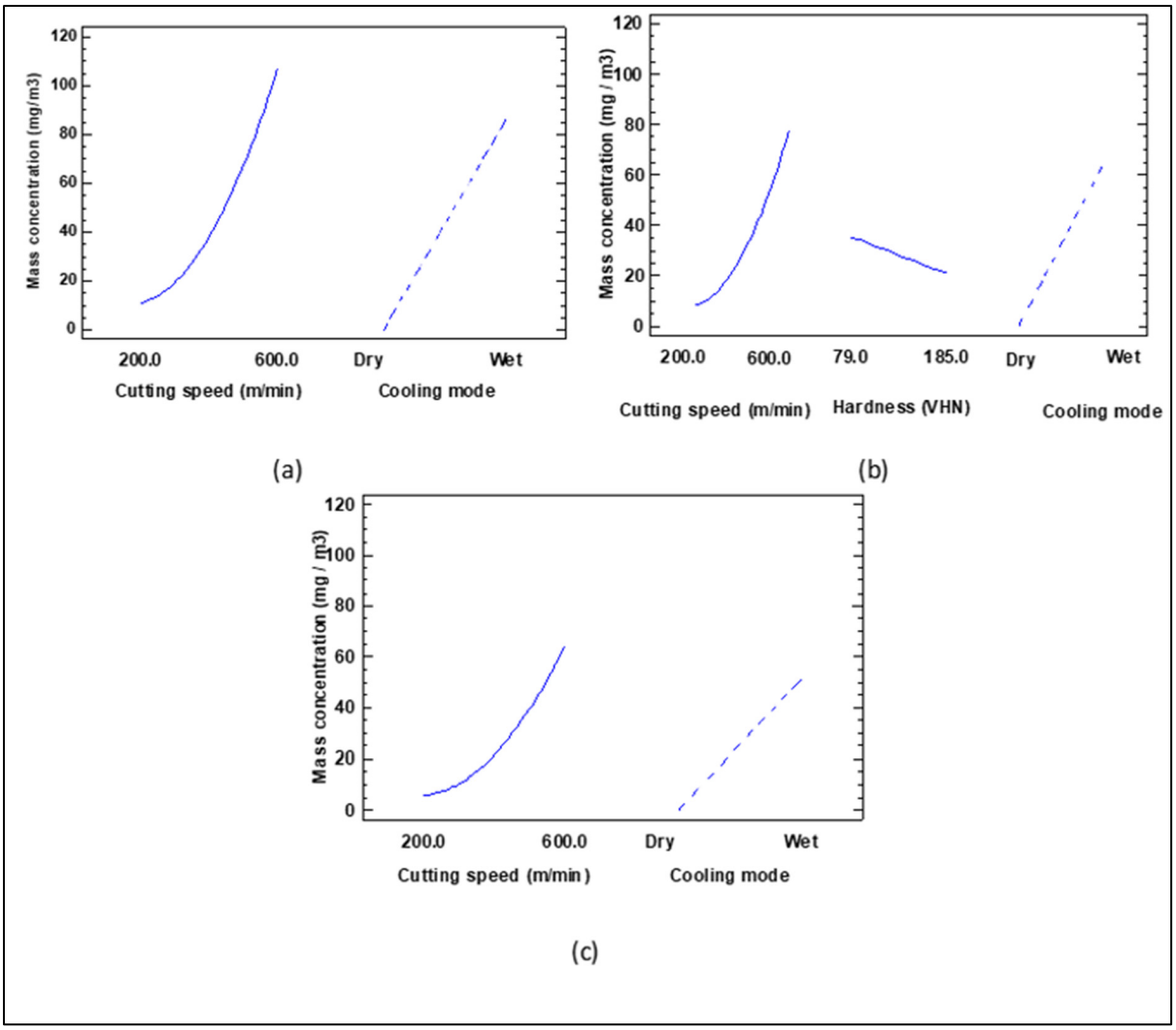

Figure 4.30 Main effects plots for mass concentration of (a) Al 7075, (b) Al 7075 – Sc, (c) Al 7075-Li-Sc

The interaction effects between cutting speed and cooling mode, illustrated in Figure 4.31, emerged as the third significant parameter affecting mass concentration in all three alloys. As depicted in the figure, at a low cutting speed of 200 m/min, in both wet and dry machining, the mass concentration of particle emissions remained around 10 mg/m³ for all three alloys. In dry machining, even at a high cutting speed of 600 m/min, this value remained relatively stable.

However, in wet machining, the mass concentration increased significantly, reaching approximately 200, 150, and 125 mg/m³ for Al 7075, 7075 - Sc, and Al 7075-Li-Sc, respectively.

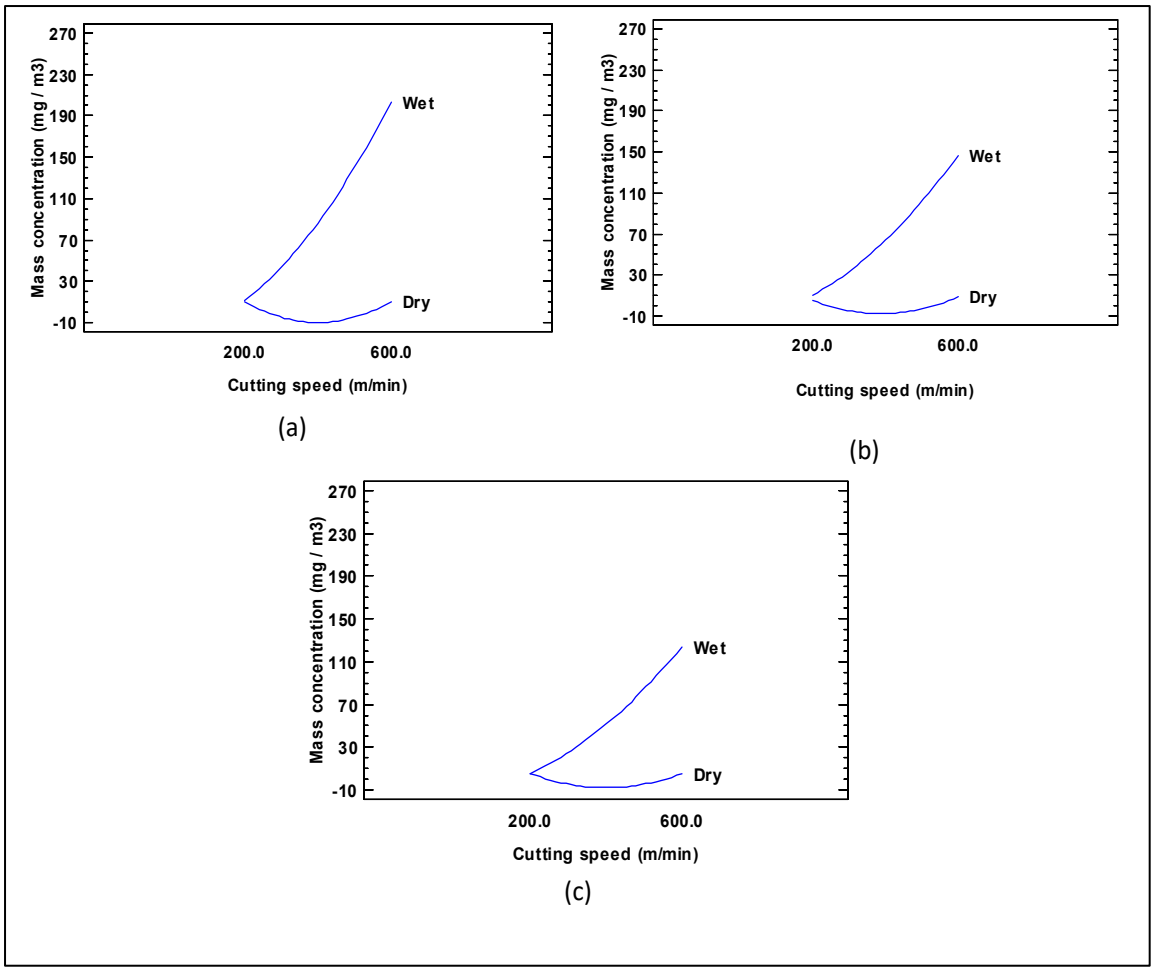

Figure 4.31 Interaction plots for mass concentration for (a) Al 7075, (b) Al 7075 – Sc, (c) Al 7075-Li-Sc

This point is important to mention that the reason why the amount of mass concentration is much higher in wet machining is that most of this amount is due to aerosols caused by using cutting fluid. So, it is recommended to investigate the metal particle emission by conducting an analysis on the machining process under dry conditions.

4.5 Conclusion

The conclusions drawn from the machining results, pertaining to surface roughness, cutting force, and particle emission, are detailed individually in the following sections.

Conclusion of Surface Roughness Analysis:

- In all three alloys used in our study, the feed rate had the most significant effect on surface roughness (Ra). However, in the case of Al 7075 - Sc, the significance of the feed rate was slightly lower than that of hardness, though it can still be considered one of the most influential parameters affecting surface roughness (Ra).
- In Al 7075, the cutting speed had a significant effect on surface roughness, ranking third in importance. It resulted in an increase of approximately 0.5 μm in roughness when the cutting speed increased from 200 to 600 m/min. In contrast, the effect was less pronounced in Al 7075 - Sc, causing only a 0.2 micrometer increase, and it was nearly insignificant in Al 7075-Li-Sc, with a decrease of less than 0.1 μm.
- Heat treating Al 7075 alloys for 24 hours at 120°C results in an increase in mechanical properties, including hardness. However, it is essential to consider the impact of this improvement on the machinability of the alloys, particularly in terms of surface roughness. In summary, our findings suggest that the hardness improvement has a negative effect on surface roughness. This effect is particularly pronounced in the case of Al 7075-Sc, where the Ra (average surface roughness) is 0.65 micrometers higher than that of the softest alloy. In Al 7075 alloy, a similarly significant negative effect is observed with a 0.35 micrometer increase in hardness. Interestingly, the direct effect of hardening on Ra in Al 7075-Li-Sc is negligible.
- Logically, the use of cutting fluid should lead to better surface quality and lower roughness. However, in our study, specifically with the Al 7075 alloy, not only did fully wet machining fail to yield a positive effect on the surface, but it also resulted in an increased Ra value. In the case of Al 7075 - Sc, the influence of the cooling mode was found to be entirely insignificant. Conversely, in Al 7075-Li-Sc, the cooling's direct

effect was positive on surface quality. However, upon closer examination and comparison of the charts and 3D surface graphs, it becomes evident that in machining of Al 7075 the interaction between the cooling mode and hardness played a significant role and wet machining more enhance Ra in hard sample. This observation held true even more strongly in the case of Al 7075-Li-Sc, where the significant reduction in Ra was pronounced in wet machining of the softer workpiece, and using a high level of cutting fluid in machining of harder samples still led to an increase in Ra.

In general, this study reveals that achieving a high level of hardness through 24-hour heat treatment at 120°C had a negative direct effect on surface quality.

Additionally, when considering its interaction with other variables, including cooling mode and feed rate, the negative impact on surface quality becomes more apparent. This is evident in the Pareto charts and 3D surface plots that increasing the feed rate, which is the most significant cutting variable, had a greater negative effect on surface quality, particularly in the case of harder samples.

Conclusion of Cutting force Analysis:

- The feed rate has the most significant effect on cutting force in all the studied alloys. However, it's worth noting that in Al 7075, this effect was more pronounced in wet machining, whereas in the two other alloys, the impact of feed rate was more significant in hardened workpieces.
- Wet machining significantly reduces cutting force, with a more pronounced effect on harder materials. Consequently, it can be concluded that dry machining yields satisfactory results when machining these alloys in their soft conditions specifically in Al 7075-Li-Sc alloy.
- An interesting and practical conclusion drawn from the cutting force analysis is that while increasing cutting speed generally reduces cutting force, this trend is more pronounced at lower feed rates. The practical implication is that selecting lower feed rates and higher cutting speeds for machining of these alloys not only reduces cutting force but also maintains high material removal rates, making it an advantageous choice.

- As the last conclusion, it is evident that higher hardness results in increased cutting force in all three alloys. Considering the manufacturing process and other relevant factors, a practical suggestion would be to machine parts produced from these alloys in their soft condition. Subsequently, a T6 heat treatment process can be applied to the machined parts to enhance their hardness and overall mechanical properties. This approach could potentially optimize both machining efficiency and final product quality.

Conclusion of Particle emission Analysis:

- Dry machining generally results in significantly lower particle emissions. In contrast, wet machining leads to a substantial increase in particle and aerosols emissions across all three alloys.
- Higher cutting speeds are associated with an increase in particle and aerosols emissions, primarily due to the elevated presence of liquid aerosols. The high speed motion of the tool must have generated more aerosols when using a high cutting speed.
- The analysis of particle and aerosol emissions was done globally. there is a need to redo the analysis condition by condition (eg wet for all materials, then dry for all materials)

CONCLUSION

This study focused on examining surface roughness, cutting force, and particle emission as crucial machinability criteria. To investigate the influence of hardness on machinability, the alloys underwent heat treatment at various aging times and temperatures. The study then selected and machined the alloys in their hardest and softest conditions. In the machining phase, both dry and wet end milling processes were carried out on the alloys, with emphasis on cutting parameters (feed rate and cutting speed). The conclusions drawn from the heat treatment process and machining, specifically regarding surface roughness, cutting force, and particle emission, are mentioned in the following.

- In all alloys, the highest level of hardness was attained through a 24-hour heat treatment at 120°C. As temperature primarily governed alloy hardness, the impact of single or double aging was found to be insignificant. The lowest hardness values were observed in both single aging (8 hours at 280°C) and double aging (8 hours at 280°C followed by 24 hours at 120°C).
- In relation to the surface roughness results, the feed rate demonstrated the highest influence, with its increase significantly enhancing roughness. Generally, hardness had a negative impact on surface quality. However, this effect was insignificant in the case of Al 7075-Li-Sc. Cutting speed did not exhibit a significant effect on surface roughness. Additionally, the effect of cooling mode on roughness in Al 7075 showed a slight positive influence, while in other alloys, this effect was negligible.
- In terms of the effect of alloying on surface roughness, although the presence of almost 0.1 percent Sc did not show a considerable impact on roughness, adding 2.2 percent Li significantly reduced roughness and improved the machined surface finish.
- The feed rate exerts the most substantial influence on cutting force in all examined alloys. Wet machining substantially diminishes cutting force, particularly impacting harder materials. Elevating cutting speed generally decreases cutting force, with a more marked impact at lower feed rates. Greater hardness leads to heightened cutting force in all three alloys.

- The statistical analysis of the air quality in the machine-tool revealed a high effect of cooling mode on aerosols and particles emission, followed by the effect of the cutting speed; These two factors seem to have higher impact; However, the analysis of particle and aerosol emissions was done globally. There is a need to redo the analysis condition by condition (eg wet for all materials, then dry for all materials)

RECOMMENDATIONS

The recommendations for future research, pertaining to the aspects addressed in this study, include:

1- This study looked at how hard and soft materials affect machinability. To learn more, it's suggested that future research focuses on materials with a medium level of hardness. This way, we can get a better overall understanding and use the findings more effectively. So, it's recommended to study machining in materials with medium hardness for better results.

2- Acknowledging the beneficial impact of cutting fluid on surface quality and cutting force reduction, alongside its adverse effect on dust emission, it is highly recommended to explore the Minimum Quantity Lubrication (MQL) method in machining these alloys.

3- Considering the abrasive particles formed in these alloys during the precipitation hardening process, particularly due to the presence of Scandium (Sc), it proves highly beneficial to investigate tool wear in the machining of these alloys.

APPENDIX I: Machining data results

Table AI.1 Surface roughness (Ra) results of Al 7075 dependence on cutting speed and feed rate

Material	Test number	Cutting speed (m/min)	Feed Rate (mm/tooth)	Ra (μm)			
				Softest (62 VHN)		Hardest (176 VHN)	
				Dry	Wet	Dry	Wet
Al 7075	1	200	0.05	0.789	0.746	0.671	1.224
	2		0.1	0.795	1.427	1.186	2.049
	3		0.15	1.507	1.578	1.843	2.343
	4	400	0.05	0.960	1.094	0.433	1.290
	5		0.1	1.183	1.507	1.117	2.004
	6		0.15	1.322	1.481	1.773	2.346
	7	600	0.05	0.812	1.091	1.026	1.405
	8		0.1	1.216	1.483	1.377	2.223
	9		0.15	1.558	1.810	1.872	2.579

Table AI.2 Surface roughness (Ra) results of Al 7075-Sc dependence on cutting speed and feed rate

Material	Test number	Cutting speed (m/min)	Feed Rate (mm/tooth)	Ra (μm)			
				Softest (79 VHN)		Hardest (185 VHN)	
				Dry	Wet	Dry	Wet
Al 7075-Sc	1	200	0.05	0.853	0.739	1.275	0.951
	2		0.1	0.895	1.156	1.893	1.132
	3		0.15	1.125	1.304	1.984	1.823
	4	400	0.05	0.962	0.891	1.387	1.651
	5		0.1	0.931	1.024	1.701	2.142
	6		0.15	1.234	1.292	1.795	2.219
	7	600	0.05	1.019	1.076	1.387	1.372
	8		0.1	1.437	1.406	2.080	2.116
	9		0.15	1.273	1.952	2.824	2.414

Table AI.3 Surface roughness (Ra) results of Al 7075-Li-Sc dependence on cutting speed and feed rate

Material	Test number	Cutting speed (m/min)	Feed Rate (mm/tooth)	Ra (μm)			
				Softest (81 VHN)		Hardest (198 VHN)	
				Dry	Wet	Dry	Wet
Al 7075-Li-Sc	1	200	0.05	0.797	0.500	0.678	0.596
	2		0.1	1.192	0.939	1.113	1.167
	3		0.15	1.481	1.354	1.575	1.563
	4	400	0.05	1.004	0.525	0.715	0.626
	5		0.1	1.364	0.951	1.131	1.183
	6		0.15	1.332	1.350	1.431	1.573
	7	600	0.05	0.961	0.561	0.458	0.527
	8		0.1	1.200	0.926	0.825	0.815
	9		0.15	1.579	1.284	1.237	1.462

Table AI.4 Cutting force results of Al 7075 dependence on cutting speed and feed rate

Material	Test number	Cutting speed (m/min)	Feed Rate (mm/tooth)	F (N)			
				Softest (62 VHN)		Hardest (176 VHN)	
				Dry	Wet	Dry	Wet
Al 7075	1	200	0.05	203.8	261.1	61.0	73.0
	2		0.1	149.4	233.6	106.4	112.5
	3		0.15	200.4	233.8	149.0	154.8
	4	400	0.05	80.3	132.7	62.3	81.6
	5		0.1	121.2	150.9	103.4	118.0
	6		0.15	172.0	184.5	145.6	164.1
	7	600	0.05	73.7	88.1	53.9	73.5
	8		0.1	114.8	125.0	90.8	119.2
	9		0.15	155.7	170.2	124.4	165.7

Table AI.5 Cutting force results of Al 7075 Sc dependence on cutting speed and feed rate

Material	Test number	Cutting speed (m/min)	Feed Rate (mm/tooth)	F (N)			
				Softest (79 VHN)		Hardest (185 VHN)	
				Dry	Wet	Dry	Wet
Al 7075-Sc	1	200	0.05	124.3	129.9	133.3	82.3
	2		0.1	146.0	111.6	151.8	120.9
	3		0.15	163.0	119.9	191.1	162.1
	4	400	0.05	96.0	101.3	117.8	91.4
	5		0.1	106.1	111.2	144.5	118.2
	6		0.15	135.5	121.7	173.0	162.2
	7	600	0.05	75.9	82.2	109.8	80.9
	8		0.1	111.4	93.7	127.3	100.9
	9		0.15	117.9	112.6	185.8	155.9

Table AI.6 Cutting force results of Al 7075-Li-Sc dependence on cutting speed and feed rate

Material	Test number	Cutting speed (m/min)	Feed Rate (mm/tooth)	F (N)			
				Softest (81 VHN)		Hardest (198 VHN)	
				Dry	Wet	Dry	Wet
Al 7075-Li-Sc	1	200	0.05	133.4	135.7	171.4	95.3
	2		0.1	125.5	134.0	182.1	133.1
	3		0.15	135.4	148.1	204.2	170.0
	4	400	0.05	90.8	97.9	125.7	93.7
	5		0.1	109.3	113.4	158.1	131.2
	6		0.15	133.4	109.4	195.6	169.8
	7	600	0.05	61.1	64.1	109.5	82.6
	8		0.1	100.9	85.3	152.2	128.4
	9		0.15	147.5	113.4	204.1	178.4

Table AI.7 Particle emission (mass consentration) results of Al 7075

Material	Test number	Cutting speed (m/min)	Feed Rate (mm/tooth)	Mass (mg/m³)			
				Softest (62 VHN)		Hardest (176 VHN)	
				Dry	Wet	Dry	Wet
Al 7075	1	200	0.05	0.277	15.8	0.674	12.8
	2		0.1	0.103	12.7	0.227	15.9
	3		0.15	3.89E-02	14.9	0.237	17
	4	400	0.05	0.163	57.3	0.965	49.9
	5		0.1	0.208	81.9	0.511	80.7
	6		0.15	9.41E-02	66.9	0.56	77.7
	7	600	0.05	0.257	183.2	0.247	190.5
	8		0.1	0.359	222.8	0.682	208.9
	9		0.15	0.166	208.8	0.701	225.1

Table AI.8 Particle emission (Number) results of Al 7075

Material	Test number	Cutting speed (m/min)	Feed Rate (mm/tooth)	Number (#/cm³)			
				Softest (62 VHN)		Hardest (176 VHN)	
				Dry	Wet	Dry	Wet
Al 7075	1	200	0.05	23	346.2	42.6	341.4
	2		0.1	9.73	276.9	14.4	446.4
	3		0.15	8.69	333	71.4	482.7
	4	400	0.05	20.7	1.18E+03	54.3	1.37E+03
	5		0.1	33.1	2.24E+03	33	2.13E+03
	6		0.15	25.3	1.86E+03	54.8	2.17E+03
	7	600	0.05	20.9	5.35E+03	16.7	5.78E+03
	8		0.1	29.6	6.97E+03	29.6	6.47E+03
	9		0.15	22.4	6.36E+03	37.2	6.94E+03

Table AI.9 Particle emission (Surface) results of Al 7075

Material	Test number	Cutting speed (m/min)	Feed Rate (mm/tooth)	Surface (µm²/cm³)			
				Softest (62 VHN)		Hardest (176 VHN)	
				Dry	Wet	Dry	Wet
Al 7075	1	200	0.05	199.6	9.60E+03	554.3	8.06E+03
	2		0.1	76.5	7.64E+03	172.6	1.01E+04
	3		0.15	36.7	8.96E+03	232	1.08E+04
	4	400	0.05	120.1	3.40E+04	671	3.20E+04
	5		0.1	143.2	5.20E+04	375.9	5.12E+04
	6		0.15	88.2	4.26E+04	460.1	5.03E+04
	7	600	0.05	184.5	1.19E+05	184.5	1.26E+05
	8		0.1	255.7	1.49E+05	461.8	1.39E+05
	9		0.15	130.4	1.39E+05	493	1.50E+05

Table AI.10 Particle emission (mass consentration) results of Al 7075-Sc

Material	Test number	Cutting speed (m/min)	Feed Rate (mm/tooth)	Mass (mg/m³)			
				Softest (79 VHN)		Hardest (185 VHN)	
				Dry	Wet	Dry	Wet
Al 7075-Sc	1	200	0.05	0.172	13.8	7.92E-02	10.8
	2		0.1	0.105	17.6	0.306	13.6
	3		0.15	0.154	15.5	0.45	14.7
	4	400	0.05	0.28	46	0.146	49.3
	5		0.1	0.315	66.5	0.785	42.8
	6		0.15	0.904	69.7	0.922	51.4
	7	600	0.05	1.07	157.7	5.64	108.7
	8		0.1	0.529	189.6	5.2	119.6
	9		0.15	0.371	219.8	9.72	108.8

Table AI.11 Particle emission (Number) results of Al 7075-Sc

Material	Test number	Cutting speed (m/min)	Feed Rate (mm/tooth)	Number (#/cm³)			
				Softest (79 VHN)		Hardest (185 VHN)	
				Dry	Wet	Dry	Wet
Al 7075-Sc	1	200	0.05	17.3	366.7	7.96	300.2
	2		0.1	11.5	469.1	28.1	392.5
	3		0.15	11.4	435.1	27	435.1
	4	400	0.05	20.3	1.23E+03	21.9	1.41E+03
	5		0.1	23.1	1.68E+03	66.1	943.2
	6		0.15	65.6	1.85E+03	51.8	1.17E+03
	7	600	0.05	59.6	4.67E+03	260.5	2.63E+03
	8		0.1	41.9	5.66E+03	238.5	2.96E+03
	9		0.15	30.2	6.81E+03	457	2.72E+03

Table AI.12 Particle emission (Surface) results of Al 7075-Sc

Material	Test number	Cutting speed (m/min)	Feed Rate (mm/tooth)	Surface (µm²/cm³)			
				Softest (79 VHN)		Hardest (185 VHN)	
				Dry	Wet	Dry	Wet
Al 7075-Sc	1	200	0.05	135.7	8.77E+03	63.8	7.05E+03
	2		0.1	86.1	1.10E+04	244.1	8.85E+03
	3		0.15	119.9	9.87E+03	315.6	9.54E+03
	4	400	0.05	195.5	2.91E+04	127.1	3.21E+04
	5		0.1	237.6	4.15E+04	621.2	2.54E+04
	6		0.15	681	4.42E+04	667.9	3.08E+04
	7	600	0.05	763.9	1.04E+05	4.14E+03	6.63E+04
	8		0.1	406.1	1.25E+05	3.79E+03	7.29E+04
	9		0.15	278.1	1.47E+05	7.18E+03	6.64E+04

Table AI.13 Particle emission (mass consentration) results of Al 7075-Li-Sc

Material	Test number	Cutting speed (m/min)	Feed Rate (mm/tooth)	Mass (mg/m³)			
				Softest (81 VHN)		Hardest (198 VHN)	
				Dry	Wet	Dry	Wet
Al 7075-Li-Sc	1	200	0.05	0.169	7.58	0.41	7.52
	2		0.1	6.80E-02	9.85	1.02	10.1
	3		0.15	0.128	10.5	2.57	12.6
	4	400	0.05	0.135	36.6	0.288	28.4
	5		0.1	0.663	45.8	0.687	41.6
	6		0.15	0.308	42.4	0.148	58.1
	7	600	0.05	0.196	114	0.117	109.4
	8		0.1	0.515	123.6	0.245	134.1
	9		0.15	1.28	146.9	0.191	136.8

Table AI.14 Particle emission (Number) results of Al 7075-Li-Sc

Material	Test number	Cutting speed (m/min)	Feed Rate (mm/tooth)	Number (#/cm³)			
				Softest (81 VHN)		Hardest (198 VHN)	
				Dry	Wet	Dry	Wet
Al 7075-Li-Sc	1	200	0.05	9.81	185.9	24.1	170.5
	2		0.1	21	235.7	73.8	233.8
	3		0.15	66.7	244.8	1.35E+03	287.4
	4	400	0.05	20.4	791.2	73.9	624.3
	5		0.1	36.8	987.8	51.1	895.2
	6		0.15	30.7	929.6	22.8	1.28E+03
	7	600	0.05	19.5	2.80E+03	14.4	2.72E+03
	8		0.1	47.4	3.07E+03	14.6	3.43E+03
	9		0.15	95.2	3.92E+03	14.3	3.40E+03

Table AI.15 Particle emission (Surface) results of Al 7075-Li-Sc

Material	Test number	Cutting speed (m/min)	Feed Rate (mm/tooth)	Surface (µm²/cm³)			
				Softest (81VHN)		Hardest (198 VHN)	
				Dry	Wet	Dry	Wet
Al 7075-Li-Sc	1	200	0.05	126.1	4.64E+03	310.7	4.46E+03
	2		0.1	66.1	5.98E+03	780.1	6.02E+03
	3		0.15	149.8	6.31E+03	3.02E+03	7.47E+03
	4	400	0.05	114.4	2.17E+04	285.2	1.69E+04
	5		0.1	466.9	2.71E+04	501.3	2.46E+04
	6		0.15	241.5	2.52E+04	132.8	3.46E+04
	7	600	0.05	156.3	7.00E+04	81.3	6.72E+04
	8		0.1	426.3	7.57E+04	171.3	8.29E+04
	9		0.15	1.03E+03	9.18E+04	130.3	8.33E+04

Table AI.16 Surface roughness (Rt) results of Al 7075 dependence on cutting speed and feed rate

Material	Test number	Cutting speed (m/min)	Feed Rate (mm/tooth)	Rt (μm)			
				Softest (62 VHN)		Hardest (176 VHN)	
				Dry	Wet	Dry	Wet
Al 7075	1	200	0.05	4.455	5.159	3.428	5.143
	2		0.1	5.839	6.820	6.347	8.205
	3		0.15	8.956	8.095	9.075	10.995
	4	400	0.05	6.539	6.883	2.753	4.910
	5		0.1	8.654	8.442	5.226	8.027
	6		0.15	8.756	7.302	8.249	10.521
	7	600	0.05	5.826	6.352	4.360	5.633
	8		0.1	7.989	9.688	6.980	9.828
	9		0.15	9.417	10.739	9.613	11.657

Table AI.17 Surface roughness (Rv) results of Al 7075 dependence on cutting speed and feed rate

Material	Test number	Cutting speed (m/min)	Feed Rate (mm/tooth)	Rv (μm)			
				Softest (62 VHN)		Hardest (176 VHN)	
				Dry	Wet	Dry	Wet
Al 7075	1	200	0.05	1.877	2.069	1.688	2.349
	2		0.1	2.109	2.884	3.245	3.681
	3		0.15	3.608	3.679	4.849	4.862
	4	400	0.05	2.783	2.689	1.331	2.211
	5		0.1	3.282	3.789	2.704	3.565
	6		0.15	3.838	3.486	4.418	4.790
	7	600	0.05	2.251	2.824	2.289	2.610
	8		0.1	3.317	4.301	3.591	4.370
	9		0.15	4.098	4.727	4.760	5.386

Table AI.18 Surface roughness (Rt) results of Al 7075-Sc dependence on cutting speed and feed rate

Material	Test number	Cutting speed (m/min)	Feed Rate (mm/tooth)	Rt (μm)			
				Softest (79 VHN)		Hardest (185 VHN)	
				Dry	Wet	Dry	Wet
Al 7075-Sc	1	200	0.05	5.849	4.291	5.660	4.845
	2		0.1	6.149	6.348	14.654	6.184
	3		0.15	7.321	7.310	11.498	10.769
	4	400	0.05	5.559	5.497	8.639	7.327
	5		0.1	5.758	5.546	13.684	8.979
	6		0.15	7.796	9.303	11.769	11.343
	7	600	0.05	6.052	9.035	10.039	7.565
	8		0.1	8.100	13.226	16.253	16.848
	9		0.15	7.395	14.209	34.333	18.982

Table AI.19 Surface roughness (Rv) results of Al 7075-Sc dependence on cutting speed and feed rate

Material	Test number	Cutting speed (m/min)	Feed Rate (mm/tooth)	Rv (μm)			
				Softest (79 VHN)		Hardest (185 VHN)	
				Dry	Wet	Dry	Wet
Al 7075-Sc	1	200	0.05	2.782	1.810	2.729	2.496
	2		0.1	2.783	2.768	5.831	3.180
	3		0.15	3.032	3.242	6.160	4.703
	4	400	0.05	2.394	2.330	3.317	3.224
	5		0.1	2.684	2.480	5.530	5.229
	6		0.15	3.237	3.727	6.239	6.476
	7	600	0.05	2.687	3.458	4.254	3.120
	8		0.1	3.676	4.670	8.590	6.156
	9		0.15	3.240	5.443	12.712	7.397

Table AI.20 Surface roughness (Rt) results of Al 7075-Li-Sc dependence on cutting speed and feed rate

Material	Test number	Cutting speed (m/min)	Feed Rate (mm/tooth)	Rt (μm)			
				Softest (81 VHN)		Hardest (198 VHN)	
				Dry	Wet	Dry	Wet
Al 7075-Li-Sc	1	200	0.05	3.744	3.477	3.581	3.594
	2		0.1	6.816	6.139	5.673	6.561
	3		0.15	9.105	7.271	8.331	8.960
	4	400	0.05	5.787	3.753	3.785	3.702
	5		0.1	7.855	6.106	6.110	5.854
	6		0.15	7.187	8.352	8.028	9.143
	7	600	0.05	5.367	3.323	2.898	3.201
	8		0.1	7.384	7.440	4.723	5.132
	9		0.15	10.249	6.993	6.550	8.050

Table AI.21 Surface roughness (Rv) results of Al 7075-Li-Sc dependence on cutting speed and feed rate

Material	Test number	Cutting speed (m/min)	Feed Rate (mm/tooth)	Rv (μm)			
				Softest (81 VHN)		Hardest (198 VHN)	
				Dry	Wet	Dry	Wet
Al 7075-Li-Sc	1	200	0.05	1.894	1.391	1.415	1.699
	2		0.1	3.022	2.424	2.602	3.033
	3		0.15	3.973	3.305	3.927	3.964
	4	400	0.05	2.638	1.413	1.588	1.596
	5		0.1	3.175	2.088	2.654	2.651
	6		0.15	3.196	3.044	4.022	3.718
	7	600	0.05	2.604	1.333	1.061	1.590
	8		0.1	3.356	2.611	1.956	2.187
	9		0.15	4.092	3.099	2.953	3.844

APPENDIX II: ANOVA Tables

Table AII.1 The Al 7075 ANOVA table for Ra

Source	Sum of Squares	Df	Mean Square	F-Ratio	P-Value
A: Feed rate	4.56841	1	4.56841	216.82	0.0000
B: Cutting speed	0.219268	1	0.219268	10.41	0.0037
C: Hardness	1.13849	1	1.13849	54.03	0.0000
D: Cooling mode	1.88604	1	1.88604	89.51	0.0000
AA	0.0347161	1	0.0347161	1.65	0.2121
AB	0.007921	1	0.007921	0.38	0.5458
AC	0.360885	1	0.360885	17.13	0.0004
AD	0.000442042	1	0.000442042	0.02	0.8861
BB	0.0351125	1	0.0351125	1.67	0.2096
BC	0.0000601667	1	0.0000601667	0.00	0.9578
BD	0.000988167	1	0.000988167	0.05	0.8305
CD	0.464669	1	0.464669	22.05	0.0001
Total error	0.484606	23	0.0210698		
Total (corr.)	9.20161	35			

Table AII.2 The Al 7075-Sc ANOVA table for Ra

Source	Sum of Squares	Df	Mean Square	F-Ratio	P-Value
A: Feed rate	2.45504	1	2.45504	49.72	0.0000
B: Cutting speed	1.13796	1	1.13796	23.05	0.0001
C: Hardness	3.72297	1	3.72297	75.40	0.0000
D: Cooling mode	0.0101674	1	0.0101674	0.21	0.6541
AA	0.0145636	1	0.0145636	0.29	0.5921
AB	0.0886551	1	0.0886551	1.80	0.1928
AC	0.239201	1	0.239201	4.84	0.0376
AD	0.039366	1	0.039366	0.80	0.3808
BB	0.0146776	1	0.0146776	0.30	0.5906
BC	0.045414	1	0.045414	0.92	0.3471
CD	0.0726303	1	0.0726303	1.47	0.2370
Total error	1.18506	24	0.0493775		
Total (corr.)	9.02571	35			

Table AII.3 The Al 7075-Li-Sc ANOVA table for Ra

Source	Sum of Squares	Df	Mean Square	F-Ratio	P-Value
A: Feed rate	3.58286	1	3.58286	619.36	0.0000
B: Cutting speed	0.0522667	1	0.0522667	9.04	0.0061
C: Hardness	0.0108507	1	0.0108507	1.88	0.1835
D: Cooling mode	0.130923	1	0.130923	22.63	0.0001
AA	0.00272568	1	0.00272568	0.47	0.4990
AB	0.00752556	1	0.00752556	1.30	0.2653
AC	0.0609034	1	0.0609034	10.53	0.0034
AD	0.062935	1	0.062935	10.88	0.0030
BB	0.0346722	1	0.0346722	5.99	0.0220
BC	0.108811	1	0.108811	18.81	0.0002
CD	0.228643	1	0.228643	39.53	0.0000
Total error	0.138834	24	0.00578476		
Total (corr.)	4.42195	35			

Table AII.4 The ANOVA table for Ra considering all alloys

Source	Sum of Squares	Df	Mean Square	F-Ratio	P-Value
Cooling mode	0.412428	1	0.412428	12.9095	0.0005
Material	3.63521	2	1.8176	56.8932	0.0000
Heat treatment	2.78853	1	2.78853	87.2844	0.0000
Cutting speed	0.568889	1	0.568889	17.8069	0.0001
Feed rate	10.4425	1	10.4425	326.861	0.0000
AB	1.61471	2	0.807353	25.2711	0.0000
AC	0.264231	1	0.264231	8.27075	0.0051
AD	0.0280845	1	0.0280845	0.879079	0.3511
AE	0.073728	1	0.073728	2.30778	0.1324
BC	2.08378	2	1.04189	32.6124	0.0000
BD	0.840607	2	0.420304	13.156	0.0000
BE	0.163856	2	0.081928	2.56445	0.0829
CD	0.0039605	1	0.0039605	0.123968	0.7256
CE	0.595504	1	0.595504	18.64	0.0000
DD	0.00498817	1	0.00498817	0.156136	0.6937
DE	0.00496133	1	0.00496133	0.155296	0.6945
EE	0.0430107	1	0.0430107	1.34629	0.2492
Model	23.5689	22	1.07131	33.5335	0.0000
Residual	2.71555	85	0.0319476		
Lack-of-fit		85			
Pure error		0			
Total (corr.)	26.2845	107			

Table AII.5 The Al 7075 ANOVA table for Cutting force

Source	Sum of Squares	Df	Mean Square	F-Ratio	P-Value
A: Feed rate	25039.0	1	25039.0	60.09	0.0000
B: Cutting speed	14200.9	1	14200.9	34.08	0.0000
C: Hardness	6246.27	1	6246.27	14.99	0.0008
D: Cooling mode	22101.8	1	22101.8	53.04	0.0000
AA	424.376	1	424.376	1.02	0.3234
AB	2201.96	1	2201.96	5.28	0.0309
AC	100.042	1	100.042	0.24	0.6288
AD	2042.42	1	2042.42	4.90	0.0370
BB	943.227	1	943.227	2.26	0.1461
BC	206.507	1	206.507	0.50	0.4885
BD	11501.9	1	11501.9	27.60	0.0000
CD	568.028	1	568.028	1.36	0.2550
Total error	9584.03	23	416.697		
Total (corr.)	95160.4	35			

Table AII.6 The Al 7075-Sc ANOVA table for Cutting force

Source	Sum of Squares	Df	Mean Square	F-Ratio	P-Value
A: Feed rate	13804.8	1	13804.8	156.82	0.0000
B: Cutting speed	3311.15	1	3311.15	37.61	0.0000
C: Hardness	3383.36	1	3383.36	38.43	0.0000
D: Cooling mode	3433.96	1	3433.96	39.01	0.0000
AA	266.805	1	266.805	3.03	0.0951
AB	203.776	1	203.776	2.31	0.1418
AC	2679.71	1	2679.71	30.44	0.0000
AD	76.3267	1	76.3267	0.87	0.3614
BB	14.8512	1	14.8512	0.17	0.6851
BC	6048.37	1	6048.37	39.79	0.0000
BD	244.482	1	244.482	1.61	0.2174
CD	4578.78	1	4578.78	30.12	0.0000
Total error	3496.59	23	152.025		
Total (corr.)	70993.4	35			

Table AII.7 The Al 7075-Li-Sc ANOVA table for Cutting force

Source	Sum of Squares	Df	Mean Square	F-Ratio	P-Value
A: Feed rate	17501.4	1	17501.4	161.48	0.0000
B: Cutting speed	4836.52	1	4836.52	44.62	0.0000
C: Hardness	11620.8	1	11620.8	107.22	0.0000
D: Cooling mode	3528.36	1	3528.36	32.55	0.0000
AA	56.0035	1	56.0035	0.52	0.4795
AB	2606.1	1	2606.1	24.05	0.0001
AC	2394.0	1	2394.0	22.09	0.0001
AD	3.01042	1	3.01042	0.03	0.8691
BB	268.733	1	268.733	2.48	0.1290
BC	803.884	1	803.884	7.42	0.0121
BD	6.72042	1	6.72042	0.06	0.8056
CD	2246.76	1	2246.76	20.73	0.0001
Total error	2492.82	23	108.384		
Total (corr.)	48365.2	35			

BIBLIOGRAPHY

Ashkenazi, D. (2019). "How aluminum changed the world: A metallurgical revolution through technological and cultural perspectives." Technological Forecasting and Social Change **143**: 101-113.

Aslantas, K., et al. (2022). "Performance evaluation of DLC and NCD coatings in micro-milling of Al7075-T6 alloy." Journal of Manufacturing Processes **81**: 976-990.

Bhushan, R. K., et al. (2010). "Effect of machining parameters on surface roughness and tool wear for 7075 Al alloy SiC composite." The International Journal of Advanced Manufacturing Technology **50**: 459-469.

Boubekri, N., et al. (2003). "Development of an aggregate indicator to assess the machinability of steels." Journal of materials processing technology **134**(2): 159-165.

Campbell Jr, F. C. (2011). Manufacturing technology for aerospace structural materials, Elsevier.

Cheng, Y., et al. (2014). "Investigations on the dust distribution characteristics of dry milling using inserts with various groove profiles." The International Journal of Advanced Manufacturing Technology **74**: 551-562.

Coelho, R., et al. (2003). "Experimental evaluation of cutting force parameters applying mechanistic model in orthogonal milling." Journal of the Brazilian Society of Mechanical Sciences and Engineering **25**.

Darsono, F. and S. Koin (2021). The Effect of T6 Heat Treatment on 7075 Aluminum on its Hardness and Tensile Strength. IOP Conference Series: Materials Science and Engineering, IOP Publishing.

Demir, H. and S. Gündüz (2009). "The effects of aging on machinability of 6061 aluminium alloy." Materials & Design **30**(5): 1480-1483.

Deng, L., et al. (2022). Precision Forging Technology and Equipment for Aluminum Alloy, Springer.

Dorward, R. (2018). "Work Hardening and Annealing of Aluminum Alloys."

Galevsky, G., V. Rudneva and V. Aleksandrov (2018). Current state of the world and domestic aluminium production and consumption. IOP Conference Series: Materials Science and Engineering, IOP Publishing.

Georgantzia, E., et al. (2021). "Aluminium alloys as structural material: A review of research." Engineering Structures **227**: 111372.

Groover, M. P. (2010). Fundamentals of modern manufacturing: materials, processes and systems, USA: Jhon Wiley & Sons, Inc.

Groover, M. P. (2020). Fundamentals of modern manufacturing: materials, processes, and systems, John Wiley & Sons.

Gupta, M. K., et al. (2022). "Cutting forces and temperature measurements in cryogenic assisted turning of AA2024-T351 alloy: An experimentally validated simulation approach." Measurement **188**: 110594.

Han, Z., et al. (2015). Cutting force prediction models of metal machining processes: A review. 2015 International Conference on Estimation, Detection and Information Fusion (ICEDIF), IEEE.

Huang, Z., et al. (1993). "Influence of lithium additions on precipitation and age hardening of 7075 alloy." Materials science and technology **9**(11): 967-980.

Isadare, A. D., et al. (2013). "Effect of heat treatment on some mechanical properties of 7075 aluminium alloy." Materials Research **16**: 190-194.

Jiang, N., et al. (2010). "Microstructure evolution of aluminum-lithium alloy 2195 undergoing commercial production." Transactions of Nonferrous Metals Society of China **20**(5): 740-745.

Johnson, W. (1990). "Properties and selection: nonferrous alloys and special-purpose materials." Molybdenum, Metals Handbook **2**: 574.

Kaya, H., et al. (2012). "The effect of aging on the machinability of AA7075 aluminium alloy." Scientific Research and Essays **7**(27): 2424-2430.

Khettabi, R., et al. (2017). "Effect of MQL and dry processes on the particle emission and part quality during milling of aluminum alloys." The International Journal of Advanced Manufacturing Technology **92**: 2593-2598.

Khettabi, R., et al. (2007). "Effect of tool lead angle and chip formation mode on dust emission in dry cutting." Journal of materials processing technology **194**(1-3): 100-109.

Khettabi, R., et al. (2010). "Effects of speeds, materials, and tool rake angles on metallic particle emission during orthogonal cutting." Journal of materials engineering and performance **19**: 767-775.

Khettabi, R., et al. (2010). "Modeling of particle emission during dry orthogonal cutting." Journal of materials engineering and performance **19**: 776-789.

Kumar, K., et al. (2018). "Introduction to Machining Processes." Advanced Machining and Manufacturing Processes: 41-47.

Kumar, R., et al. (2019). "Influence of cutting parameters on cutting forces and surface roughness in dry turning of Al using PCD and different coated tools." Sādhanā **44**: 1-17.

LI JF, P. Z. (2008). "Mechanical properties, corrosion behaviors and microstructure of 7075 aluminum alloy with various aging statements." Transaction of Nonferrous Metals Society of China **18**(4): 755-762.

Li, W., et al. (2009). "Effects of minor Sc on the microstructure and mechanical properties of Al-Zn-Mg-Cu-Zr based alloys." Rare Metals **28**: 102-106.

Luo, H., et al. (2020). "Effect of cutting parameters on machinability of 7075-T651 aluminum alloy in different processing methods." The International Journal of Advanced Manufacturing Technology **110**: 2035-2047.

Luo, M., et al. (2018). "Cutting forces measurement for milling process by using working tables with integrated PVDF thin-film sensors." Sensors **18**(11): 4031.

Maechler, R., et al. (1991). "Structure, mechanical properties, and stress corrosion behaviour of high strength spray deposited 7000 series aluminium alloy." Materials science and technology **7**(5): 447-451.

Magabe, R. and K. Gupta (2023). "Investigation on Machinability of Aluminum 7075 Under Dry Environment." FME Transactions **51**(4): 471.

Marani, M., et al. (2020). "Neuro-fuzzy predictive model for surface roughness and cutting force of machined Al–20 Mg 2 Si–2Cu metal matrix composite using additives." Neural Computing and Applications **32**: 8115-8126.

Mathew, A. K., et al. (2010). "Effect of machining feed on surface roughness in cutting 6061 Aluminum." SAE International: 01-0218.

Meng, X., et al. (2021). "The research of tool wear mechanism for high-speed milling ADC12 aluminum alloy considering the cutting force effect." Materials **14**(5): 1054.

Miller, W., et al. (2000). "Recent development in aluminium alloys for the automotive industry." Materials Science and Engineering: A **280**(1): 37-49.

Nimase, R. and P. Khodke (2015). "Effect of machining parameters on surface roughness of Al-7075 alloy in end milling." International Research Journal of Engineering and Technology (IRJET) e-ISSN: 2395-0056.

Pathak, B., et al. (2013). "Effect of machining parameters on cutting forces and surface roughness in Al-(1-2) Fe-1V-1Si alloys." Materials and Manufacturing Processes **28**(4): 463-469.

Ping, Z., et al. (2021). "Surface integrity and tool wear mechanism of 7050-T7451 aluminum alloy under dry cutting." Vacuum **184**: 109886.

Prasad, N. E., et al. (2013). Aluminum-lithium alloys: processing, properties, and applications, Butterworth-Heinemann.

Pruthvi, H. and H. G. Shenoy (2022). Effect of Zn, Mg and heat treatment on Al base alloy on hardness using Taguchi Technique. IOP Conference Series: Materials Science and Engineering, IOP Publishing.

Rana, R., et al. (2012). "Reviews on the influences of alloying elements on the microstructure and mechanical properties of aluminum alloys and aluminum alloy composites." International Journal of Scientific and research publications **2**(6): 1-7.

Rawangwong, S., et al. (2012). "An investigation of optimum cutting conditions in face milling semi-solid AA 7075 using carbide tool." International Journal of Innovation, Management and Technology **3**(6): 692.

Rivière-Lorphèvre, E. and E. Filippi (2009). "Mechanistic cutting force model parameters evaluation in milling taking cutter radial runout into account." The International Journal of Advanced Manufacturing Technology **45**(1-2): 8-15.

Sadeghifar, M., et al. (2022). "A comparative analysis of chip shape, residual stresses, and surface roughness in minimum-quantity-lubrication turning with various flow rates." The International Journal of Advanced Manufacturing Technology **121**(5-6): 3977-3987.

Sales, W. F., et al. (2001). "Application of cutting fluids in machining processes." Journal of the Brazilian Society of Mechanical Sciences **23**: 227-240.

Santos, M. C., et al. (2016). "Machining of aluminum alloys: a review." The International Journal of Advanced Manufacturing Technology **86**(9): 3067-3080.

Shankar, S., et al. (2017). "Influence of vegetable based cutting fluids on cutting force and vibration signature during milling of aluminium metal matrix composites." Jurnal Tribologi **12**: 1-17.

Slamani, M., et al. (2016). "Comparison of surface roughness quality obtained by high speed CNC trimming and high speed robotic trimming for CFRP laminate." Robotics and Computer-Integrated Manufacturing **42**: 63-72.

Soren, T. R., et al. (2019). "Machinability behavior of aluminium alloys: A brief study." Materials Today: Proceedings **18**: 5069-5075.

Stephenson, D. A. and J. S. Agapiou (2018). Metal cutting theory and practice, CRC press.

Stojanovic, B. and I. Epler (2018). "Application of aluminum and aluminum alloys in engineering." Applied Engineering Letters: Journal of Engineering and Applied Sciences.

Tajally, M. and E. Emadoddin (2011). "Mechanical and anisotropic behaviors of 7075 aluminum alloy sheets." Materials & Design **32**(3): 1594-1599.

Toenshoff, H. K. and B. Denkena (2013). "Basics of cutting and abrasive processes."

Trent, E. M. and P. K. Wright (2000). Metal cutting, Butterworth-Heinemann.

Tsao, C. (2009). "Grey–Taguchi method to optimize the milling parameters of aluminum alloy." The International Journal of Advanced Manufacturing Technology **40**: 41-48.

ud Din, S., et al. (2016). "The synergistic effect of Li addition on microstructure, texture and mechanical properties of extruded Al–Mg–Si alloys." Materials Chemistry and Physics **174**: 11-22.

Verma, M. and P. Saha (2023). "Effect of micro-grooves featured tool and their depths on dissimilar micro-friction stir welding (μFSW) of aluminum alloys: A study of process responses and weld characteristics." Materials Characterization **196**: 112614.

Wan, M., et al. (2016). "Study on the correction of cutting force measurement with table dynamometer." Procedia CIRP **56**: 119-123.

Wang, W.-R., et al. (2012). "Effects of Al addition on the microstructure and mechanical property of AlxCoCrFeNi high-entropy alloys." Intermetallics **26**: 44-51.

Wanhill, R. and G. Bray (2014). Aerostructural design and its application to aluminum–lithium alloys. Aluminum-lithium alloys, Elsevier**:** 27-58.

Wei, B., et al. (2000). "Aging behavior of Li containing Al–Zn–Mg–Cu alloys." Materials Science and Engineering: A **280**(1): 161-167.

Wieroński, W., et al. (2016). "Effect of Heat Treatment on Machining Properties of the AlSi9Cu3 (Fe) Alloy." Archives of Foundry Engineering **16**(3): 137-140.

Williams, J. C. and E. A. Starke Jr (2003). "Progress in structural materials for aerospace systems." Acta materialia **51**(19): 5775-5799.

X.-M., L. and M. Starink (2001). "Effect of compositional variations on characteristics of coarse intermetallic particles in overaged 7000 aluminium alloys." Materials science and technology **17**(11): 1324-1328.

Xia, P., et al. (2021). "Effect of Sc and Zr additions on recrystallization behavior and intergranular corrosion resistance of Al-Zn-Mg-Cu alloys." Materials **14**(19): 5516.

Xu, Y., et al. (2021). "Effect of main elements (Zn, Mg and Cu) on the microstructure, castability and mechanical properties of 7xxx series aluminum alloys with Zr and Sc." Materials Characterization **182**: 111559.

Ye, Z., et al. (2022). "Study on the reaming process of aluminum alloy 7050-T7451 under different cooling conditions." Advances in Manufacturing: 1-15.

Yeganefar, A., et al. (2019). "Machinability study of aircraft series aluminium alloys 7075-T6 and 7050-T7451." Transactions of the Canadian Society for Mechanical Engineering **44**(3): 427-439.

Yilbas, B. S., et al. (2010). "Laser cutting of 7050 Al alloy reinforced with Al 2 O 3 and B 4 C composites." The International Journal of Advanced Manufacturing Technology **50**: 185-193.

Yoshimura, H., et al. (2006). "Study on near dry machining of aluminum alloys." JSME International Journal Series C Mechanical Systems, Machine Elements and Manufacturing **49**(1): 83-89.

Zagórski, I. and T. Warda (2018). "Effect of technological parameters on the surface roughness of aluminium alloys after turning." Advances in Science and Technology. Research Journal **12**(2): 144-149.

Zhang, J. Z., et al. (2007). "Surface roughness optimization in an end-milling operation using the Taguchi design method." Journal of materials processing technology **184**(1-3): 233-239.

Zhenjing, D., et al. (2021). "Milling surface roughness for 7050 aluminum alloy cavity influenced by nozzle position of nanofluid minimum quantity lubrication." Chinese Journal of Aeronautics **34**(6): 33-53.